Electromagnetic Scattering By Random Rough Surfaces

The problem of electromagnetic scattering from random rough surfaces has been the subject of intense investigation over the past several decades for its applications in a number of important remote sensing problems. With the advent of the polarimetric synthetic aperture radar (SAR), radar remote sensing has attained significant prominence in the past decade. SAR systems are capable of producing the backscatter map of the terrain with high resolution from an airborne or space-borne platform. Radar remote sensing of soil moisture is one example for which the knowledge of electromagnetic wave interaction with rough surfaces is needed. Soil moisture, and its temporal and spatial variations are influential parameters in both climatic and hydrologic models. Soil dielectric constant at microwave frequencies exhibits a strong dependence on the soil's moisture content. At L-band, for example, the real part of the dielectric constant ranges from 3 for dry soil to about 25 for saturated soil. This variation can result in a change on the order of 10 dB in the magnitude of the radar backscatter coefficient [1]. Another such example is radar remote sensing of ocean surfaces. The interest in radar remote sensing of ocean stems from the fact that the upper ocean has a large influence on global weather and climate processes through its role in the exchange of matter (aerosols and gases) momentum and energy with atmosphere [2]. From the electromagnetics point of view, remote sensing of rough surfaces can be modeled as an inverse scattering problem, where the dielectric constant and surface roughness statistics are to be determined from a set of backscatter measurements.

The problem of wave scattering from random rough surfaces has been the subject of ongoing research over the past several decades. Generally speaking, the available electromagnetic scattering models can be categorized into three major groups: (1) analytical, (2) empirical, and (3) numerical. The analytical scattering solutions for rough surfaces can be obtained in approximate forms and under certain limiting conditions which allow the required mathematical simplifications. There are two classical approaches available for this problem, 1) a high frequency method known as Kirchhoff approach [7], and 2) a low frequency method knows as the small perturbation method [3, 4]. The high and low frequency in this context refer to the relative dimensions of the statistical parameters of the surface roughness profile to the wavelength of the incident wave. For example when the root-mean-squared (rms) of the surface height profile and the surface correlation length are much smaller than the wavelength the small perturbation method can be used, whereas in the other extreme when the rms height and correlation length are large compared to the wavelength the Kirchhoff approach is appropriate.

In the small perturbation method (SPM) the surface fields are expanded in terms of a

power series in the small roughness parameter and then, using either the Rayleigh hypothesis or the extended boundary condition [5], the expansion coefficients are obtained recursively. The scattering formulations based on SPM exist for dielectric and perfectly conducting rough surfaces. For these surfaces, only first-order expressions for the co-polarized and second-order expressions for the cross-polarized backscattering coefficients are reported [6]. On the other hand, if the irregularities of the surface have relatively small slopes and large radii of curvature, the Kirchhoff approximation (KA) can be used [7]. In this approach, the surface fields at a given point are approximated by those of the local tangent plane. In the past two decades, many attempts have been made to extend the validity region of SPM and KA. Among these, the phase perturbation method (PPM) [8] and the unified perturbation expansion (UPE) [9] for extending the low-frequency techniques, and the integral equation method (IEM) [10] for extending the high-frequency techniques, can be mentioned. In the PPM, the perturbation solution is obtained by expanding the phase of the field instead of the field itself, whereas in the UPE method, the solution is obtained by expanding the field in terms of a parameter (momentum transfer) that remains small over a region larger than the perturbation parameter used in SPM. Scattering formulation based on PPM and UPM are reported only for one-dimensional rough surfaces. The scattering solution based on IE method is obtained by inserting the KA into the surface field integral equation. This method is significant in that it reduces to the SPM solution, thereby seemingly bridging the gap between the low- and high-frequency solutions [11].

In this chapter we confine our attention to the classical approaches, and present fully polarimetric solutions for dielectric surfaces at high and low frequencies.

1 Kirchhoff Approximation

In the Kirchhoff approach the unknown surface fields are approximated by the physical optics currents assuming that the surface at each point is locally flat (tangent plane approximation). This approximation is valid for surfaces with large radii of curvature at every point on the surface. For perfectly conducting surfaces the Kirchhoff diffraction integrals can be evaluated much easier than those for dielectric surfaces. The excess complexity of the Kirchhoff approach for dielectric surfaces stems from the fact that the reflection coefficients locally are complex functions of the incidence angle whereas for a perfectly conducting surface the TE and TM reflection coefficients are respectively -1 and $+1$ independent of the local incident angle. To overcome this difficulty, further simplifications are made for evaluating the diffraction integral assuming either the surface slope is small with a very high probability or using the stationary phase approximation which only accounts for the contribution from certain points on the surface known as the specular points. The solution with the small slope approximation is referred to as the physical optics approximation (P.O.) and the solution using the stationary phase ap-

proximation is known as the geometrical optics approximation (G.O.). The result based on GO approximation is frequency independent as it is proportional to the probability of the occurrence of the surface slopes for which the reflected or transmitted rays are parallel to the observation direction.

Consider two homogeneous dielectric media whose interface is described in the global coordinate system by a function $z = f(x, y)$. Let us denote the permittivity and permeability of the upper and lower regions by ϵ_o and μ_o and ϵ_1 and μ_o respectively. Suppose the interface is illuminated by a plane wave whose direction of propagation $\hat{k}_i$ is given by (4) as shown in Figure 1. In this figure $f(x, y)$ denotes a sample of a two dimensional stochastic process which is assumed to be a zero-mean stationary Gaussian process with a known power spectral density. The bistatic scattered field from different sample functions of the stochastic process is a random process which depending on the surface roughness may fluctuate significantly. As described before in most clutter characterization studies, the second moments of the scattered field such as the bistatic scattering coefficient are of interest. In this treatment the basic assumption is that the radius of

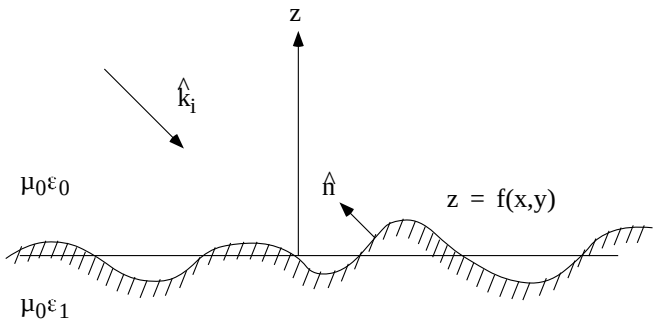

Figure 1: A rough interface between two homogeneous dielectric media.

curvature at any point on the surface is much larger than the incident wavelength. With this assumption, the electric and magnetic fields at every point on the surface can be approximated by those of a semi-infinite medium with planar interface (tangent plane) for which exact solution exist. As shown before (in the proof of Ewald-Oseen extinction theorem) once the tangential fields on the surface of a scatterer are known the scattered field in regions 0 and 1 can, respectively, be obtained from

$$E_s^0(\bar{r}) = \int_s \int \left[ik_0 Z_0 \left(\hat{n} \times \overline{H}(\bar{r}') \right) \cdot \bar{\bar{G}}_0 \left(\bar{r}, \bar{r}' \right) - \left(\hat{n} \times \overline{E}(\bar{r}') \right) \cdot \nabla \times \bar{\bar{G}}_0 \left(\bar{r}, \bar{r}' \right) \right] ds' \quad (1)$$

$$E_s^1(\bar{r}) = -\int_s \int \left[ik_1 Z_1 (\hat{n} \times \overline{H}(\bar{r}') \cdot \bar{\bar{G}}_1 \left(\bar{r}, \bar{r}' \right) - (\hat{n} \times \overline{E}(\bar{r}')) \cdot \nabla \times \bar{\bar{G}}_1 \left(\bar{r}, \bar{r}' \right) \right] ds' \quad (2)$$

Where $\bar{\bar{G}}_0 \left(\bar{r}, \bar{r}' \right)$ and $\bar{\bar{G}}_1 \left(\bar{r}, \bar{r}' \right)$ are the dyadic Green's functions for regions 0 and 1, and $\hat{n}$ is the unit normal to the surface pointing towards region 0 and is given by

$$\hat{n} = \frac{\nabla(z - f(x,y))}{|\nabla(z - f(x,y))|} = \frac{-f_x\hat{x} - f_y\hat{y} + \hat{z}}{\sqrt{1 + f_x^2 + f_y^2}} \tag{3}$$

where

$$\begin{aligned} f_x &= \frac{\partial f(x,y)}{\partial x} \\ f_y &= \frac{\partial f(x,y)}{\partial y} \end{aligned}$$

Since the antenna footprint usually covers a finite portion of the rough surface, the notion of far-field region can be exploited. Let us assume that the observation points in region 0 or 1 are in the far-field region of the illuminated portion of the rough surface (A). In this case the far-field expression of the dyadic Green's functions (equation (2.21)) can be employed in the diffraction integrals (1) and (2). Suppose the direction of observation points in region 0 and 1 are denoted by $\hat{k}_s^0$ and $\hat{k}_s^1$ respectively, then

$$\bar{\bar{G}}_0\left(\bar{r}, \bar{r}'\right) \simeq \left[\bar{\bar{I}} - \hat{k}_s^0 \hat{k}_s^0\right] \frac{e^{ik_0 r}}{4\pi r} e^{-ik_0 \hat{k}_s^0 \cdot \bar{r}'} \tag{4}$$

$$\bar{\bar{G}}_1\left(\bar{r}, \bar{r}'\right) \simeq \left[\bar{\bar{I}} - \hat{k}_s^1 \hat{k}_s^1\right] \frac{e^{ik_1 r}}{4\pi r} e^{-ik_i \hat{k}_s^1 \cdot \bar{r}'} \tag{5}$$

Recalling that $\nabla\times \bar{\bar{G}}\left(\bar{r}, \bar{r}'\right)$ is anti- symmetric, that is

$$(\hat{n} \times \overline{E}(r')) \cdot \nabla\times \bar{\bar{G}}\left(\bar{r}, \bar{r}'\right) = -\nabla\times \bar{\bar{G}}\left(r, r'\right) \cdot (\hat{n} \times \overline{E}(\bar{r}')),$$

and in the far-field region

$$\nabla\times \bar{\bar{G}}\left(\bar{r}, \bar{r}'\right) = \nabla g(\bar{r}, \bar{r}')\times \bar{\bar{I}} \simeq \frac{e^{ik_0 r}}{4\pi r} e^{ik_0 \hat{k}_s^0 \cdot \bar{r}'} ik_0 \hat{k}_s^0 \times \bar{\bar{I}}$$

which can be written as

$$\nabla\times \bar{\bar{G}}\left(\bar{r}, \bar{r}'\right) \simeq \frac{e^{ik_0 r}}{4\pi r} e^{ik_0 \hat{k}_s^0 \cdot \bar{r}'} ik_0 \hat{k}_s^0 \times \left(\bar{\bar{I}} - \hat{k}_s^0 \hat{k}_s^0\right)$$

it can easily be shown that

$$\left(\hat{n} \times \overline{E}(\bar{r}')\right) \cdot \nabla\times \bar{\bar{G}}\left(\bar{r}, \bar{r}'\right) \simeq \frac{e^{ik_0 r}}{4\pi r} e^{ik_0 \hat{k}_s^0 \cdot \bar{r}'} ik_0 \left[(\hat{n} \times \overline{E}(\bar{r}')) \times \hat{k}_s^0\right] \cdot \left(\bar{\bar{I}} - \hat{k}_s^0 \hat{k}_s^0\right) \tag{6}$$

In view of (4) and (6), (1) can be written as

$$E_s^0(\bar{r}) \simeq \frac{ik_0 e^{ik_0 r}}{4\pi r}\left(\bar{\bar{I}} - \hat{k}_s^0 \hat{k}_s^0\right) \cdot \iint_s \left\{Z_0\left(\hat{n} \times \overline{H}(\bar{r}')\right) + \hat{k}_s^0 \times \left(\hat{n} \times \overline{E}(\bar{r}')\right)\right\} e^{-ik_0 \hat{k}_s^0 \cdot \bar{r}'} ds' \quad (7)$$

In a similar manner it can be shown that

$$E_s^1(\bar{r}) \simeq \frac{-ik_1 e^{ik_1 r}}{4\pi r}\left(\bar{\bar{I}} - \hat{k}_s^1 \hat{k}_s^1\right) \cdot \int_s \int \left\{Z_1\left(\hat{n} \times \overline{H}(\bar{r}')\right) + \hat{k}_s^1 \times \left(\hat{n} \times \overline{E}(\bar{r}')\right)\right\} e^{ik_1 \hat{k}_s^1 \cdot \bar{r}'} ds' \quad (8)$$

where the negative sign, as explained before, is due to the fact that the same unit normal vector to the surface is used.

The next step is to characterize the surface field quantities using the Kirchhoff approximation. At a given point $\bar{r}'$ on the surface let $\hat{t}$ be a unit vector perpendicular to the local plane of incidence, i.e.,

$$\hat{t} = \frac{\hat{k}_i \times \hat{n}}{|\hat{k}_i \times \hat{n}|} \quad (9)$$

Also we define a unit vector in the plane of incidence perpendicular to $\hat{k}_i$

$$\hat{u} = \hat{t} \times \hat{k}_i \quad (10)$$

The reflected wave locally propagates along

$$\hat{k}_r = \hat{k}_i - 2\hat{n}(\hat{n} \cdot \hat{k}_i) \quad (11)$$

To calculate the reflected waves, the incident field is decomposed into its perpendicular and parallel polarization components where each component then is modified according to the local Fresnel reflection coefficient. For the incident plane wave

$$\overline{E}^i = \overline{E}_0 e^{ik_0 \hat{k}_i \cdot \bar{r}} \quad , \quad \overline{H}^i = \overline{H}_0 e^{ik_0 \hat{k}_i \cdot \bar{r}}$$

where $\overline{H}_0 = \frac{\hat{k}_i \times \overline{E}_0}{Z_0}$ one can write

$$\overline{E}^i = \left\{A\left(\hat{k}_i \times \hat{t}\right) + B\hat{t}\right\} e^{ik_0 \hat{k}_i \cdot \bar{r}}$$

and

$$\overline{H}^i = Y_0 \left\{ B \left(\hat{k}_i \times \hat{t} \right) - A\hat{t} \right\} e^{ik_0 \hat{k}_i \cdot \bar{r}}$$

The reflected waves are

$$\overline{E}^r = \left\{ AR_h \left(\hat{k}_r \times \hat{t} \right) + BR_e \hat{t} \right\} e^{ik_0 \hat{k}_r \cdot \bar{r}} \tag{12}$$

$$\overline{H}^r = Y_0 \left\{ BR_e \left(\hat{k}_r \times \hat{t} \right) - AR_h \hat{t} \right\} e^{ik_0 \hat{k}_r \cdot \bar{r}} \tag{13}$$

Where R_e and R_h are the perpendicular and parallel Fresnel reflection coefficients and

$$A = -Z_0 \overline{H}_0 \cdot \hat{t} \qquad B = \overline{E}_0 \cdot \hat{t}$$

Noting that

$$\hat{n} \times \left(\hat{k}_i \times \hat{t} \right) = -\hat{n} \times \left(\hat{k}_r \times \hat{t} \right) = - \left(\hat{n} \cdot \hat{k}_i \right) \hat{t}$$

it can be shown that

$$\hat{n} \times \left(\overline{E}^i + \overline{E}^r \right) = e^{ik_0 \hat{k}_i \cdot \bar{r}} \left\{ Z_0 \left(\overline{H}_0 \cdot \hat{t} \right) \left(\hat{n} \cdot \hat{k}_i \right) (1 - R_h) \, \hat{t} + \left(\overline{E}_0 \cdot \hat{t} \right) (1 + R_e) \right. \tag{14}$$
$$\left. \left(\hat{n} \times \hat{t} \right) \right\}$$

$$\hat{n} \times \left(\overline{H}^i + \overline{H}^r \right) = e^{ik_0 \hat{k}_i \cdot \bar{r}} \left\{ -Y_0 \left(\overline{E}_0 \cdot \hat{t} \right) \left(\hat{n} \cdot \hat{k}_i \right) (1 - R_e) \, \hat{t} + \left(\overline{H}_0 \cdot \hat{t} \right) (1 + R_h) \right. \tag{15}$$
$$\left. \left(\hat{n} \times \hat{t} \right) \right\}$$

Substituting (14) and (15) into (7) and (8) the explicit form for the scattered fields are obtained and are given by

$$\overline{E}_s^j(\bar{r}) = \frac{ik_j e^{ik_j r}}{4\pi r} \left(\bar{\bar{I}} - \hat{k}_s^j \hat{k}_s^j \right) \cdot \iint_s \overline{C}_j \left(f_x, f_y \right) e^{i(k_0 \hat{k}_i - k_j \hat{k}_s^j) \cdot \bar{r}'} dx' dy' \tag{16}$$

with $j = 0$ or 1 and

$$\overline{C}_j \left(f_x, f_y \right) = \sqrt{1 + f_x^2 + f_y^2} (-1)^j \left\{ - (\overline{E}_0 \cdot \hat{t}) \left[\frac{Z_j}{Z_0} \left(\hat{n} \cdot \hat{k}_i \right) (1 - R_e) + \left(\hat{n} \cdot \hat{k}_s^j \right) \right. \right. \tag{17}$$
$$\left. \left. (1 + R_e) \right] \hat{t} \right.$$
$$+ \left(Z_j \overline{H}_0 \cdot \hat{t} \right) (1 + R_h) \left(\hat{n} \times \hat{t} \right) + \left(Z_0 \overline{H}_0 \cdot \hat{t} \right) \left(\hat{n} \cdot \hat{k}_i \right) (1 - R_h) \left(\hat{k}_s^j \times \hat{t} \right) \}$$

It should be noted that equation (16) is not specific to rough surfaces and can be applied to compute the scattered field from any arbitrary dielectric scatterer[1] where the limit of

[1] 1

the integral is over the lit region. In derivation of (16) we used the following relationship as well

$$ds' = \frac{dxdy}{(\hat{n} \cdot \hat{z})} = \sqrt{1 + f_x^2 + f_y^2}\; dxdy.$$

The Kirchhoff integrals (7) and (8) are valid when the surface slopes are relatively small and/or medium 1 is lossy as these integrals do not account for the shadowing effects and re-entry of the transmitted rays back to region 0. Figure 2 depicts the shadowing and ray re-entry effects that are more significant at near grazing incidence angles. Ray re-entry contribution is the dominant surface field component, in the absence of multiple scattering, over the shadowed areas.

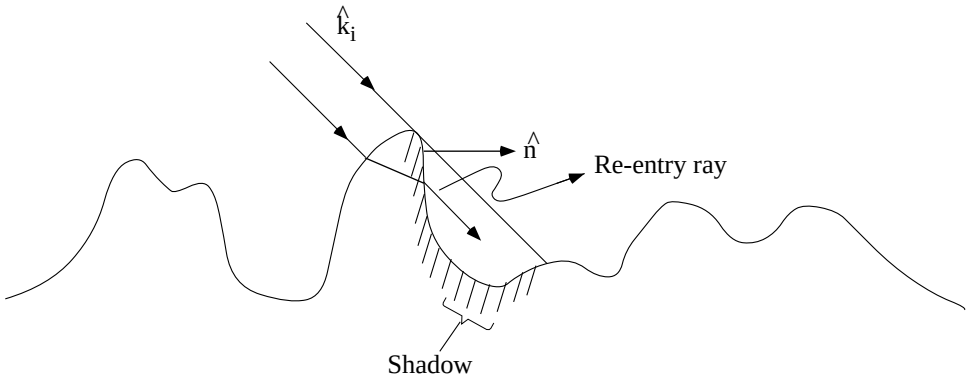

Figure 2: Surface with shadow region due to $\hat{k}_i$ showing re-entry ray effects.

As the surface height profile varies, the scattered field quantities given by (7) and (8) vary accordingly. Assuming that the illuminated area of the rough surface is large compared to the wavelength, it is expected that the number of scattering points on the surface that contribute to the scattered field is statistically large. In this case, according to the central limit theorem, the statistics of the scattered fields are Gaussian. Hence a complete description of the field statistics can be obtained once the first and second moments of the scattered fields are characterized. The scattered field in each region may be written as

$$\overline{E}_s^j(\bar{r}) = \langle \overline{E}_{sco}^j(\bar{r}) \rangle + \overline{E}_{sinco}^j(\bar{r}) \tag{18}$$

where $\langle \overline{E}_{sco}^j(\bar{r}) \rangle$ is the mean scattered field which will be referred to as the coherent term and $\overline{E}_{sinco}^j(\bar{r})$ is the fluctuating component of the scattered field which will be referred to as the incoherent component of the scattered field. It is obvious that

$$\langle \overline{E}_{sinco}^j(\bar{r}) \rangle = 0 \tag{19}$$

and that the total scattered power is proportional to

$$\langle|\overline{E}_s^j(\bar{r})|^2\rangle = |\langle\overline{E}_{sco}^j(\bar{r})\rangle|^2 + \langle|\overline{E}_{sinco}^j(\bar{r})|^2\rangle \tag{20}$$

To compute (20) further approximation must be used. Two standard approximate solutions for (20) are based on small slope expansion and stationary phase method which are respectively known as the Physical Optics approximation and Geometric Optics approximation.

1.1 Physical Optics Approximation

In this method, the coefficient in the integrand (16) is expanded in terms of its Taylor series around zero slope, i.e.,

$$\overline{C}_j(f_x, f_y) \simeq \overline{C}_j(0,0) + \frac{\partial\overline{C}_j}{\partial f_x}|_{f_x=f_y=0} f_x + \frac{\partial\overline{C}_j}{\partial f_y}|_{f_x=f_y=0} f_y + \cdots \tag{21}$$

If the surface roughness is a gentle function of position, only the first term of (21) is sufficient to provide an approximate solution. Retaining only the first term of (21), (16) is reduced to

$$\overline{E}_j(\bar{r}) = \frac{ik_j e^{ik_j r}}{4\pi r}\left(\bar{\bar{I}} - \hat{k}_s^j\hat{k}_s^j\right)\cdot\overline{C}_j(0,0)I^j \tag{22}$$

where

$$I^j = \iint_A e^{i(k_0\hat{k}_i - k_j\hat{k}_s^j)\cdot\bar{r}'}dx'dy' \tag{23}$$

In this approximation only I is stochastic and the coherent and incoherent scattered powers are proportional to $|\langle I^j\rangle|^2$ and $\langle|I^j|^2\rangle - |\langle I^j\rangle|^2$ respectively. These can be calculated directly once the statistics of the height profile is known. For many natural rough surfaces a stationary Gaussian process is an accurate description of the surface roughness statistics. Assuming $Z = f(x,y)$ is a zero-mean Gaussian process, then for any arbitrary number of points (x_m, y_m), $f_m s$ are jointly Gaussian. For two arbitrary points (x_1, y_1) and (x_2, y_2) the joint probability density function is given by

$$P(f_1, f_2) = \frac{1}{2\pi\sigma^2\sqrt{1-C^2}} e^{\frac{-\left[f_1^2 - 2Cf_1f_2 + f_2^2\right]}{2\sigma^2(1-C^2)}} \tag{24}$$

where σ is the rms height of the surface and $C = C(x_1, y_1; x_2, y_2)$ is the correlation coefficient between the two points. For a surface with azimuthal symmetry C is only a function of radial distance between the two points, that is,

$$C(x_1, y_1; x_2, y_2) = C(\sqrt{(x_1 - x_2)^2 + (y_1 - y_2)^2}) = C(\rho)$$

C is basically the normalized auto correlation function of the process which is defined by

$$\langle f(x_1, y_1) f(x_2, y_2) \rangle = \sigma^2 C(x_1, y_1; x_2, y_2)$$

Rewriting (23) as

$$I^j = \int_A \int_A e^{i(\nu_x^j x' + \nu_y^j y')} e^{i\nu_z^j f(x', y')} \, dx' dy' \tag{25}$$

where

$$\bar{\nu}^j = \nu_x^j \hat{x} + \nu_y^j \hat{y} + \nu_z^j \hat{z} = k_0 \hat{k}_i - k_j \hat{k}_s^j \tag{26}$$

the mean value of I can be computed from

$$\langle I^j \rangle = \int_{-L_x}^{L_x} \int_{-L_y}^{L_y} e^{i(\nu_x^j x' + \nu_y^j y')} \langle e^{i\nu_z^j f(x', y')} \rangle dx' dy' \tag{27}$$

where it is assumed that the lit area is a rectangle with dimensions $2L_x \times 2L_y$. Noting $\langle e^{i\nu_z^j f(x', y')} \rangle$ is the characteristic function of Gaussian process f, we have

$$\langle e^{i\nu_z^j f(x', y')} \rangle = e^{-\frac{1}{2}\sigma^2 (\nu_z^j)^2} \tag{28}$$

In view of (28)

$$\langle I^j \rangle = 4 L_x L_y \mathrm{sinc}(\nu_x^j L_x) \mathrm{sinc}(\nu_y^j L_y) e^{-\frac{1}{2}\sigma^2 (\nu_z^j)^2}$$

Allowing L_x and L_y to become very large and noting that

$$\lim_{L_x \to \infty} L_x \mathrm{sinc}(\nu_x^j L_x) = \pi \delta(\nu_x^j).$$

It can easily be shown that

$$|\langle I^j \rangle|^2 = 4\pi^2 A \, e^{-(\nu_z^j)^2 \sigma^2} \delta(\nu_x^j) \delta(\nu_y^j) \tag{29}$$

Equation (29) indicates that the coherent scattered field exist only for scattering direction k_s^j where $\nu_x^j = \nu_y^j = 0$.

For region 0 we have

$$\hat{x} \cdot (\hat{k}_i - \hat{k}_s^0) = \hat{y} \cdot (\hat{k}_i - \hat{k}_s^0) = 0$$

or

$$\begin{aligned} \sin\theta_i \cos\phi_i &= \sin\theta_s^0 \cos\phi_s^0 \\ \sin\theta_i \sin\phi_i &= \sin\theta_s^0 \sin\phi_s^0 \end{aligned}$$

which has the solution $\theta_s^0 = \pi - \theta_i, \phi_s^0 = \phi_s^i$. In other words, the coherent field exist only in the specular (with respect to the mean flat surface with $\hat{n} = \hat{z}$) direction in region 0 for which $\nu_z^0 = 2k_0 \cos\theta_i$. In a similar manner it can be shown that the coherent field in region 1 exists only along the transmitted field for a planar interface for which $\nu_z^1 = k_0 \left(\cos\theta_i - \sqrt{\left(\frac{k_1}{k_0}\right)^2 - \sin^2\theta_i} \right)$. From (29) it can be shown that the surface roughness modifies the surface reflectivity of the mean flat surface ($|R_{e,h}|^2$) by a factor $e^{-4(k_0\cos\theta_i)^2\sigma^2}$ and its transmissivity ($|T_{e,h}|^2$) by $e^{-k_0^2\left(\cos\theta_i - \sqrt{\left(\frac{k_1}{k_0}\right)^2 - \sin^2\theta_i}\right)^2 \sigma^2}$.

To calculate the incoherent scattered power, the integral for $\langle |I|^2 \rangle$ must first be calculated

$$\langle |I^j|^2 \rangle = \iint\limits_A \iint\limits_A e^{i[\nu_x^j(x_1 - x_2) + \nu_y^j(y_1 - y_2)]} \langle e^{i\nu_z^j(f(x_1,y_1) - f(x_2,y_2))} \rangle dx_1 dx_2 dy_1 dy_2 \qquad (30)$$

Any linear transformation on a jointly Gaussian random vector would produce a jointly Gaussian random vector. In other words, if $\overline{W} = (W_1, W_2, \cdots W_n)$ is Gaussian, then $\overline{U} = \overline{\overline{A}}\, \overline{W}$ is jointly Gaussian where $\overline{\overline{A}}$ is an $(m \times n)$ matrix. The covariance of $\overline{U}(\overline{\overline{\Lambda}}_v)$ in terms of $\overline{\overline{\Lambda}}_w$ is simply obtained from

$$\overline{\overline{\Lambda}}_u = \overline{\overline{A}} \Lambda_w \overline{\overline{A}}^t$$

where $\overline{\overline{A}}^{\rm t}$ is the transpose of $\overline{\overline{A}}$. Hence $f(x_1, y_1) - f(x_2, y_2)$ is a Gaussian random variable with variance $2\sigma^2[1 - C(\rho)]$ and characteristic function

$$\langle e^{i\nu_z^j(f(x_1,y_1) - f(x_2,y_2))} \rangle = e^{-\sigma^2(1 - C(\rho))(\nu_z^j)^2} \qquad (31)$$

where as before $\rho = \sqrt{(x_1 - x_2)^2 + (y_1 - y_2)^2}$ for a surface with statistical azimuthal symmetry. In view of (31) the integrand of (30) is a function of difference variables and can be simplified through a change of variables: $x = x_1 - x_2, x' = x_2$ (a similar change of variables is performed for y_1 and y_2). With this change of variables $x_1 = x + x'$ and $x_2 = x'$ which has a Jacobian of unity, however, the limits of the integral must be changed as shown in Figure 3. Actually the area of the square can be covered by first integrating along the line of constant x where the integrand is constant. The integrand along x is proportional to the length of constant x line confined within the space as shown in Figure 3.

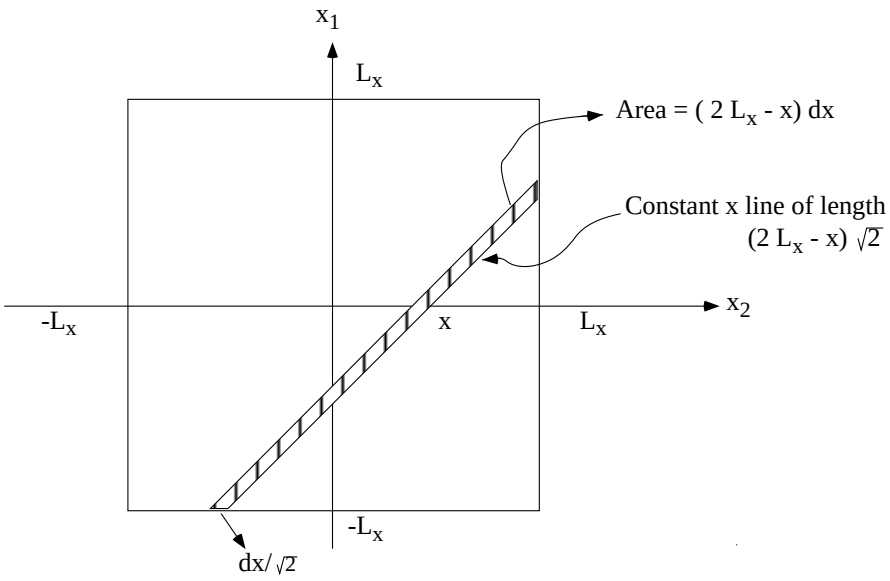

Figure 3: Geometry of area over which the integrand of (30) is carried out and the associated change of variables.

Therefore (30) can now be written as

$$\begin{aligned}\langle |I^j|^2 \rangle &= \int_{-2L_x}^{2L_x} dx \int_{-2L_y}^{2L_y} dy (2L_x - |x|)(2L_y - |y|) \\ &\quad \times e^{i[\nu_x^j x + \nu_y^j y]} e^{-\sigma^2 (1 - C(\rho))(\nu_z^j)^2}\end{aligned} \tag{32}$$

Using a similar change of variables $|\langle I^j \rangle|^2$ can be written as

$$|\langle I^j \rangle|^2 = \int_{-2L_x}^{2L_x} dx \int_{-2L_y}^{2L_y} dy (2L_x - |x|)(2L_y - |y|) \times e^{i(\nu_x^j x + \nu_y^j y)} e^{-\sigma^2 (\nu_z^j)^2} \tag{33}$$

Subtracting (33) from (32)

$$\begin{aligned}\langle |I^j|^2 \rangle - \left| \langle I^j \rangle \right|^2 &= \int_{-2L_x}^{2L_x} dx \int_{-2L_y}^{2L_y} (2L_x - |x|)(2L_y - |y|) \\ &\quad \times e^{i(\nu_x^j x + \nu_y^j y)} \left[e^{-\sigma^2 (1 - C(\rho))(\nu_z^j)^2} - e^{-\sigma^2 (\nu_z^j)^2} \right]\end{aligned} \tag{34}$$

Allowing L_x and L_y to become very large, it can be shown that

$$\lim_{L_x \to \infty} (2L_x - |x|) \sim 2L_x$$

for $|x| \ll L_x$. Considering the fact that the term in the bracket vanishes quickly as x increases, (34) can be simplified to:

$$\langle |I^j|^2 \rangle - |\langle I^j \rangle|^2 = A \iint_{-\infty}^{+\infty} \left[e^{-\sigma^2(1-C(\rho))(\nu_z^j)^2} - e^{-\sigma^2(\nu_z^j)^2} \right] e^{i(\nu_x^j x + \nu_y^j y)} dx dy \tag{35}$$

Making a change of variables $\nu_x^j = \nu_\rho^j \cos\delta, \nu_y^j = \nu_\rho^j \sin\delta$ and $x = \rho\cos\phi, y = \rho\sin\phi$ and noting that

$$\int_0^{2\pi} e^{i\nu_\rho^j \rho \cos(\phi - \delta)} d\phi = 2\pi J_0(\nu_\rho^j \rho)$$

where J_o is the Bessel function of the first kind and zeroth order, (35) reduces to

$$\langle |I^j|^2 \rangle - |\langle I^j \rangle|^2 = 2\pi A \int_0^\infty \rho J_0(\nu_\rho^j \rho) \left[e^{-\sigma^2(1-C(\rho))(\nu_z^j)^2} - e^{-\sigma^2(\nu_z^j)^2} \right] d\rho \tag{36}$$

In general the integral in (36) must be evaluated numerically, however, in some special cases the integral can be transformed into an infinite series. Consider the Taylor series expansion

$$e^{-\sigma^2(\nu_z^j)^2} \left[e^{\sigma^2(\nu_z^j)^2 C(\rho)} - 1 \right] = e^{-\sigma^2(\nu_z^j)^2} \sum_{m=1}^{\infty} \frac{(\sigma\nu_z^j)^{2m}}{m!} C^m(\rho)$$

If the normalized surface correlation function is Gaussian, that is,

$$C(\rho) = e^{-\rho^2/\ell^2}$$

where ℓ is known as the correlation length, and using the identity

$$\int_0^\infty \rho J_0(\nu_\rho^j \rho) e^{-m\rho^2/\ell^2} d\rho = \frac{\ell^2}{2m} e^{-\frac{(\nu_\rho^j \ell)^2}{4m}},$$

then (36) takes the following form:

$$\langle |I^j|^2 \rangle - |\langle I^j \rangle|^2 = \pi A e^{-(\sigma\nu_z^j)^2} \sum_{m=1}^{\infty} \frac{(\sigma\nu_z^j)^{2m} \ell^2}{m(m!)} e^{-\frac{(\nu_\rho^j \ell)^2}{4m}} \tag{37}$$

In cases where convergence of (37) is poor, for large values of m, it is recommended that Sterling's formula be used for $m!$, that is for $m > 10$, $m! \simeq m^m e^{-m}\sqrt{2\pi m}$. We are now in a position to calculate the backscattering coefficients. We need to evaluate $(\overline{\overline{I}} - \hat{k}_s^j \hat{k}_s^j) \cdot \overline{C}_j(0,0)$ where in (17) $\hat{n} = \hat{z}, \hat{t} = \frac{\hat{k}_i \times \hat{z}}{|\hat{k}_i \times \hat{z}|} = \hat{h}_i, R_e = R_e(\theta_i)$, and $R_h = R_h(\theta_i)$ must be substituted. To evaluate σ_{hh}^o and σ_{vh}^o, $\overline{E}_o$ is set parallel to $\hat{h}_i$ and $\overline{C}_j(0,0)$ will be

denoted by $\overline{C}_j^h$. It is obvious that σ_{hh}^o and σ_{vh}^o are proportional to $|\hat{h}_s^j \cdot \overline{C}_j^h|^2$ and $|\hat{v}_s^j \cdot \overline{C}_j^h|^2$ respectively. After some simple algebraic manipulations it can be shown that

$$\hat{h}_s^j \cdot \overline{C}_j^h = (-1)^{j+1} \left[\frac{Z_j}{Z_0} \cos\theta_i (1 - R_e(\theta_i)) + \cos\theta_s^j (1 + R_e(\theta_i)) \right] \cos(\phi_s^j - \phi_i) \quad (38)$$

$$\hat{v}_s^j \cdot \overline{C}_j^h = (-1)^{j+1} \left[\frac{Z_j}{Z_0} \cos\theta_i (1 - R_e(\theta_i)) + \cos\theta_s^j (1 + R_e(\theta_i)) \right] \cos\theta_s^j \sin(\phi_s^j - \phi_i) \quad (39)$$

Similarly $\hat{h}_s^j \cdot \overline{C}_j^v$ and $\hat{v}_s^j \cdot \overline{C}_j^v$ are needed to compute σ_{hv}^o and σ_{vv}^o where $\overline{C}_j^v$ is $\overline{C}_j(0,0)$ when the incident field is parallel to $\hat{v}_i$. The explicit expressions are given by

$$\hat{h}_s^j \cdot \overline{C}_j^v = (-1)^j \left[\frac{Z_j}{Z_0} (1 + R_h(\theta_i)) + \cos\theta_i \cos\theta_s^j (1 - R_h(\theta_i)) \right] \sin(\phi_s^j - \phi_i) \quad (40)$$

$$\hat{v}_s^j \cdot \overline{C}_j^v = (-1)^j \left[-\frac{Z_j}{Z_0} (1 + R_h(\theta_i)) \cos\theta_s^j - \cos\theta_i (1 - R_h(\theta_i)) \right] \cos(\phi_s^j - \phi_i) \quad (41)$$

Therefore the following expressions for the bistatic scattering coefficients are obtained

$$\sigma_{pq}^o(\theta_s^j, \phi_s^j; \theta_i, \phi_i) = \frac{|k_j|^2 Z_0}{4\pi Z_j} |\hat{p}_s^j \cdot \overline{C}_j^q|^2 D \qquad p, q \in \{v, h\} \quad (42)$$

where $\hat{p}_s^j$ can be either $\hat{v}_s^j$ or $\hat{h}_s^j$ and q can be v or h and

$$D = \left[\langle |I^j|^2 \rangle - |\langle I^j \rangle|^2 \right] / A \quad (43)$$

Also the covariance between the scattered field elements are given by

$$\langle S_{pq} S_{p'q'}^* \rangle^o = \frac{|k_j|^2 Z_0}{(4\pi)^2 Z_j} (\hat{p}_s^j \cdot \overline{C}_j^q)(\hat{p}_s'^j \cdot \overline{C}_j^q)^* D \quad p, q, p', q' \in \{v, h\} \quad (44)$$

1.2 Geometrical Optics Approximation

The small slope approximation which resulted in the P.O. solution may be too restrictive. Another approach for evaluating the statistical behavior of (16) is an approximation in the limit as the wavelength compared to the radii of curvature at any points approaches zero. Under this approximation the involved integrals can be evaluated using the stationary phase approximation. Although the stationary phase approximation does not put any restriction on the surface slope, the surface slopes still have to be moderate as (16) does not account for the effects of multiple scattering and shadowing.

Since $\overline{C}_j(f_x, f_y)$ is a relatively slowly varying function of position and the exponential phase varies rapidly (k_0 is large) as x' and y' change, the contribution of the integrand to the overall integral comes from the points near the stationary phase point. The stationary phase points for the scattered field in region 0 are obtained from:

$$\frac{\partial}{\partial x'}\left[\bar{\nu}^j \cdot \bar{r}'\right] = 0 \ , \ \frac{\partial}{\partial y'}\left[\bar{\nu}^j \cdot \bar{r}'\right] = 0 \tag{45}$$

Recalling that $\bar{\nu}^j = k_0\hat{k}_i - k_j\hat{k}_s^j$ and $\bar{r}' = x'\hat{x} + y'\hat{y} + f(x', y')\hat{z}$ at stationary point

$$f_x^s = -\frac{\nu_x^j}{\nu_z^j} \ ; \ f_y^s = -\frac{\nu_y^j}{\nu_z^j} \tag{46}$$

The unit normal to the surface at the stationary phase point (in region 0), using (46) in (3), is found to be

$$\hat{n}_0^s = \frac{\nu_x^0\hat{x} + \nu_y^0\hat{y} + \nu_z^0\hat{z}}{\sqrt{(\nu_x^0)^2 + (\nu_y^0)^2 + (\nu_z^0)^2}} = \frac{\hat{k}_s - \hat{k}_i}{|\hat{k}_i - \hat{k}_s|} \tag{47}$$

Equation (47) clearly indicates that the stationary points are those points on the surface where the observation direction is in the local plane of incidence and along the specular direction. Evaluating $\overline{C}_j(f_x, f_y)$ at the stationary phase points, (16) becomes

$$E_s^j(\bar{r}) = \frac{ik_j e^{ik_j r}}{4\pi r}(\bar{\bar{I}} - k_s^j\hat{k}_s^j) \cdot \overline{C}_j(f_x^s, f_y^s) I^j \tag{48}$$

where I^j is the same integral defined by (23).

Since in the G.O. approximation $k_0\sigma >> 1$, according to (29), the coherent scattered power is negligible at incidence angles away from grazing incidence. The second moments of the scattered fields are proportional to $\langle |I^j|^2 \rangle$ which is given by

$$\langle |I^j|^2 \rangle = \langle \int_A \int_A e^{i\left[\nu_x^j(x-x') + \nu_y^j(y-y') + \nu_z^j(f(x,y) - f(x',y'))\right]} dx dx' dy dy' \rangle \tag{49}$$

Since $\bar{\nu}^j$ is proportional to k, $\bar{\xi}^j = \bar{\nu}^j/k_j$ is independent of frequency. Expanding $f(x', y')$ in terms of its Taylor series around $x = x'$ and $y = y'$

$$f(x', y') = f(x, y) + f_x(x - x') + f_y(y - y') + \cdots$$

and using a change of variables

$$\begin{aligned} u &= k_j(x - x') \\ v &= k_j(y - y') \end{aligned}$$

(49) can be written as

$$\langle |I^j|^2 \rangle = \left\langle \frac{1}{k_j^2} A \iint e^{i\left[(\xi_x^j + f_x\xi_z^j)u + (\xi_y^j + f_y\xi_z^j)v + \frac{1}{k_j}(\cdots)\right]} du dv \right\rangle$$

As $k_j \to \infty$ only the first two terms of the integrand exponent remain. Therefore

$$\langle |I^j|^2 \rangle = \frac{4\pi^2 A}{k_j^2} \langle \delta(\xi_x^j + f_x\xi_z^j)\delta(\xi_y^j + f_y\xi_z^j) \rangle \tag{50}$$

Knowing the joint probability density function of the surface slopes ($P(f_x, f_y)$), (50) can be evaluated readily. In fact

$$\langle |I^j|^2 \rangle = \frac{4\pi^2 A}{(\nu_z^j)^2} P\left(-\frac{\nu_x^j}{\nu_z^j}, -\frac{\nu_y^j}{\nu_z^j}\right) \tag{51}$$

For a Gaussian process $f(x, y)$, f_x and f_y, which are obtained from $f(x, y)$ using a linear operation, are jointly Gaussian. Since $f(x, y)$ is zero-mean

$$f_x = \lim_{\Delta x \to 0} \frac{f(x + \Delta x, y) - f(x, y)}{\Delta x}$$

and

$$f_y = \lim_{\Delta y \to 0} \frac{f(x, y + \Delta y) - f(x, y)}{\Delta y}$$

are also zero-mean. It can easily be shown that $\langle f_x f_y \rangle = 0, \langle f_x^2 \rangle = \langle f_y^2 \rangle = \sigma^2 |C''(0)|$ and therefore

$$P(f_x, f_y) = \frac{1}{2\pi\sigma^2 |C''(0)|} e^{-\frac{f_x^2 + f_y^2}{2\sigma^2 |C''(0)|}} \tag{52}$$

Using (52) in (51), we have

$$\langle |I^j|^2 \rangle = \frac{2\pi A}{(\nu_z^j)^2 \sigma^2 |C''(0)|} e^{-\frac{(\nu_x^j)^2 + (\nu_y^j)^2}{2(\nu_z^j)^2 \sigma^2 |C''(0)|}} \tag{53}$$

To evaluate the backscattering coefficients $\overline{C}_j^h$ and $\overline{C}_j^v$ must be evaluated (where $\overline{C}_j^h$ is the value of $\overline{C}_j$ for $\bar{h}_i$ incident polarization and $\overline{C}_j^v$ is the value of $\overline{C}_j$ for $\hat{v}_i$ incident polarization). When the observation point is in region 0

$$\begin{aligned}
\hat{t} &= \tfrac{\hat{k}_i \times \hat{n}_0^s}{|\hat{n}_o^s \times \hat{k}_i|} \quad , \qquad \hat{n}_o^s = \frac{\hat{k}_s^0 - \hat{k}_i}{|\hat{k}_s^0 - \hat{k}_i|} \\
\hat{t} \cdot \hat{h}_i &= -\tfrac{(\hat{n}_0^s \cdot \hat{v}_i)}{|n_0^s \times k_i|} \quad , \qquad \hat{t} \cdot \hat{h}_s = -\frac{\hat{n}_0^s \cdot \hat{v}_s}{|\hat{k}_0^s \times \hat{k}_i|} \\
\hat{t} \cdot \hat{v}_i &= \tfrac{(n_0^s \cdot \hat{h}_i)}{|n_0^s \times \hat{k}_i|} \qquad\qquad \hat{t} \cdot \hat{v}_s = \frac{\hat{n}_0^s \cdot \hat{h}_s}{|\hat{n}_0^s \times \hat{k}_i|}
\end{aligned}$$

After some tedious algebra it can be shown that

$$\begin{aligned}
\overline{C}_0^h &= \frac{2\ (\hat{n}_0^s \cdot \hat{k}_i) k_0 |\hat{k}_s^0 - \hat{k}_i|}{|\hat{k}_s^0 \times \hat{k}_i|^2 |\nu_z^0|} \Big\{ \Big[(\hat{v}_i \cdot \hat{k}_s^0)(\hat{h}_s \cdot \hat{k}_i) R_e - (\hat{h}_i \cdot \hat{k}_s^0)(\hat{v}_s \cdot \hat{k}_i) R_h \Big] \hat{v}_s \qquad (54) \\
&\quad - \Big[(\hat{v}_i \cdot \hat{k}_s^0)(\hat{v}_s \cdot \hat{k}_i) R_e + (\hat{h}_i \cdot \hat{k}_s^0)(\hat{h}_s \cdot \hat{k}_i) R_h \Big] \hat{h}_s - \frac{1}{2} (\hat{h}_i \cdot \hat{k}_s^0)(1 + \hat{k}_s^0 \cdot \hat{k}_i)(1 + R_h) \hat{k}_s^0 \Big\} \\
\overline{C}_0^v &= \frac{2\ (\hat{n}_0^s \cdot \hat{k}_i) k_0 |\hat{k}_s^0 - \hat{k}_i|}{|\hat{k}_s^0 \times \hat{k}_i|^2 |\nu_z^0|} \Big\{ - \Big[(\hat{v}_i \cdot \hat{k}_s^0)(\hat{v}_s \cdot \hat{k}_i) R_h + (\hat{h}_i \cdot \hat{k}_s^0)(\hat{h}_s \cdot \hat{k}_i) \Big] \hat{v}_s \qquad (55) \\
&\quad + \Big[-(\hat{v}_i \cdot \hat{k}_s^0)(\hat{h}_s \cdot \hat{k}_i) R_h + (\hat{h}_i \cdot \hat{k}_s^0)(\hat{v}_s \cdot \hat{k}_i) R_e \Big] \hat{h}_s - \frac{1}{2} (\hat{v}_i \cdot \hat{k}_s^0)(1 + \hat{k}_s^s \cdot \hat{k}_i)(1 + R_h) \hat{k}_s^0 \Big\}
\end{aligned}$$

Here R_e and R_h are evaluated at $\theta = \cos^{-1}\left(-\hat{n}_0^s \cdot \hat{k}_i\right)$.

In the special case of backscattering ($\phi_s = \pi + \phi_i, \theta = \pi - \theta_i$) where $\hat{k}_s^0 = -\hat{k}_i$ in the denominator of (54) and (55) the cross product $\hat{k}_s^0 \times \hat{k}_i = 0$, however, at the same time the numerator also goes to zero. To determine the values of $\overline{C}_0^h$ and $\overline{C}_0^v$ in the backscatter direction, we first calculate these quantities at $\theta_i = \theta, \theta_s = \theta + \Delta\theta$ and then let $\Delta\theta \to 0$, that is,

$$\begin{aligned}
\lim_{\Delta\theta \to 0} \frac{(\hat{v}_i \cdot \hat{k}_s^0)(\hat{h}_s \cdot \hat{k}_i)}{|\hat{k}_s^0 \times \hat{k}_i|^2} &= 0 \\
\lim_{\Delta\theta \to 0} \frac{(\hat{h}_i \cdot \hat{k}_s^0)(\hat{v}_s \cdot \hat{k}_i)}{|\hat{k}_s^0 \times \hat{k}_i|^2} &= 0 \\
\lim_{\Delta\theta \to 0} \frac{(\hat{v}_i \cdot \hat{k}_s^0)(\hat{v}_s \cdot \hat{k}_i)}{|\hat{k}_s^0 \times \hat{k}_i|^2} &= 1
\end{aligned}$$

$$\lim_{\Delta\theta\to 0}\frac{(\hat{h}_i\cdot\hat{k}_s^0)(\hat{h}_s\cdot\hat{k}_i)}{|\hat{k}_s^0\times\hat{k}_i|^2}=0$$
$$\lim_{\Delta\theta\to 0}\frac{(\hat{h}_i\cdot\hat{k}_s^0)(1+\hat{k}_s^0\cdot\hat{k}_i)}{|\hat{k}_s^0\times\hat{k}_i|^2}=0$$
$$\lim_{\Delta\theta\to 0}\frac{(\hat{v}_i\cdot\hat{k}_s^0)(1+\hat{k}_s^0\cdot\hat{k}_i)}{|\hat{k}_s^0\times\hat{k}_i|^2}=0$$

Furthermore, noting that in the backscatter direction $\hat{n}_0^s\cdot|\hat{k}_s^0-\hat{k}_i|=2$ and $|\nu_z^0|=2k_0|\cos(\theta_i)|$, we have

$$\overline{C}_0^h=-\frac{2}{|\cos(\theta_i)|}R_e\hat{h}_s \tag{56}$$
$$\overline{C}_0^v=-\frac{2}{|\cos(\theta_i)|}R_e\hat{v}_s \tag{57}$$

Using (54) and (55) the bistatic scattering coefficients and the covariance between the scattered field elements can be obtained. For q-polarized transmit wave ($\hat{q}=\hat{v}_i$ or $\hat{h}_i$) and p-polarized receive antenna the bistatic scattering coefficient is given by

$$\sigma_{pq}^0(\theta_s^0,\phi_s^0;\theta_i,\phi_i)=\frac{k_0^2}{2(\nu_z^0)^2\sigma^2|C''(0)|}|\hat{p}_s\cdot\overline{C}_0^q|^2e^{-\frac{(\nu_x^0)^2+(\nu_y^0)^2}{2(\nu_z^0)^2\sigma^2|C''(0)|}} \tag{58}$$

where $\hat{p}_s=\hat{v}_s$ or $\hat{h}_s$. Also the bistatic field covariance is given by:

$$\langle S_{pq}S_{p'q'}^*\rangle^o = \frac{k_0^2}{8\pi(\nu_z^o)^2\sigma^2|C''(0)|}(\hat{p}_s\cdot\overline{C}_o^q)(\hat{p}_s'\cdot\overline{C}_o^{q'})^*\left(e^{-\frac{(\nu_x^o)^2+(\nu_y^o)^2}{2(\nu_z^o)^2\sigma^2|C''(0)|}}\right) \tag{59}$$

It should be noted that (58) is a special case of (59) since

$$\sigma_{pq}^o=4\pi\langle S_{pq}S_{pq}^*\rangle^o$$

Equation (56) clearly demonstrates that the bistatic scattering coefficient is independent of frequency as expected for geometric optics approximation.

To calculate the bistatic scattering coefficients when the observation point is in region 1, we note that at the stationary point (see (46))

$$\hat{n}_1^s=\frac{k_1\hat{k}_s^1-k_0\hat{k}_i}{|k_1\hat{k}_s^1-k_0\hat{k}_i|} \tag{60}$$

At this point the k-vectors satisfy the phase matching condition, i.e.

$$k_o(\hat{k}_i - (\hat{n}_1^s \cdot \hat{k}_i)\hat{n}_1^s) = k_1(\hat{k}_s^1 - (\hat{n}_1^s \cdot \hat{k}_s^1)\hat{n}_1^s) \tag{61}$$

which can be shown directly from (58). In other words, stationary phase points on the surface are those points where $\hat{k}_i, \hat{k}_s^1$, and $\hat{n}$ are in the same plane and $\hat{k}_s^1$ is along the transmitted ray from region 0 to 1. Using a similar procedure it can be shown that

$$\begin{aligned}
\overline{C}_1^h &= \frac{2(\hat{n}_1^s \cdot \hat{k}_s^1)k_1|\hat{k}_s^1 - \frac{k_o}{k_1}\hat{k}_i|}{|\hat{k}_s^1 \times \hat{k}_i|^2|\nu_z^1|} \Big\{ \Big[(\hat{v}_i \cdot \hat{k}_s^1)(\hat{h}_s \cdot \hat{k}_i)(1+R_e) - (\hat{h}_i \cdot \hat{k}_s^1)(\hat{v}_s \cdot \hat{k}_i) \\
&\quad \cdot \frac{Z_1}{Z_o}(1+R_h)\Big]\hat{v}_s - \Big[(\hat{v}_i \cdot \hat{k}_s^1)(\hat{v}_s \cdot \hat{k}_i)(1+R_e) + (\hat{h}_i \cdot \hat{k}_s^1)(\hat{h}_s \cdot \hat{k}_i)\frac{Z_1}{Z_0} \\
&\quad (1+R_h)]\,\hat{h}_s + \frac{1}{2}(\hat{h}_i \cdot \hat{k}_s^1)(1+R_h)\frac{Z_1}{Z_0}[(\hat{h}_s \cdot \hat{k}_i)(\hat{h}_s \cdot \hat{n}_s^1) + (\hat{v}_s \cdot \hat{k}_i)(\hat{v}_s \cdot \hat{n}_s^1)]\hat{k}_s^1 \Big\}
\end{aligned}$$

$$\begin{aligned}
\overline{C}_1^v &= \frac{2(\hat{n}_1^s \cdot \hat{k}_s^1)k_1|\hat{k}_s^1 - \frac{k_0}{k_1}\hat{k}_i|}{|\hat{k}_s^1 \times \hat{k}_i|^2|\nu_z^1|} \Big\{ - \Big[(\hat{h}_i \cdot \hat{k}_s^1)(\hat{h}_s \cdot \hat{k}_i)(1+R_e) + \\
&\quad (\hat{v}_i \cdot \hat{k}_s^1)(\hat{v}_s \cdot \hat{k}_i)\frac{Z_1}{Z_0}(1+R_h)\,]\,\hat{v}_s + \Big[-(\hat{h}_i \cdot \hat{k}_s^1)(\hat{v}_s \cdot \hat{k}_i)(1+R_e) \\
&\quad + (\hat{v}_i \cdot \hat{k}_s^1)(\hat{h}_s \cdot \hat{k}_i)\frac{Z_1}{Z_0}(1+R_v)\,]\,\hat{h}_s + \frac{1}{2}(\hat{v}_i \cdot \hat{k}_s^1)(1+R_h)\frac{Z_1}{Z_0}[(\hat{h}_s \cdot \hat{k}_i)(\hat{h}_s \cdot \hat{n}_s^1) + (\hat{v}_s \cdot \hat{k}_i)(\hat{v}_s \cdot \hat{n}_s^1)]\hat{k}_s^1 \Big\}
\end{aligned}$$

where the explicit form of the reflection coefficients are

$$\begin{aligned}
R_e &= \frac{k_0(\hat{n}_1^s \cdot \hat{k}_i) - k_1(\hat{n}_1^s \cdot \hat{k}_s^1)}{k_0(\hat{n}_1^s \cdot \hat{k}_i) + k_1(\hat{n}_1^s \cdot \hat{k}_s^1)} \\
R_h &= \frac{\epsilon_1 k_0(\hat{n}_1^s \cdot \hat{k}_i) - \epsilon_0 k_1(\hat{n}_1^s \cdot \hat{k}_s^1)}{\epsilon_1 k_0(\hat{n}_1^s \cdot \hat{k}_i) + \epsilon_0 k_1(\hat{n}_1^s \cdot \hat{k}_s^1)}
\end{aligned}$$

2 Small Perturbation Method

Perturbation method is a powerful mathematical tool for complex electromagnetic problems. This method is usually useful for boundary-value problems where there are small variations on a parameter, such as the permittivity or permeability of the medium or the boundary conditions, that influences the solution. In this procedure the solution of the unperturbed problem must be known. By expanding the fluctuating parameter and the

unknowns in terms of a power series of the perturbation factor, an iterative solution can be obtained. In the context of the electromagnetic scattering from rough surfaces with small surface roughness parameters, the fluctuating parameter is the boundary between the two homogeneous media. The unperturbed problem is the problem of plane wave reflection and transmission between two homogeneous media with a planar interface for which an exact solution exist. Two methods will be presented in this chapter: 1) based on the expansion of surface fields using the extinction theorem, and 2) based on the expansion of the volumetric currents induced in the top rough layer. The second method is appropriate for rough surfaces with inhomogeneous dielectric profiles as will be shown later.

2.1 Extended Boundary Condition Method

The problem of electromagnetic scattering from a metallic rough surface was first treated by Rice [3]. More advanced techniques based on the extended boundary condition for dielectric surfaces were later developed by Nieto-Vesprian [9] and Agarwal[5]. The method described here is based on the extended boundary condition for two homogeneous dielectric media with a slightly rough interface and closely follows the procedure outlines by Tsang, et al [6]. In the following section a recently developed approach based on polarization current will be discussed.

The geometry of the problem is the same as the one shown in Figure 1. In this case it is assumed that the height profile and its derivatives are small compared to the wavelength. As before we assume the height profile is deterministic in order to formulate the scattering problem. The extended boundary condition establishes a relationship between the surface fields and the scattered and incident fields in each region. Denoting the surface height profile by $\Delta f(x,y)$ where Δ is a small scalar quantity, we have

$$\begin{aligned} \overline{E}_i(\overline{r}) \quad + \quad & \iint_s \left[ik_0 Z_0 \, \overline{\overline{G}}_0 \, (\overline{r},\overline{r}') \cdot (\hat{n} \times \overline{H}(\overline{r}')) + \nabla \times \overline{\overline{G}}_0 \, (\overline{r},\overline{r}') \cdot (\hat{n} \times \overline{E}(\overline{r}')) \right] ds' \\ = \quad & \begin{cases} \overline{E}_0(\overline{r}) & z > \Delta f_{max} \qquad (1) \\ 0 & z < \Delta f_{min} \qquad (2) \end{cases} \end{aligned}$$

$$\begin{aligned} - \quad & \iint_s \left[ik_1 Z_1 \, \overline{\overline{G}}_1 \, (\overline{r},\overline{r}') \cdot (\hat{n} \times \overline{H}(\overline{r}')) + \nabla \times \overline{\overline{G}}_1 \, (\overline{r},\overline{r}') \cdot (\hat{n} \times \overline{E}(\overline{r}')) \right] ds' \\ = \quad & \begin{cases} 0 & z > \Delta f_{max} \qquad (3) \\ \overline{E}_1(\overline{r}) & z < \Delta f_{min} \qquad (4) \end{cases} \end{aligned}$$

where $\hat{n}$ is the unit normal to the surface pointing towards region 0 and f_{min} and f_{max} refer to the minimum and maximum of $f(x,y)$, and $\overline{\overline{G}}_j \, (\overline{r},\overline{r}')$ is the free-space dyadic

Green's function for region j. The inclusion of the multiplicative factor Δ in the expression for height profile is for keeping track of scattered fields which are produced by the perturbed surface. In the equations above, we have used the fact that $\hat{n} \times \overline{E}(\overline{r}')$ and $\hat{n} \times \overline{H}(\overline{r}')$ are continuous across the dielectric boundary and thus no subscript is assigned to them.

Calculations of the unknown surface fields is accomplished through simulataneous application of equations (2) and (3). In (2) the Fourier representation of the dyadic Green's function given by

$$\bar{\bar{G}}_0\ (\overline{r}, \overline{r}') = \frac{i}{(8\pi)^2} \iint \frac{1}{k_{0z}} \left[\hat{e}(-k_{0z}) \hat{e}(-k_{0z}) + \hat{h}(-k_{0z}) \hat{h}(-k_{0z}) \right] e^{i(\overline{k}_\perp - k_{0z}\hat{z}) \cdot (\overline{r} - \overline{r}')} dk_x dk_y \tag{5}$$

and its curl ($\nabla \times \bar{\bar{G}}_o\ (\overline{r}, \overline{r}')$) given by

$$\begin{aligned} \nabla \times \bar{\bar{G}}_0\ (\overline{r}, \overline{r}') &= \nabla g \times \bar{\bar{I}} \\ &= \frac{i}{(8\pi)^2} \iint i \frac{\overline{K}_0}{k_{0z}} \times \bar{\bar{I}}\ e^{i\overline{K}_o \cdot (\overline{r} - \overline{r}')} dk_x dk_y \end{aligned}$$

or simply

$$\nabla \times \bar{\bar{G}}_0\ (\overline{r}, \overline{r}') = \frac{-1}{8\pi^2} \int_{-\infty}^{+\infty} \int 1/k_{0z} \left[-\hat{h}(-k_{0z}) \hat{e}(-k_{0z}) + \hat{e}(-k_{0z}) \hat{h}(-k_{0z}) \right] e^{i(\overline{k}_\perp - k_{0z}\hat{z}) \cdot (\overline{r} - \overline{r}')} dk_x dk_y \tag{6}$$

will render an equation suitable from the perturbation analysis where plane waves are used as the basis functions for the unknown surface fields.

Similar expression for $\bar{\bar{G}}_1\ (\overline{r}, \overline{r}')$ and $\nabla \times \bar{\bar{G}}_1\ (\overline{r}, \overline{r}')$ can be obtained by replacing the subscript 0 with 1 in (5) and (6). For simplicity of equations, instead of defining the surface fields $(\hat{n} \times \overline{E})$ and $(\hat{n} \times \overline{H})$ as the unknown, we define a new set of unknown vectors

$$\overline{a}(\overline{r}'_\perp) = \frac{\hat{n} \times \overline{H}(\overline{r}')}{(\hat{n} \cdot \hat{z})} \tag{7}$$

$$\overline{b}(\overline{r}'_\perp) = \frac{\hat{n} \times \overline{E}(\overline{r}')}{(\hat{n} \cdot \hat{z})} \tag{8}$$

Substituting (5), (6), (7) and (8) into (2) and (3) the following coupled integral equations are obtained:

$$\begin{aligned}\overline{E}_i(\overline{r}) &= \frac{-1}{8\pi^2}\iint dk_x dk_y e^{i(\overline{K}_0\cdot\overline{r})}\frac{1}{k_{oz}}\iint e^{-i\overline{k}_\perp\cdot\overline{r}'_\perp}e^{ik_{0z}\Delta f(x',y')}\left\{k_0 Z_0\left[\hat{e}(-k_{0z})\hat{e}(-k_{0z})\right.\right. \\ &+ \left.\left.\hat{h}(-k_{0z})\hat{h}(-k_{0z})\right]\cdot\overline{a}(\overline{r}'_\perp)+i\left[-\hat{h}(-k_{0z})\hat{e}(-k_{0z})+\hat{e}(-k_{0z})\hat{h}(-k_{0z})\right]\cdot\overline{b}(\overline{r}'_\perp)\right\}dx'dy' \end{aligned} \tag{9}$$

$$\begin{aligned}0 &= \frac{-1}{8\pi^2}\iint dk_x dk_y e^{i(\overline{k}_1\cdot\overline{r})}\frac{1}{k_{1z}}\iint e^{-i\overline{k}_\perp\cdot\overline{r}'_\perp}e^{ik_{1z}\Delta f(x',y')}\left\{k_1 Z_1\left[\hat{e}(k_{1z})\hat{e}(k_{1z})\right.\right. \\ &+ \left.\left.\hat{h}(k_{1z})\hat{h}(k_{1z})\right]\cdot\overline{a}(\overline{r}'_\perp)+i\left[-\hat{h}(k_{1z})\hat{e}(k_{1z})+\hat{e}(k_{1z})\hat{h}(k_{1z})\right]\cdot\overline{b}\,(\overline{r}'_\perp)\right\}dx'dy' \end{aligned} \tag{10}$$

It should be emphasized that the three components of $\overline{a}(\overline{r}'_\perp)$ and $\overline{b}(\overline{r}'_\perp)$ are not independent since

$$\hat{n}\cdot\overline{a}(\overline{r}'_\perp)=\hat{n}\cdot\overline{b}(\overline{r}'_\perp)=0$$

In fact

$$a_z(\overline{r}'_\perp) = \Delta(f_x(\overline{r}'_\perp)\hat{x}+f_y(\overline{r}'_\perp)\hat{y})\cdot\overline{a}(\overline{r}'_\perp) \tag{11}$$

$$b_z(\overline{r}'_\perp) = \Delta(f_x(\overline{r}'_\perp)\hat{x}+f_y(\overline{r}'_\perp)\hat{y})\cdot\overline{b}(\overline{r}'_\perp) \tag{12}$$

In the limit as $\Delta\to 0$ the surface roughness disappears and the surface fields approach those of a flat surface denoted by $\overline{a}_o(\overline{r}'_\perp)$ and $\overline{b}_o(\overline{r}'_\perp)$. When Δ is sufficiently small the surface fields may be expanded by convergent series given:

$$\overline{a}(\overline{r}'_\perp) = \sum_{m=0}^{\infty}\frac{\overline{a}_m(\overline{r}'_\perp)}{m!}\Delta^m \tag{13}$$

$$\overline{b}(\overline{r}'_\perp) = \sum_{m=0}^{\infty}\frac{\overline{b}_m(\overline{r}'_\perp)}{m!}\Delta^m \tag{14}$$

where $\overline{a}_m$ and $\overline{b}_m$ are referred to as the mth-order solution. In the integral equations (9) and (10), $\overline{r}'$ is on the surface, that is, $\overline{r}'=\overline{r}'_\perp+\Delta f(x',y')\hat{z}$ which makes the integrand a function of $f(x',y')$. Using the Taylor series expansion we have

$$e^{\pm ik_{jz}\Delta f(x',y')}=\sum_{m=0}^{\infty}\frac{(\pm ik_{jz}f(x',y'))^m}{m!}\Delta^m \quad j=0,1 \tag{15}$$

Substituting (13) and (14) in (11) and (12) and requiring that f_x and f_y be of the same order as the function itself, that is, with a high probability f_x/f and f_y/f are not large quantities, $a_{zm}(\overline{r}'_\perp)$ can be related to $\overline{a}_{(m-1)}(\overline{r}'_\perp)$ as follows

$$a_{zm}(\overline{r}'_\perp) = m(f_x(\overline{r}'_\perp)\hat{x}+f_y(\overline{r}'_\perp)\hat{y})\cdot\overline{a}_{(m-1)}(\overline{r}'_\perp)\ . \tag{16}$$

$$b_{zm}(\overline{r}'_\perp) = m(f_x(\overline{r}'_\perp)\hat{x}+f_y(\overline{r}'_\perp)\hat{y})\cdot\overline{b}_{(m-1)}(\overline{r}'_\perp)\ . \tag{17}$$

with m is a non-negative integer. In other words we require that the surface slope be moderate.

Note that to the zeroth order in $\Delta, \hat{n} = \hat{z}$ and surface fields do not have $\hat{z}$ components, i. e.,

$$a_{zo}(\overline{r}'_\perp) = b_{z0}(\overline{r}'_\perp) = 0 \ .$$

Now substituting (13), (14), and (15) in (9) and (10) and noting that

$$\overline{E}_i(\overline{r}) = \hat{p}_i e^{i\overline{k}^i_\perp \cdot \overline{r}_\perp} e^{-ik^i_z z} = \hat{p}_i \iint_{-\infty}^{+\infty} dk_x dk_y e^{i\overline{K}_0 \cdot \overline{r}} \delta(\overline{k}_\perp - \overline{k}^i_\perp)$$

we have

$$\hat{p}_i \iint_{-\infty}^{+\infty} dk_x dk_y \delta(\overline{k}_\perp - \overline{k}^i_\perp) e^{i\overline{K}_0 \cdot \overline{r}} = \frac{-1}{8\pi^2} \iint_{-\infty}^{+\infty} dk_x dk_y e^{i\overline{K}_0 \cdot \overline{r}} \frac{1}{k_{0z}} \left\{ \iint dx' dy' \right. \tag{18}$$
$$\left. \times e^{-i\overline{k}_\perp \cdot \overline{r}'_\perp} \sum_{m=0}^{\infty} \sum_{m'=0}^{\infty} \frac{(ik_{oz} f(x', y'))^m}{m! m'!} \left[\overline{\overline{Q}}_0^- \cdot \overline{a}_{m'}(\overline{r}'_\perp) + \overline{\overline{P}}_0^- \cdot \overline{b}_{m'}(\overline{r}'_\perp) \right] \Delta^{m+m'} \right\}$$

where $\overline{\overline{Q}}_0^-$ and $\overline{\overline{P}}_0^-$ are given by

$$\overline{\overline{Q}}_0^{\pm} = k_0 Z_0 \left[\hat{e}(\pm k_{0z}) \hat{e}(\pm k_{0z}) + \hat{h}(\pm k_{0z}) \hat{h}(\pm k_{0z}) \right] \tag{19}$$

$$\overline{\overline{P}}_0^{\pm} = i \left[-\hat{h}(\pm k_{0z}) \hat{e}(\pm k_{0z}) + \hat{e}(\pm k_{0z}) \hat{h}(\pm k_{0z}) \right] \tag{20}$$

Recognizing the expression in $\{ \quad \}$ of equation (18) as a 2-D Fourier transform, the following equation is obtained after performing the Fourier transform

$$\sum_{m=0}^{\infty} \sum_{m'=0}^{\infty} \frac{-i(ik_{0z})^{m-1}}{(2m!)(m'!)} \left[\overline{\overline{Q}}_0^- \cdot \otimes^m F(\overline{k}_\perp) * \tilde{a}_{m'}(\overline{k}_\perp) + \overline{\overline{P}}_0^- \cdot \otimes^m F(\overline{k}_\perp) * \tilde{b}_{m'}(\overline{k}_\perp) \right] \Delta^{m+m'} \tag{21}$$
$$= \hat{p}_i \delta(\overline{k}_\perp - \overline{k}^i_\perp)$$

where $F(\overline{k}_\perp)$ is the Fourier transform of $f(x, y)$ and $\tilde{a}_{m'}(\overline{k}_\perp)$ and $\tilde{b}_{m'}(\overline{k}_\perp)$ are also Fourier transform of $\overline{a}_{m'}(\overline{r}'_\perp)$ and $\tilde{b}_{m'}(r'_\perp)$. The symbols $*$ denotes the convolution operation and $\otimes^m$ denotes the m-fold self-convolution

$$\otimes^m F = \frac{1}{(4\pi^2)^{m-1}} \overbrace{F * F * \cdots * F}^{m}$$

with a definition $\otimes^0 F = 1/(4\pi)^2$. Similarly from (10) we have

$$\sum_{m=0}^{\infty}\sum_{m'=0}^{\infty}\frac{-i(ik_{1z})^{m-1}}{2(m!)(m'!)}\left[\bar{\bar{Q}}_1^{+}\cdot\otimes^m F(\overline{k}_\perp)*\tilde{a}_{m'}(\overline{k}_\perp)+\bar{\bar{P}}_1^{+}\cdot\otimes^m F(\overline{k}_\perp)*\tilde{b}_{m'}(\overline{k}_\perp)\right]\Delta^{m+m'}=0 \tag{22}$$

where $\bar{\bar{Q}}_1^{+}$ and $\bar{\bar{P}}_1^{+}$ are given by (19) and (20) with subscripts 0 replaced by 1 and $-k_{0z}$ to k_{1z}. Since (21) and (22) must be valid for all values of Δ, then the coefficients of equal powers of Δ on both sides of the equations must be equal. For the zeroth-order solution ($m = m' = 0$) the following vector equations are obtained:

$$\frac{-1}{8\pi^2 k_{0z}}\left[\bar{\bar{Q}}_0^{-}\cdot\tilde{a}_0(\overline{k}_\perp)+\bar{\bar{P}}_0^{-}\cdot\tilde{b}_0(\overline{k}_\perp)\right] = \hat{p}_i\delta(\overline{k}_\perp-\overline{k}_\perp^i) \tag{23}$$

$$\left[\bar{\bar{Q}}_1^{+}\cdot\tilde{a}_0(\overline{k}_\perp)+\bar{\bar{P}}_1^{+}\cdot\tilde{b}_0(\overline{k}_\perp)\right] = 0 \tag{24}$$

Since $\tilde{a}_{z0}(\overline{k}_\perp)$ and $\tilde{b}_{z0}(\overline{k}_\perp)$ are zero, (23) and (24) constitute 4 equations for the 4 unknowns $\tilde{a}_{\perp 0}$ and $\tilde{b}_{\perp 0}$. Once $\tilde{a}_0(\overline{k}_\perp)$ and $\tilde{b}_0(\overline{k}_\perp)$ are obtained the higher order solutions can be derived in a recursive manner. It can easily be shown that the m-th order solution ($m > 0$) in terms of the lower order solutions is given by

$$\begin{aligned}\bar{\bar{Q}}_j\cdot\tilde{a}_m(\overline{k}_\perp)+\bar{\bar{P}}_j\cdot\tilde{b}_m(\overline{k}_\perp) &= -4\pi^2\sum_{\ell=1}^{m}\binom{m}{\ell}(ik_{jz})^\ell[\bar{\bar{Q}}_j\cdot\otimes^\ell F(\overline{k}_\perp)*\tilde{a}_{(m-\ell)}(\overline{k}_\perp)\\ &\quad+\bar{\bar{P}}_j\cdot\otimes^\ell F(\overline{k}_\perp)*\tilde{b}_{(m-\ell)}(\overline{k}_\perp)]\end{aligned} \tag{25}$$

where $j = 0$ or 1 and $\binom{m}{\ell}$ is the binomial coefficient. Equation (25) constitutes 2 vector equations (one for $j = 0$ and one for $j = 1$) which together with

$$a_{mz}(\overline{k}_\perp) = im\overline{k}_\perp\cdot F(\overline{k}_\perp)*\tilde{a}_{(m-1)}(\overline{k}_\perp) \tag{26}$$

$$b_{mz}(\overline{k}_\perp) = im\overline{k}_\perp\cdot F(\overline{k}_\perp)*\tilde{b}_{(m-1)}(\overline{k}_\perp), \tag{27}$$

obtained from (16) and (17), provide a total of 6 scalar equations for the six unknown quantities.

Once the surface fields to any desired order are calculated from (25)-(27), equations (1) and (4) will be used to derive the scattered field in each region. When $z > \Delta f_{max}$

$$\begin{aligned}\overline{E}_s(\overline{r}) = -\frac{1}{8\pi^2}\iint dk_x dk_y e^{i\overline{k}_0\cdot\overline{r}}\frac{1}{k_{0z}}\iint e^{-i\overline{k}_\perp\cdot\overline{r}'_\perp}e^{-ik_{0z}f(x',y')}\\ \left\{k_0 Z_0\left[\hat{e}(k_{0z})\hat{e}(k_{0z})+\hat{h}(k_{0z})\hat{h}(k_{0z})\right]\cdot\overline{a}(\overline{r}_\perp)+\right.\\ \left.i\left[-\hat{h}(k_{0z})\hat{e}(k_{0z})+\hat{e}(k_{0z})\hat{h}(k_{0z})\right]\cdot\overline{b}(\overline{r}_\perp)\right\}dx'dy'\end{aligned} \tag{28}$$

and when $z < \Delta f_{min}$

$$\begin{aligned}\overline{E}_1(\overline{r}) = \frac{-1}{8\pi^2}\iint dk_x dk_y e^{i\overline{K}_1\cdot\overline{r}}\frac{1}{k_{1z}}\iint e^{-i\overline{k}_\perp\cdot\overline{r}'}e^{ik_{1z}f(x',y')} \\ \{K_1 Z_1\left[\hat{e}(-k_{1z})\hat{e}(-k_{1z})+\hat{h}(-k_{1z})\hat{h}(-k_{1z})\right]\cdot\overline{a}(\overline{r}_\perp) \\ + i\left[-\hat{h}(-k_{1z})\hat{e}(-k_{1z})+\hat{e}(-k_{1z})\hat{h}(-k_{1z})\right]\cdot\overline{b}(\overline{r}_\perp)\Big\}\,dx'dy'\end{aligned} \tag{29}$$

Following a similar procedure as outlined for deriving (21), (28) and (29) can be, respectively, written in terms of their perturbation expansion as

$$\begin{aligned}\overline{E}_0^s(\overline{r}) &= \frac{-1}{2}\iint_{-\infty}^{+\infty} dk_x dk_y e^{i\overline{k}_0\cdot\overline{r}}\frac{1}{k_{0z}}\sum_{m=0}^{\infty}\sum_{m'=0}^{\infty}\frac{(ik_{0z})^m}{m!m'!}\Big[\overline{\overline{Q}}_0^{+}\cdot\otimes^m F(\overline{k}_\perp)*\tilde{a}_{m'}(\overline{k}_\perp) \\ &\quad + \overline{\overline{P}}_0^{+}\cdot\otimes^m F(\overline{k}_\perp)*\tilde{b}_{m'}(\overline{k}_\perp)\,\Big]\Delta^{m+m'}\end{aligned} \tag{30}$$

$$\begin{aligned}\overline{E}_1^s(\overline{r}) &= \frac{-1}{2}\iint_{+\infty}^{-\infty} dk_x dk_y e^{i\overline{K}_1\cdot\overline{r}}\frac{1}{k_{1z}}\sum_{m=0}^{\infty}\sum_{m'=0}^{\infty}\frac{(ik_{1z})^m}{m!m'!}\Big[\overline{\overline{Q}}_1^{-}\cdot\otimes^m F(\overline{k}_\perp)*\tilde{a}_{m'}(\overline{k}_\perp) \\ &\quad + \overline{\overline{P}}_1^{-}\cdot\otimes^m F(\overline{k}_\perp)*\tilde{b}_{m'}(\overline{k}_\perp)\,\Big]\Delta^{m+m'}\end{aligned} \tag{31}$$

We are now in a position to derive the explicit expressions for the scattered fields. The starting point is equations (23) and (24). A convenient way of solving (23) and (24) is to express $\tilde{a}_o(\overline{k}_\perp)$ and $\tilde{b}_o(\overline{k}_\perp)$ in a Cartesian coordinate system composed of $\hat{z}, \hat{q} = \hat{e}(k_z^i)$, and $\hat{t}$ which is perpendicular to $\hat{z}$ and $\hat{q}$, that is,

$$\begin{aligned}\tilde{a}(\overline{k}_\perp) &= a_q(\overline{k}_\perp)\hat{q} + a_t(\overline{k}_\perp)\hat{t} + a_z(\overline{k}_\perp)\hat{z} \\ \tilde{b}(\overline{k}_\perp) &= b_q(\overline{k}_\perp)\hat{q} + b_t(\overline{k}_\perp)\hat{t} + b_z(\overline{k}_\perp)\hat{z}\end{aligned} \tag{32}$$

where

$$\begin{aligned}\hat{q} &= \frac{\hat{k}_i\times\hat{z}}{|\hat{k}_i\times\hat{z}|} \\ \hat{t} &= \hat{z}\times\hat{q}\end{aligned} \tag{33}$$

After some algebraic manipulations

$$
\begin{aligned}
a_{0q}(\overline{k}_\perp) &= \frac{k_z^i}{k_0 Z_0}\left[\hat{e}(-k_z^i)\cdot\hat{p}_i\right](1-R_h(\theta_i))4\pi^2\delta(\overline{k}_\perp-\overline{k}_\perp^i) \\
a_{0t}(\overline{k}_\perp) &= \frac{1}{Z_0}\left[\hat{h}(-k_z^i)\cdot\hat{p}_i\right](1+R_v(\theta_i))4\pi^2\delta(\overline{k}_\perp-\overline{k}_\perp^i) \\
b_{0q}(\overline{k}_\perp) &= -ik_0k_z^i\left[\hat{h}(-k_z^i)\cdot\hat{p}_i\right](1-R_v(\theta_i))4\pi^2\delta(\overline{k}_\perp-\overline{k}_\perp^i) \\
b_{0t}(\overline{k}_\perp) &= ik_0\left[\hat{e}(-k_z^i)\cdot\hat{p}_i\right](1+R_h(\theta_i))4\pi^2\delta(\overline{k}_\perp-\overline{k}_\perp^i)
\end{aligned} \tag{34}
$$

where R_h and R_v are the Fresnel reflection coefficients for TE and TM waves evaluated at the incidence angle θ_i. Substituting (34) into (30) and (31) the zeroth-order scattered fields ($m = m' = 0$) are given by

$$
\begin{aligned}
\overline{E}_s^{(0)}(\overline{r}) &= \left\{R_h(\theta_i)\left[\hat{e}(-k_z^i)\cdot\hat{p}_i\right]\hat{e}(k_z^i)+R_v(\theta_i)\left[\hat{h}(-k_z^i)\cdot\hat{p}_i\right]\hat{h}(k_z^i)\right\} \\
&\quad\times e^{i(\overline{k}_\perp^i\cdot\overline{r}_\perp+ik_z^iz)}
\end{aligned} \tag{35}
$$

$$
\begin{aligned}
\overline{E}_1^{(0)}(\overline{r}) &= \Bigg\{(1+R(\theta_i))\left[\hat{e}(-k_z^i)\cdot\hat{p}_i\right]\hat{e}(-k_z^i)+\frac{k_0}{k_1}(1+R_v(\theta_i))\left[\hat{h}(-k_z^i)\cdot\hat{p}_i\right] \\
&\quad\times\hat{h}(-k_{1z}^i)\ \Bigg\}\, e^{i(\overline{k}_\perp^1\cdot\overline{r}_\perp-ik_{1z}^iz)}
\end{aligned} \tag{36}
$$

Derivation of the first order solution is more involved. Starting from (26) and (27) with $m = 1$, we find

$$
a_{1z}(\overline{k}_\perp) = i\left[\frac{k_xk_{yi}-k_yk_{xi}}{k_{\rho i}}a_{oq}(\overline{k}_\perp^i)+\left(\frac{k_xk_{xi}+k_yk_{yi}}{k_{\rho i}}-k_{\rho i}\right)a_{0t}(\overline{k}_\perp^i)\right]\times F(\overline{k}_\perp-\overline{k}_\perp^i) \tag{37}
$$

$$
b_{1z}(\overline{k}_\perp) = i\left[\frac{k_xk_{yi}-k_yk_{xi}}{k_{\rho i}}b_{0z}(\overline{k}_\perp)+\left(\frac{k_xk_{xi}+k_yk_{yi}}{k_{\rho i}}-k_{\rho i}\right)b_{0q}(\overline{k}_\perp^i)\right]\times F(\overline{k}_\perp-\overline{k}_\perp^i) \tag{38}
$$

where $k_{\rho i} = \sqrt{k_{xi}^2+k_{yi}^2}$. Now using (25), $a_{1q}(\overline{k}_\perp), a_{1t}(\overline{k}_\perp), b_{1q}(\overline{k}_\perp)$, and $b_{1t}(\overline{k}_\perp)$ can be obtained. Using (30) with $m = 1, m' = 0$ and $m = 0, m' = 1$ the first-order scattered field is given by:

$$
\begin{aligned}
\overline{E}_s^{(1)}(\overline{r}) &= -\frac{\Delta}{8\pi^2}\iint_{-\infty}^{+\infty}dk_xdk_ye^{i\overline{k}_0\cdot\overline{r}}\left\{\frac{1}{k_{0z}}\left[\overline{\overline{Q}}_o^{+}(k_{0z})\cdot\tilde{a}_1(\overline{k}_\perp)+\overline{\overline{P}}_0^{+}(k_{oz})\cdot\tilde{b}_1(\overline{k}_\perp)\right]\right. \\
&+ \left. i\left[\overline{\overline{Q}}_0^{+}(k_{oz})\cdot\tilde{a}_0(\overline{k}_\perp^i)+\overline{\overline{P}}_0^{+}(k_{0z})\cdot\tilde{b}_0(\overline{k}_\perp^i)\right]F(\overline{k}_\perp-\overline{k}_\perp^i)\ \right\}
\end{aligned} \tag{39}
$$

It is found that $\tilde{a}_1(\overline{k}_\perp)$ and $\tilde{b}_1(\overline{k}_1)$ are linearly proportional to $F(\overline{k}_\perp - \overline{k}^i_\perp)$ and noting that

$$\langle F(\overline{k}_\perp - \overline{k}^i_\perp)\rangle = \iint dx'dy' e^{i(\overline{k}_\perp - \overline{k}^i_\perp)\cdot\overline{r}'_\perp}\langle f(x',y')\rangle = 0,$$

then it is obvious that the mean scattered field is zero, i.e.,

$$\langle \overline{E}^{(1)}_s\rangle = 0 \tag{40}$$

In a similar manner, the mean value of the first-order transmitted field is zero,

$$\langle \overline{E}^{(1)}_1\rangle = 0 \tag{41}$$

Assuming that the perturbation on the surface is confined over a finite region or assuming that the illuminated beam on the surface is finite, the stationary phase approximation can be used to evaluate (39). The stationary phase point is $\overline{k}^s_0 = k_0\cos\phi_s\sin\theta_s\hat{x} + k_0\sin\phi_s\sin\theta_s\hat{y} + k_0\cos\theta_s\hat{z}$ where θ_s and ϕ_s denote the direction of observation. Using the stationary phase approximation we have

$$\begin{aligned}\overline{E}^{(1)}_s(\overline{r}) &\simeq -i\Delta\frac{e^{ik_0 r}}{4\pi r}\left\{\overline{\overline{Q}}^{+}_0(k^s_{0z})\cdot\tilde{a}_1(\overline{k}^s_\perp) + \overline{\overline{P}}^{+}_0(k^s_{0z})\tilde{b}_1(\overline{k}^s_\perp)\right. \\ &+ \left.\left[\overline{\overline{Q}}^{+}_0(k^s_{0z})\cdot\tilde{a}_0(\overline{k}^i_\perp) + \overline{\overline{P}}^{+}_0(k^s_{0z})\tilde{b}_0(\overline{k}^i_\perp)\right]F(\overline{k}^s_\perp - \overline{k}^i_\perp)\right\}\end{aligned} \tag{42}$$

where $k^s_{0z} = k_0\cos\theta_s$ and $\overline{k}^s_\perp$ is $\overline{k}_\perp$ evaluated at the stationary phase point. The only random quantity in (42) is $F(\overline{k}^s_\perp - \overline{k}^i_\perp)$. Noting that the power spectral density of the random process $f(x,y)$ is defined by

$$W(\overline{k}_\perp) = \lim_{A\to\infty}\frac{1}{A}\langle|F(\overline{k}_\perp)|^2\rangle$$

the backscattering coefficients can be computed from (42) and are given by

$$\begin{aligned}\sigma^\circ_{vv}(\hat{k}_s,\hat{k}_i) &= 16\pi k_0^4\cos^2\theta_s\cos^2\theta_i\left|\frac{(k_1^2-k_0^2)}{(k_1^2k^s_z + k_0^2k^s_{1z})(k_1^2k^i_z + k_0^2k^i_{1z})}\right. \\ &\times \left.\left[k_1^2k_0^2\sin\theta_s\sin\theta_i - k_0^2k^s_{1z}k^i_{1z}\cos(\phi_s-\phi_i)\right]\right|^2 W(\overline{k}^s_\perp - \overline{k}^i_\perp) \\ \sigma^\circ_{vh}(\hat{k}_s,\hat{k}_i) &= 16\pi k_0^4\cos^2\theta_s\cos^2\theta_i\left|\frac{(k_1^2-k_0^2)k_0k_{1zs}}{(k_1^2k^s_z + k_0^2k^s_{1z})(k^i_z + k^i_{1z})}\right|^2\sin^2(\phi_s-\phi_i) \\ &\times W(\overline{k}^s_\perp - \overline{k}^i_\perp) \\ \sigma^\circ_{hv}(\hat{k}_s,\hat{k}_i) &= 16\pi k_0^4\cos^2\theta_s\cos^2\theta_i\left|\frac{(k_1^2-k_0^2)k_0k^i_{1z}}{(k^s_z + k^s_{1z})(k_1^2k^i_z + k_0^2k^i_{1z})}\right|^2\sin^2(\phi_s-\phi_i)\end{aligned}$$

$$
\begin{aligned}
& \times \quad W(\overline{k}_{\perp}^{s} - \overline{k}_{\perp}^{i}) \\
\sigma_{hh}^{\circ}(\hat{k}_s, \hat{k}_i) &= 16\pi k_0^4 \cos^2\theta_s \cos^2\theta_i \left| \frac{(k_1^2 - k_o^2)}{(k_z^s + k_{1z}^s)(k_z^i + k_{1z}^i)} \right|^2 \cos^2(\phi_s - \phi_i) \\
& \times \quad W(\overline{k}_{\perp}^{s} - \overline{k}_{\perp}^{i})
\end{aligned}
$$

2.2 Rough Surface with Inhomogeneous Profile: A Volumetric Integral Equation Method

In this section analytical expressions for the bistatic scattering coefficients of soil surfaces with slightly rough interface and stratified permittivity profile are derived [15]. The scattering formulation is based on a new approach where the perturbation expansion of the volumetric polarization current instead of the tangential fields is used to obtain the scattered field. Study of this problem is modivated for its application in radar remote sensing of soil moisture. In nature, most soil surfaces have a non-uniform moisture profile. The soil moisture profile is usually a complex function of soil type, temperature profile, surface evaporation and moisture content [16]. This variations in moisture profile can be translated to variations in the permittivity of a soil medium using the existing empirical dielectric models. In this approach, the top rough layer is replaced with an equivalent polarization current and using the volumetric integral equation in conjunction with the dyadic Green's function of the remaining stratified half-space medium, the scattering problem is formulated.

Closed form analytical expressions for the induced polarization currents to any desired order are derived which are then used to evaluate the bistatic scattered fields up to and including the third order. The analytical solutions for the scattered fields are used to derive the complete second-order expressions for the backscattering coefficients as well as the statistics of phase difference between the scattering matrix elements. In what follows, the theoretical formulation for the scattering problem is given and the closed-form complete second order solution for backscattering coefficients and phase-difference statistics are derived. Then, the theoretical solution will be compared with experimental backscatter measurements of rough surfaces with known dielectric profiles and roughness statistics.

2.2.1 Theoretical Analysis

Consider an inhomogeneous half-space medium with a rough interface as shown in Fig. 1. In the following derivation, it is assumed that the medium is stratified, that is, the relative permittivity is only a function of z, and is given by

$$\epsilon_r(x, y, z) = \epsilon_r(z) \ .$$

Suppose a plane wave is illuminating the rough interface from the upper medium

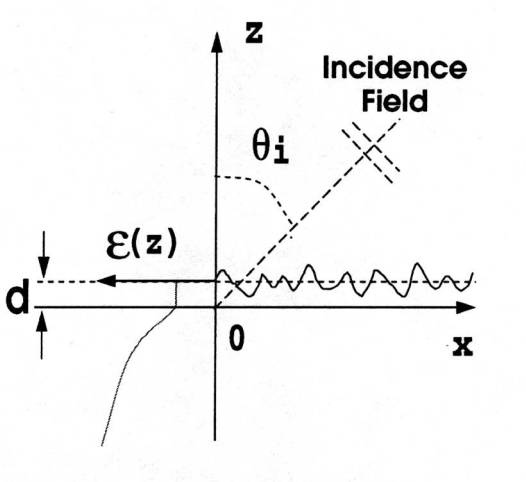

Figure 4: An inhomogeneous half-space medium with a rough interface. Left side of this figure shows the dielectric profile.

and, with a very high probability, the surface height variation is small compared with the wavelength of the incident wave. To make the solution tractable, the permittivity of the top layer down to a depth of d is considered to be uniform, where -d $<$ $min\{$surface profile$\}$. As before, let us denote the surface height profile by a function $z = \triangle f(x, y)$, where $f(x, y)$ is a zero-mean stationary random process with a known autocorrelation function, and $\triangle << \lambda$ is a small constant representing the perturbation parameter. The incident wave can be written as

$$\mathbf{E}^i(\bar{r}) = \mathbf{P}_i \, e^{ik_0 \hat{k}^i \cdot \mathbf{r}} \ ,$$

where $\mathbf{P}_i$ denotes the polarization of the incident wave, $k_0 = \frac{2\pi}{\lambda}$ is the free space propagation constant, and $\hat{k}^i$ is the unit vector along the direction of propagation, given by

$$\hat{k}^i = \sin\theta_i \cos\phi_i \hat{x} + \sin\theta_i \sin\phi_i \hat{y} - \cos\theta_i \hat{z} \ .$$

In the absence of the top homogeneous rough layer (with thickness d), the incident wave would be reflected at the smooth interface between the free space and the inhomogeneous half space soil medium. The reflected wave can be expressed by

$$\mathbf{E}^r(\bar{r}) = \mathbf{P}_r \, e^{ik_0 \hat{k}^r \cdot \mathbf{r}} \ ,$$

where $\hat{k}^r$ is the direction of propagation of the reflected wave, given by

$$\hat{k}^r = \hat{k}^i - 2(\hat{z} \cdot \hat{k}^i)\hat{z} \ ,$$

and $\mathbf{P}_r$ is the polarization vector of the reflected wave, which can be obtained from

$$\mathbf{P}_r = r_v(\mathbf{P}_i \cdot \hat{v}_i)\hat{v}_r + r_h(\mathbf{P}_i \cdot \hat{h}_i)\hat{h}_r \ .$$

Here r_v and r_h are the Fresnel reflection coefficients, and the horizontal and vertical unit vectors are given by

$$\hat{h}_s = \frac{\hat{k}_s \times \hat{z}}{|\hat{k}_s \times \hat{z}|}, \qquad \hat{v}_s = \hat{h}_s \times \hat{k}_s \ , \tag{43}$$

where the subscript s can be i or r for the incident and reflected waves. In presence of the homogeneous rough layer, the incident and reflected waves induce a polarization current within the top dielectric layer which is the source of the scattered field. The polarization current in terms of the total field and the permittivity of the layer is

$$\mathbf{J}(\mathbf{r}) = -ik_0 Y_0(\epsilon - 1)\mathbf{E}^t \ , \tag{44}$$

where $Y_0 = \frac{1}{Z_0}$ is the characteristic admittance of the free space, and

$$\mathbf{E}^t = \mathbf{E}^i + \mathbf{E}^r + \mathbf{E}^s \ .$$

The scattered field $\mathbf{E}^s$ can in turn be expressed in terms of the polarization current and is given by

$$\mathbf{E}^s = ik_0 Z_0 \int\limits_{V_{slab}} \bar{\bar{\mathbf{G}}}(\mathbf{r}, \mathbf{r}') \cdot \mathbf{J}(\mathbf{r}')\, dv' \ , \tag{45}$$

where $\bar{\bar{\mathbf{G}}}(\mathbf{r}, \mathbf{r}')$ is the dyadic Green's function of the half-space inhomogeneous medium (in the absence of the top rough layer). Substituting (45) into (43), the following integral equation for the polarization current can be obtained:

$$\frac{1}{\epsilon - 1}\mathbf{J}(\mathbf{r}) = -ik_0 Y_0(\mathbf{E}^i + \mathbf{E}^r) + k_0^2 \int\limits_{-\infty}^{\infty} \int\limits_{0}^{d+\triangle f(x',y')} \bar{\bar{\mathbf{G}}}(\mathbf{r}, \mathbf{r}') \cdot \mathbf{J}(\mathbf{r}')\, dv' \ . \tag{46}$$

An approximate solution for the integral equation can be obtained using a perturbation technique. By breaking the z' integral into two integrals, one with limits from 0 to d and the other with limits from d to $d + \triangle f(x', y')$, and noting $\triangle f(x', y')$ is a small quantity, up to the Nth order in $\triangle$, (46) can be written as

$$\begin{aligned} \frac{1}{\epsilon - 1}\mathbf{J}(\mathbf{r}) \simeq \quad & -ik_0 Y_0(\mathbf{E}^i + \mathbf{E}^r) + k_0^2 \int\limits_{-\infty}^{\infty} \int\limits_{0}^{d} \bar{\bar{\mathbf{G}}}(\mathbf{r}, \mathbf{r}') \cdot \mathbf{J}(\mathbf{r}')\, dx' dy' dz' \\ & + k_0^2 \sum_{n=0}^{N-1} \int\limits_{-\infty}^{\infty} \frac{[\triangle f(x', y')]^{n+1}}{(n+1)!} \frac{\partial^n}{\partial z'^n} \left\{ \bar{\bar{\mathbf{G}}}(\mathbf{r}, \mathbf{r}'_d) \cdot \mathbf{J}(\mathbf{r}'_d) \right\} dx' dy' \ , \end{aligned} \tag{47}$$

where $\mathbf{r}'_d = x'\hat{x} + y'\hat{y} + d\hat{z}$. Taking the two-dimensional Fourier transform of both sides of (47) and noting that the integrals in x' and y' are of convolution type, it can be shown that

$$\frac{1}{\epsilon - 1}\widetilde{\mathbf{J}}(\mathbf{k}_\perp, z) \ = \ -i4\pi^2 k_0 Y_0 \delta(\mathbf{k}_\perp - \mathbf{k}^i_\perp) \left[\mathbf{P}_i e^{-ik^i_z z} + \mathbf{P}_r e^{ik^i_z z} \right]$$

$$+ \quad k_0^2 \int_0^d \overline{\overline{\mathbf{G}}}\,(\mathbf{k}_\perp; z, z') \cdot \widetilde{\mathbf{J}}(\mathbf{k}_\perp, z')\, dz' + k_0^2 \sum_{n=0}^{N-1} \sum_{m=0}^{n} \frac{\binom{n}{m} \triangle^{n+1}}{(n+1)!}$$

$$\cdot \quad \frac{\partial^m}{\partial z'^m}\, \overline{\overline{\mathbf{G}}}\,(\mathbf{k}_\perp; z, d) \cdot \left[\frac{\partial^{n-m}}{\partial z'^{n-m}} \widetilde{\mathbf{J}}(\mathbf{k}_\perp, d) * \bigotimes^{n+1} F(\mathbf{k}_\perp) \right] \quad , \tag{48}$$

where $*$ is the convolution operator, $F(\mathbf{k}_\perp)$ is the Fourier transform of $f(x', y')$, $\overset{n}{\bigotimes}$ represents n-fold self-convolution ($\overset{n}{\bigotimes} F = \overbrace{F * F * \ldots * F}^{n}$), $k_z^i = k_0 \cos\theta_i$, and $\overline{\overline{\mathbf{G}}}\,(\bar{k}_\perp; z, z')$ is the Fourier transform of the Green's function, given by

$$\begin{aligned} \overline{\overline{\mathbf{G}}}\,(\mathbf{k}_\perp; z, z') &= -\hat{z}\hat{z}\frac{\delta(z-z')}{k_0^2} \\ &+ \frac{i}{2k_z} \begin{cases} \left\{ \left[r_h \hat{h}(k_z) e^{ik_z z} + \hat{h}(-k_z) e^{-ik_z z} \right] \cdot \hat{h}(-k_z) e^{ik_z z'} \right. \\ \left. + \left[r_v \hat{v}(k_z) e^{ik_z z} + \hat{v}(-k_z) e^{-ik_z z} \right] \cdot \hat{v}(-k_z) e^{ik_z z'} \right\} \\ \qquad\qquad z < z', \\ \left\{ \hat{h}(k_z) \left[r_h \hat{h}(-k_z) e^{ik_z z'} + \hat{h}(k_z) e^{-ik_z z'} \right] e^{ik_z z} \right. \\ \left. + \hat{v}(k_z) \left[r_v \hat{v}(-k_z) e^{ik_z z'} + \hat{v}(k_z) e^{-ik_z z'} \right] e^{ik_z z} \right\} \\ \qquad\qquad z > z'. \end{cases} \end{aligned} \tag{49}$$

In (49), $k_z = \sqrt{k^2 - k_x^2 - k_y^2}$, $\mathbf{k}_\perp = k_x\hat{x} + k_y\hat{y}$, and $\hat{h}(\pm k_z)$ and $\hat{v}(\pm k_z)$ can be obtained from (43) with $\hat{k}_s = (k_x\hat{x} + k_y\hat{y} \pm k_z\hat{z})/k_0$.

Since the surface height variations are much smaller than the wavelength ($\triangle << \lambda_0$), the induced polarization current on the top rough layer closely resembles that of a smooth layer with the same dielectric constant and thickness d. Under this assumption, the polarization current may be expanded in terms of a convergent perturbation series in $\triangle$, and is given by

$$\mathbf{J}(\mathbf{r}) = \sum_{n=0}^{\infty} \mathbf{J}_n(\mathbf{r}) \triangle^n \quad , \tag{50}$$

where $\mathbf{J}_0(\mathbf{r})$ is the induced polarization current in the unperturbed layer. Then by substituting this expansion into (48) and collecting terms of equal powers in $\triangle$, a recursive set of equations for the components of the polarization current can be obtained, and is given by

$$\begin{aligned} \frac{1}{\epsilon - 1} \widetilde{\mathbf{J}}_0(\mathbf{k}_\perp, z) &= -i4\pi^2 k_0 Y_0 \delta(\mathbf{k}_\perp - \mathbf{k}_\perp^i) \left[\mathbf{P}_i e^{-ik_z^i z} + \mathbf{P}_r e^{ik_z^i z} \right] \\ &+ k_0^2 \int_0^d \overline{\overline{\mathbf{G}}}\,(\mathbf{k}_\perp; z, z') \cdot \widetilde{\mathbf{J}}_0(\mathbf{k}_\perp, z')\, dz', \end{aligned} \tag{51}$$

$$\frac{1}{\epsilon - 1} \widetilde{\mathbf{J}}_N(\mathbf{k}_\perp, z) = k_0^2 \int_0^d \overline{\overline{\mathbf{G}}}\,(\mathbf{k}_\perp; z, z') \cdot \widetilde{\mathbf{J}}_N(\mathbf{k}_\perp, z')\, dz'$$

$$+ \quad k_0^2 \, \widetilde{\widetilde{\mathbf{G}}} \, (\mathbf{k}_\perp; z, d) \cdot \widetilde{\mathbf{V}}_N \; . \tag{52}$$

Here $\widetilde{\mathbf{V}}_N$ is the source function for the Nth-order integral equation with a closed form representation

$$\widetilde{\mathbf{V}}_N \;=\; \sum_{n=0}^{N-1} \sum_{m=0}^{N-n-1} \frac{\binom{N-n-1}{m} (ik_z)^m}{(N-n)!} \cdot \left[\frac{\partial^{N-n-m-1}}{\partial \, (z')^{N-n-m-1}} \widetilde{\mathbf{J}}_n(\mathbf{k}_\perp, d) \right] * \bigotimes^{N-n} F(\mathbf{k}_\perp) \; .$$

The integral equations so obtained are Fredholm integral equations of the second kind, for which analytical solutions can be obtained. Note that the solution of the zeroth-order equation is the source function for the first-order equation and the Nth-order equation has an excitation function which consists of N-1 lower order polarization currents. To solve (51), let us first split the integral into two integrals : one over the interval $[0, z]$ and the other over the interval $[z, d]$. Extending the integration limits of the second integral over the entire interval $[0, d]$ by adding and subtracting an integral over the interval $[0, z]$ and noting $\hat{h}(k_z) = \hat{h}(-k_z)$, (51) can be written as

$$\begin{aligned}
\frac{1}{\epsilon - 1} \widetilde{\mathbf{J}}_0(\mathbf{k}_\perp, z) \;&=\; -i4\pi^2 k_0 Y_0 \delta(\mathbf{k}_\perp - \mathbf{k}_\perp^i) \; \left[\mathbf{P}_i e^{-ik_z^i z} + \mathbf{P}_r e^{ik_z^i z} \right] - \hat{z}\hat{z} \cdot \widetilde{\mathbf{J}}_0(\mathbf{k}_\perp, z) \\
&+ \; \frac{ik_0^2}{2k_z} \int_0^z \Big\{ \hat{h}(k_z) \hat{h}(k_z) \left[e^{-ik_z(z'-z)} - e^{ik_z(z'-z)} \right] \\
&+ \; \left[\hat{v}(k_z) \hat{v}(k_z) e^{-ik_z(z'-z)} - \hat{v}(-k_z) \hat{v}(-k_z) e^{ik_z(z'-z)} \right] \Big\} \cdot \widetilde{\mathbf{J}}_0(\mathbf{k}_\perp, z') \, dz' \\
&+ \; \frac{ik_0^2}{2k_z} \Big\{ \left[r_h e^{ik_z z} + e^{-ik_z z} \right] \hat{h}(k_z) \hat{h}(k_z) + \left[r_v e^{ik_z z} \hat{v}(k_z) + e^{-ik_z z} \hat{v}(-k_z) \right] \\
&\quad \hat{v}(-k_z) \Big\} \cdot \int_0^d \widetilde{\mathbf{J}}_0(\mathbf{k}_\perp, z') \, dz' \; .
\end{aligned} \tag{53}$$

Noting that the second integral in (53) is a constant function of z and that the first integral is of convolution type in z, (53) is recognized as a vector Volta integral equation that can be solved analytically using the Laplace transformation or Picard's Process of successive approximation [17]. Since the involved integral in (53) is explicit in terms of variable $\mathbf{k}_\perp$, it can be shown that $\widetilde{\mathbf{J}}_0(\mathbf{k}_\perp, z)$ is of the form

$$\widetilde{\mathbf{J}}_0(\mathbf{k}_\perp, z) = (2\pi)^2 \, \delta(\mathbf{k}_\perp - \mathbf{k}_\perp^i) \, \widetilde{\mathbf{J}}_0(z) \, . \tag{54}$$

The polarization current can be decomposed into its principal components, given by

$$\widetilde{\mathbf{J}}_0(z) = J_{0h}(z) \, \hat{h}(k_z^i) + J_{0t}(z) \, \hat{t}(k_z^i) + J_{0z}(z) \, \hat{z} \; , \tag{55}$$

where $\hat{t}(k_z^i) = \hat{z} \times \hat{h}(k_z^i)$. Evaluating the inner product of (53) with $\hat{h}(k_z^i)$, $\hat{t}(k_z^i)$ and $\hat{z}$, three uncoupled scalar Volta integral equations are obtained. Solutions to the resulted integral equations for the three components of the current are of the following form:

$$
\begin{aligned}
J_{0h}(z) &= A_h^0 e^{ik_{1z}^i z} + B_h^0\, e^{-ik_{1z}^i z} \ , \\
J_{0t}(z) &= A_v^0 e^{ik_{1z}^i z} + B_v^0\, e^{-ik_{1z}^i z} \ , \\
J_{0z}(z) &= -\frac{k_\rho^i}{k_{1z}} \left\{ A_v^0\, e^{ik_{1z}^i z} - B_v^0\, e^{-ik_{1z}^i z} \right\} \ . \qquad (56)
\end{aligned}
$$

After a long algebraic manipulation, closed form expressions for the zeroth-order polarization current are obtained

$$
\begin{aligned}
J_{0h}(z) = &\quad -i\, \tfrac{2k_0 k_z^i}{k_z^i + k_{1z}^i} Y_0\, (\epsilon - 1)\ C_0^h(\mathbf{k}^i, z)\ \left[\mathbf{P}_i \cdot \hat{h}(k_z^i) \right]\ e^{-ik_z^i d} \ , \\
J_{0t}(z) = &\quad -i \tfrac{2k_0 k_z^i k_{1z}^i}{k_\rho^i \left(\epsilon k_z^i + k_{1z}^i \right)} Y_0 (\epsilon - 1)\, C_0^v(\mathbf{k}^i, z)\ [\mathbf{P}_i \cdot \hat{z}]\ e^{-ik_z^i d} \ , \\
J_{0z}(z) = &\quad -i \tfrac{2k_0 k_z^i}{\epsilon k_z^i + k_{1z}^i} Y_0 (\epsilon - 1)\, C_1^v(\mathbf{k}^i, z)\ [\mathbf{P}_i \cdot \hat{z}]\ e^{-ik_z^i d} \ ,
\end{aligned}
$$

where

$$
k_{1z}^i = k_0 \sqrt{\epsilon - \sin^2 \theta_i}\ \ k_\rho^i = k_0 \sin\theta_i\ \ R_h^i = \tfrac{k_z^i - k_{1z}^i}{k_z^i + k_{1z}^i}\ \ R_v^i = \tfrac{\epsilon k_z^i - k_{1z}^i}{\epsilon k_z^i + k_{1z}^i}
$$

$$
\begin{aligned}
C_n^h(\mathbf{k}, z) &= \frac{(-1)^n \left(R_h - r_h \right) e^{ik_{1z} z} + \left(R_h r_h - 1 \right) e^{-ik_{1z} z}}{R_h \left(R_h - r_h \right) e^{ik_{1z} d} + \left(R_h r_h - 1 \right) e^{-ik_{1z} d}} \\
C_n^v(\mathbf{k}, z) &= \frac{(-1)^n \left(r_v - R_v \right) e^{ik_{1z} z} + \left(R_v r_v - 1 \right) e^{-ik_{1z} z}}{R_v \left(R_v - r_v \right) e^{ik_{1z} d} + \left(R_v r_v - 1 \right) e^{-ik_{1z} d}} .
\end{aligned}
$$

The source function of (52) can be written as

$$
k_0^2\, \widetilde{\widetilde{\mathbf{G}}}\, (\mathbf{k}_\perp; z, d) \cdot \widetilde{\mathbf{V}}_N = -ik_0 Y_0 \left(\mathbf{q}_{Ni} e^{-ik_z z} + \mathbf{q}_{Nr} e^{ik_z z} \right) \ , \qquad (57)
$$

where

$$
\begin{aligned}
\mathbf{q}_{Ni} &= \frac{-Z_0 k_0}{2k_z} e^{ik_z d} \cdot \left\{ \left(\hat{h}(k_z) \cdot \widetilde{\mathbf{V}}_N \right) \hat{h}(k_z) + (\hat{v}(-k_z) \cdot \widetilde{\mathbf{V}}_N) \hat{v}(-k_z) \right\} \\
\mathbf{q}_{Nr} &= \frac{-Z_0 k_0}{2k_z} e^{ik_z d} \cdot \left\{ \left(\hat{h}(k_z) \cdot \widetilde{\mathbf{V}}_N \right) \hat{h}(k_z) + (\hat{v}(-k_z) \cdot \widetilde{\mathbf{V}}_N) \hat{v}(k_z) \right\} .
\end{aligned}
$$

Note that the vector integral equation (52) and the source function for the Nth-order polarization current are identical to those of the zeroth-order polarization current, and therefore a similar solution can be easily obtained. By decomposing the Nth-order polarization current in terms of its three principle components, it can be shown that

$$
\begin{aligned}
\widetilde{J}_{Nh}(\mathbf{k}_\perp, z) = &\quad \tfrac{ik_0^2(\epsilon - 1)}{k_z + k_{1z}} C_0^h(\mathbf{k}, z) \left[\widetilde{\mathbf{V}}_N \cdot \hat{h}(k_z) \right] \\
\widetilde{J}_{Nt}(\mathbf{k}_\perp, z) = &\quad \tfrac{ik_0 k_{1z}(\epsilon - 1)}{\epsilon k_z + k_{1z}} C_0^v(\mathbf{k}, z) \left[\widetilde{\mathbf{V}}_N \cdot \hat{v}(-k_z) \right] \\
\widetilde{J}_{Nz}(\mathbf{k}_\perp, z) = &\quad \tfrac{ik_0 k_\rho (\epsilon - 1)}{\epsilon k_z + k_{1z}} C_1^v(\mathbf{k}, z) \left[\widetilde{\mathbf{V}}_N \cdot \hat{v}(-k_z) \right] .
\end{aligned}
$$

2.2.2 Scattering Coefficients

Once the polarization current is obtained, the scattered field in region $z > d$ can be obtained from (45). Assuming that the surface perturbation is localized and the observation point $\mathbf{r} = r(\sin\theta_s\cos\phi_s\hat{x} + \sin\theta_s\sin\phi_s\hat{y} + \cos\theta_s\hat{z})$ is far from the scatterer, the far field approximation can be used to find the scattered fields. Using the stationary phase approximation in the far fields region, the Green's function is reduced to

$$\begin{aligned}\bar{\bar{\mathbf{G}}}(\mathbf{r},\mathbf{r}') = \; & \tfrac{e^{ik_0 r}}{4\pi r}\left\{\left[\hat{h}(k_z^s)\hat{h}(k_z^s)r_h^s + \hat{v}(k_z^s)\hat{v}(-k_z^s)r_v^s\right]e^{-i\mathbf{K}^s r'}\right. \\ & \left. + \left[\hat{h}(k_z^s)\hat{h}(k_z^s) + \hat{v}(k_z^s)\hat{v}(k_z^s)\right]e^{-i\mathbf{k}^s r'}\right\} \quad . \end{aligned} \tag{58}$$

Substituting (58) and the polarization currents into (45) and expanding the integral similar to those used in (47), the Nth-order scattered field is given by a power series in $\triangle f(x,y)$ (similar to (45)). In this process, the Nth-order scattered field components are found to be

$$\begin{aligned}\mathbf{E}_N^s(\mathbf{r})\cdot\hat{h}(k_z^s) \; = \; & ik_0 Z_0 \triangle^N \frac{e^{ik_0 r}}{4\pi r}\, e^{-ik_z^s d}\sum_{n=0}^{N-1}\sum_{m=0}^{N-n-1}\frac{\binom{N-n-1}{m}(ik_z^s)^m}{(N-n)!}[R_h^s + (-1)^m] \\ & \cdot C_m^h(\mathbf{k}^s, d)\left[\frac{\partial^{N-n-m-1}}{\partial\,(z')^{N-n-m-1}}\widetilde{\mathbf{J}}_n(\mathbf{k}_\perp^s, d)\right] * \bigotimes^{N-n} F(\mathbf{k}_\perp^s) \\ & \cdot\hat{h}(k_z^s)\end{aligned} \tag{59}$$

$$\begin{aligned}\mathbf{E}_N^s(\mathbf{r})\cdot\hat{v}(k_z^s) = \; & ik_0 Z_0 \triangle^N \tfrac{e^{ik_0 r}}{4\pi r}\, e^{-ik_z^s d}\sum_{n=0}^{N-1}\sum_{m=0}^{N-n-1}\frac{\binom{N-n-1}{m}(ik_z^s)^m}{(N-n)!}\left\{[R_v^s - (-1)^m]\right. \\ & \left. \cdot C_m^v(\mathbf{k}^s, d)\,\cos\theta_s\,\hat{t}(k_z^s) + [R_v^s + (-1)^m]\,C_{m+1}^v(\mathbf{k}^s, d)\,\sin\theta_s\,\hat{z}\right\} \\ & \cdot\left[\tfrac{\partial^{N-n-m-1}}{\partial(z')^{N-n-m-1}}\widetilde{\mathbf{J}}_n(\mathbf{k}_\perp^s, d)\right] * \bigotimes^{N-n} F(\mathbf{k}_\perp^s)\cdot\hat{v}(k_z^s) \quad .\end{aligned} \tag{60}$$

The polarimetric response of a target can be obtained from its complex scattering matrix, defined by

$$\mathbf{E}^s = \frac{e^{ikr}}{r}\,\bar{\bar{\mathbf{S}}}\,\mathbf{E}^i \quad . \tag{61}$$

The elements of the bistatic scattering matrix can simply be computed by setting $\mathbf{P}_i = \hat{h}(k_z^i)$ and $\mathbf{P}_i = \hat{v}(k_z^i)$ in (59) and (60). For distributed targets, such as rough surfaces, the quantities of interest are the elements of the differential covariance matrix, defined by

$$\sigma_{ijpq}^0 = \lim_{A\to\infty}\frac{4\pi}{A}\left\langle S_{ij}S_{pq}^*\right\rangle \;, \qquad\qquad i,\, j,\, p,\, q \in \{h,\, v\}\,. \tag{62}$$

Here $\langle\cdot\rangle$ denotes ensemble averaging. These elements are in general complex quantities, except when $i = p$ and $j = q$, in which case the elements are the usual scattering

coefficients. In the perturbation analysis, each element of the scattering matrix can be evaluated up to the Nth-order, that is

$$S_{ij} = \sum_{n=1}^{N} S_{ij}^{(n)} \triangle^n \ , \qquad\qquad i,\, j \in \{h,\, v\} \, . \tag{63}$$

It turns out that simple expressions for the first-order elements can be obtained and are given by

$$S_{hh}^{(1)} = \frac{k_0^2 k_z^i k_z^s (\epsilon-1) e^{-i(k_z^i+k_z^s)d}}{\pi\left(k_z^i+k_{1z}^i\right)\left(k_z^s+k_{1z}^s\right)} C_0^h(\mathbf{k}^s, d)\, C_0^h(\mathbf{k}^i, d)\, \cos(\phi_s - \phi_i)\, F(\mathbf{k}_\perp^s - \mathbf{k}_\perp^i) \ , \tag{64}$$

$$S_{hv}^{(1)} = \frac{k_0 k_z^i k_z^s k_{1z}^i (\epsilon-1) e^{-i(k_z^i+k_z^s)d}}{\pi\left(\epsilon k_z^i+k_{1z}^i\right)\left(k_z^s+k_{1z}^s\right)} C_0^h(\mathbf{k}^s, d)\, C_0^v(\mathbf{k}^i, d)\, \sin(\phi_s - \phi_i)\, F(\mathbf{k}_\perp^s - \mathbf{k}_\perp^i) \ , \tag{65}$$

$$S_{vh}^{(1)} = \frac{k_0 k_z^i k_z^s k_{1z}^s (\epsilon-1) e^{-i(k_z^i+k_z^s)d}}{\pi\left(\epsilon k_z^s+k_{1z}^s\right)\left(k_z^i+k_{1z}^i\right)} C_0^h(\mathbf{k}^i, d)\, C_0^v(\mathbf{k}^s, d)\, \sin(\phi_s - \phi_i)\, F(\mathbf{k}_\perp^s - \mathbf{k}_\perp^i) \ , \tag{66}$$

$$\begin{aligned} S_{vv}^{(1)} = \frac{k_z^i k_{1z}^i (\epsilon-1) e^{-i(k_z^i+k_z^s)d}}{\pi\left(\epsilon k_z^i+k_{1z}^i\right)\left(\epsilon k_z^s+k_{1z}^s\right)} \Big[& -k_z^s k_{1z}^s C_0^v(\mathbf{k}^s, d) C_0^v(\mathbf{k}^i, d) \cos(\phi_s - \phi_i) + \frac{\epsilon k_z^s k_\rho^s k_\rho^i}{k_{1z}^i} \\ & \cdot C_1^v(\mathbf{k}^s, d) C_1^v(\mathbf{k}^i, d) \Big] F(\mathbf{k}_\perp^s - \mathbf{k}_\perp^i) \ . \end{aligned} \tag{67}$$

In these expressions $F(\mathbf{k}_\perp^s - \mathbf{k}_\perp^i)$ is the only indeterministic factor and therefore the elements of the differential covariance matrix can easily be obtained by noting that

$$\lim_{A\to\infty} \frac{1}{A} \left\langle \left| \triangle F(\mathbf{k}_\perp^s - \mathbf{k}_\perp^i) \right|^2 \right\rangle = W(\mathbf{k}_\perp^s - \mathbf{k}_\perp^i) \ , \tag{68}$$

where $W(\mathbf{k}_\perp)$ is the power spectral density of the surface.

To examine the validity of the first-order results, a special case is considered. In the case of backscattering ($\mathbf{k}_\perp^s = -\mathbf{k}_\perp^i$) and for a homogeneous profile where $R_v = r_v$ and $R_h = r_h$, the first-order backscattering coefficients are given by

$$\begin{aligned} \sigma_{hhhh}^0 &= \frac{4}{\pi} k_0^4 \cos^4\theta_i \left| R_h^i \right|^2 W(-2\mathbf{k}_\perp^i) \\ \sigma_{vvvv}^0 &= \frac{4}{\pi} \cos^4\theta_i \left| \frac{(k_1^2 - k_0^2)\left(k_{1z}^2 + k_1^2 \sin^2\theta_i\right)}{\left(k_{1z}^i + \epsilon k_z^i\right)^2} \right|^2 W(-2\mathbf{k}_\perp^i) \\ \sigma_{hvhv}^0 &= \sigma_{vhvh}^0 = 0 \end{aligned}$$

which are in agreement with the results reported in the literature [6]. Before we proceed with the higher order scattering solutions, the following observations are in order. The analysis is simplified if we assume that the surface height profile $f(x, y)$ is a Gaussian random field. There is some evidence that this assumption is reasonable for some surfaces of practical importance [1]. Since Fourier transformation is a linear operation, $F(\mathbf{k}_\perp)$ is

also Gaussian. It is well known that the following identities hold for a zero-mean jointly Gaussian random vector $\{X_1, \ldots, X_n\}$:

$$\langle X_i X_j X_k \rangle = 0 \tag{69}$$

$$\langle X_i X_j X_k X_l \rangle = \langle X_i X_j \rangle \langle X_k X_l \rangle + \langle X_i X_k \rangle \langle X_j X_l \rangle + \langle X_i X_l \rangle \langle X_j X_k \rangle . \tag{70}$$

On the other hand, it can be shown that

$$S_{ij}^{(1)} \propto \quad F(\mathbf{k}_\perp^s - \mathbf{k}_\perp^i) \ , \tag{71}$$

$$S_{ij}^{(2)} \propto \quad \int_{-\infty}^{\infty} d\mathbf{k}_\perp \, F(\mathbf{k}_\perp^s - \mathbf{k}_\perp) F(\mathbf{k}_\perp - \mathbf{k}_\perp^i) \, I_{ij}^{(2)}(\mathbf{k}_\perp) \ , \tag{72}$$

$$S_{ij}^{(3)} \propto \quad \int_{-\infty}^{\infty} d\mathbf{k}_\perp d\mathbf{k}'_\perp \, F(\mathbf{k}_\perp^s - \mathbf{k}_\perp) F(\mathbf{k}_\perp - \mathbf{k}'_\perp) F(\mathbf{k}'_\perp - \mathbf{k}_\perp^i) \, I_{ij}^{(3)}(\mathbf{k}_\perp, \mathbf{k}'_\perp) \ , \tag{73}$$

where $I_{ij}^{(2)}$ and $I_{ij}^{(3)}$ are functions of polarization currents (see (64)$\sim$(67) and Appendix A). For the evaluation of the covariance matrix, we confine our interest in perturbation terms up to $\triangle^4$. Substituting (71)$\sim$(73) in (63) and then using (69), the elements of covariance matrix simplify to

$$\left\langle S_{ij} S_{pq}^* \right\rangle \approx \left\langle S_{ij}^{(1)} S_{pq}^{(1)*} \right\rangle \triangle^2 + \left[\left\langle S_{ij}^{(2)} S_{pq}^{(2)*} \right\rangle + \left\langle S_{ij}^{(1)} S_{pq}^{(3)*} \right\rangle + \left\langle S_{ij}^{(3)} S_{pq}^{(1)*} \right\rangle \right] \triangle^4 . \tag{74}$$

Noting that property (69) is valid for any odd number of random variables, the elements of covariance matrix are only functions of even power of $\triangle$. Therefore the next higher order of approximation in calculation of $\left\langle S_{ij} S_{pq}^* \right\rangle$ can be obtained by inclusion of products of the first and the fifth, the second and the fourth, and the third-order scattering terms. However, evaluation of high-order scattered fields such as fourth and fifth order are rather complex and tedious. Noting that $\triangle$ is a small quantity compared to the wavelength, the benefit of inclusion of $\triangle^6$ term is not significant. This argument cannot be used for the second order solution ($\triangle^4$ term), since this term is the dominant factor for some important scattering parameters such as cross-polarized backscattering coefficient and co-polarized degree of correlation.

The scattering matrix elements up to third order are derived. These expressions are very lengthy and are not included in this paper. Interested readers are referred to reference [12]. Using these expressions in (74), the elements of the covariance matrix can be obtained. The ensemble averaging process can be carried out easily using (70), and

$$\triangle^2 \langle F(\mathbf{k}_\perp) F^*(\mathbf{k}'_\perp) \rangle = \triangle^2 \langle F(\mathbf{k}_\perp) F(-\mathbf{k}'_\perp) \rangle = (2\pi)^2 \, \delta(\mathbf{k}_\perp - \mathbf{k}'_\perp) W(\mathbf{k}_\perp) \ . \tag{75}$$

Using the above mentioned properties, and noting that in backscatter direction ($\phi_s = \phi_i + \pi$, $\theta_s = \theta_i$) $S_{hv}^{(1)} = S_{vh}^{(1)} = 0$, the cross-polarized backscattering coefficients can be

obtained and are given by

$$\sigma^0_{hvhv} = \sigma^0_{vhvh} = \frac{\left|k_0 k_z^i (\epsilon-1)^2\right|^2}{16\pi^3} \left|(1-R_v^i)\,(1+R_h^i)\,C_0^h(\mathbf{k}^i,d)C_0^v(\mathbf{k}^i,d)\right|^2 \cdot \int_{-\infty}^{\infty} W(\mathbf{k}_\perp - \mathbf{k}_\perp^i)W(\mathbf{k}_\perp + \mathbf{k}_\perp^i)\sin^2(\phi-\phi_i)\cos^2(\phi-\phi_i) \cdot \left|\frac{k_0^2}{k_z+k_{1z}}\,C_0^h(\mathbf{k},d) - \frac{k_z k_{1z}}{k_{1z}+\epsilon k_z}\,C_0^v(\mathbf{k},d)\right|^2 d\mathbf{k}_\perp \ , \tag{76}$$

which satisfies the reciprocity condition. To examine the validity of (76), a homogeneous profile is considered having $R_h = r_h$ and $R_v = r_v$. In this case

$$\sigma^0_{hvhv} = \sigma^0_{vhvh} = \frac{2}{\pi^3}\left|\frac{k_0 (k_z^i)^2 k_{1z}^i \left(k_1^2 - k_0^2\right)^2}{(k_0^2 k_{1z}^i + k_1^2 k_z^i)\,(k_z^i + k_{1z}^i)}\right|^2 \cdot \int_{-\infty}^{+\infty}\left|\frac{\left(k_x^i k_y - k_y^i k_x\right)\left(k_x^i k_x + k_y^i k_y\right)}{(k_\rho^i)^2\,(k_0^2 k_{1z} + k_1^2 k_z)}\right|^2 W(\mathbf{k}_\perp - \mathbf{k}_\perp^i)W(\mathbf{k}_\perp + \mathbf{k}_\perp^i)d\mathbf{k}_\perp \tag{77}$$

which is in agreement with result reported in [6].

2.2.3 Phase Statistics

Traditionally, scattering models for rough surfaces provide formulations for co- and cross-polarized scattering coefficients. With the advances in the development of polarimetric radar, the statistics of the phase difference of scattering matrix elements can be measured and used in inversion algorithms to retrieve the target parameters. In a polarimetric backscatter measurement, apart from the backscattering coefficients, the co- and cross-polarized phase differences, defined by $\phi_c = \phi_{hh} - \phi_{vv}$ and $\phi_x = \phi_{hv} - \phi_{vv}$, are two additional independent parameters which can be used in an inversion process. In a recent paper [13], it was shown that the statistics of the phase difference can be derived from the elements of the target covariance matrix ($\langle S_{ij} S_{pq}^* \rangle$) and that the pdf of each phase-difference can be fully determined in terms of two parameters : (1) coherent phase difference (ζ) and (2) degree of correlation (α). The coherent phase difference is the phase difference at which the pdf assumes its maximum. The degree of correlation is a real number that can vary from 0 to 1 and is proportional to the spread of the pdf around ζ, where $\alpha = 0$ corresponds to a uniform distribution and $\alpha = 1$ corresponds to a delta function. In terms of covariance matrix elements, ζ and α are given by

$$\zeta = \tan^{-1}\frac{Im[\langle S_{ij} S_{vv}^* \rangle]}{Re[\langle S_{ij} S_{vv}^* \rangle]} \ , \qquad \alpha = \sqrt{\frac{|\langle S_{ij} S_{vv}^* \rangle|^2}{\langle |S_{ij}|^2 \rangle \langle |S_{vv}|^2 \rangle}} \ , \tag{78}$$

where subscript $ij = hh$ for co-polarized and $ij = vh$ or hv for cross-polarized phase difference respectively. Referring to (64)$-$(67) it can easily be shown that $\alpha_c = 1$ and $\alpha_x = 0$ for the first-order scattering solution. Hence α_c and α_x do not contain any

information about the surface power spectral density or the surface dielectric constant. Noting that to the first-order elements of the covariance matrix are linearly proportional to the power spectral density, ζ_c is only a function of the surface dielectric profile.

To characterize the dependency of α_c and α_x on the surface power spectral density, we have to resort to the second-order scattering solution. Combining the first-order solution given by (64)−(67) and the second-order and third-order solutions, closed form expressions for the parameters of phase-difference statistics can be obtained. It is found that α_x vanishes when the surface power spectral density is azimuthally symmetric, that is, if $W(k_x, k_y) = W(\sqrt{k_x^2 + k_y^2})$. This is usually the case for most practical situations, which implies the co- and cross-polarized backscattered fields are mutually uncorrelated.

2.2.4 Data Simulation and Experimental Results

In the previous section, an analytical model for predicting polarimetric scattering behavior of inhomogeneous rough surfaces based on a perturbation expression of induced polarization current was obtained. Here, data simulation based on the complete second-order analytical model is carried out to investigate the sensitivity of the radar backscatter measurements to physical parameters of the surface, such as the surface dielectric profile and surface power spectral density. Also, polarimetric backscatter measurements were conducted to examine the significance of the second-order solution on the overall backscatter response as a function of surface parameters and radar attributes.

Figures 5a and 5b demonstrate the significance of the second-order solution, where the ratio of the first-order to the complete co-polarized second-order solutions $(\sigma^{0(1)})/\sigma^{0(2)})$ are plotted versus incidence angle. An exponential correlation function given by

$$\rho(x, y) = s^2 \, e^{-\frac{\sqrt{x^2+y^2}}{l}} \ , \tag{79}$$

where s is the rms height and l is the surface correlation length, is used in these simulations. In Figs. 5a and 5b, ks and kl are varied as free parameters, and the soil surface is assumed to be a homogeneous medium with $\epsilon = 8.0 + i\,2.51$. This dielectric constant corresponds to a moist soil surface with volumetric moisture content $m_v = 0.2$ and is computed using the empirical formula given in [14] at 1.25 GHz with $S = 0.1$ and $C = 0.3$. It is shown that the second-order scattering term is more sensitive to variations in rms height(s) than it is to the surface correlation length (l). The sensitivity to s is higher at lower angles of incidence for σ^0_{vvvv} unlike σ^0_{hhhh}. Figures 6a and 6b show the ratio of the first-order to the complete co-polarized second-order solutions of the homogeneous rough surface as a function of soil moisture at $\theta = 45^o$. Here it is shown that as the soil moisture increases from 0.01 ($\epsilon = 2.21 + i\,0.002$) to 0.4 ($\epsilon = 14.68 + i\,7.5$), the contribution from the second-order scattering term to the overall backscattering increases slightly. This effect is more pronounced for σ^0_{hhhh}. Figures 5 and 6 demonstrate that the inclusion of the second-order solution is more important for calculation of σ^0_{hhhh}

than for σ^0_{vvvv}. Figures 7 and 8 show the co-polarized coherent phase difference ζ_c calculated from the first-order and complete second-order solutions for the homogeneous surface as a function of incidence angle and soil moisture. To the first order, ζ_c is independent of surface roughness parameters, however, the second-order solution shows a weak dependency on ks and kl. It is interesting to note that the sensitivity to roughness parameters disappears for incidence angles larger than 50^o. As shown in Fig. 8, ζ_c is relatively insensitive to moisture content for a homogeneous surface.

As mentioned before, the second-order solution is the dominant component for the cross-polarized backscattering coefficient. σ^0_{hvhv} is directly proportional to the square of the rms height, thus the dependency to s is not examined. Figure 9 shows σ^0_{hvhv} of the homogeneous surface as a function of incidence angle for different values of kl and m_v while $ks = 0.2$ is kept constant. Note that σ^0_{hvhv} increases with increasing dielectric constant and decreases with increasing surface correlation length. The co-polarized degree of correlation is another potential parameter that can be used in retrieval of surface physical parameters. The first-order scattering solution predict $\alpha_c = 1$ independent of the surface physical parameters. Figures 10 and 11 show α_c for the homogeneous rough surface as a function of incidence angle and dielectric constant for different values of ks and kl. Note that α_c, in general, has a decreasing trend with increasing incidence angle, rms height, and soil moisture. It is also noted that α_c increases when kl is decreased. The total dynamic range of α_c as a function of the surface parameters is rather limited.

Next we examine the sensitivity of the polarimetric backscatter data to the surface dielectric inhomogeneity. Three dielectric profiles are considered here: (1) exponentially increasing moisture with depth, (2) exponentially decreasing moisture with depth, and (3) a two-layer step profile, as shown in Fig. 12. The exponential profiles are chosen according to [16] and are given by:

$$m_v(z) = \begin{cases} m_{vs} + \triangle m_v \, \frac{e^{\beta z}-1}{e^{-\beta d}-1} & -d \le z \le 0 \ , \\ m_v(z) = m_v(-d) & z \le -d \ , \end{cases} \tag{80}$$

where m_{vs} is the surface moisture content and $\triangle m_v$ is the increment of moisture at a depth d below the surface. The moisture content below depth d is considered to be uniform. In all cases the backscatter parameters are compared with a homogeneous profile having a dielectric constant equal to that of the inhomogeneous profile at the interface. Figures 13 and 14 show the backscattering coefficients for a surface with the increasing and decreasing exponential dielectric profiles and having $ks = 0.2$, $kl = 2$. Note that the backscattering coefficients are insensitive to moisture profiles, and the backscattering coefficients are basically indistinguishable from those of the homogeneous profile having the same dielectric constant as that of the inhomogeneous profile at the interface. This is due to the tapered impedance matching nature of the profile. However, this is not the case for the step profile as shown in Fig. 15. The difference in σ^o, depending on the incidence angle, can be as high as 10 dB. The only sensitive parameter to moisture variations in depth for continuous profiles is the co-polarized coherent phase

difference as is shown in Fig. 16, where ζ_c for the homogeneous, increasing, and step moisture profiles are shown. ζ_c does not shown any sensitivity for decreasing profiles. It should be pointed out that the calculation of the complete second-order solution involves numerical evaluation of two-fold integrals. To provide a feeling for the required computation time, the calculation of backscattering coefficients and phase difference statistics for one incidence angle would take about one minute on a Sun workstation Ultra 2.

The validity of the analytical results are also examined by conducting backscatter measurements. The backscatter measurements were performed polarimetrically using the indoor bistatic facilities of the Radiation Laboratory at the University of Michigan [18]. The backscatter data were collected from a rough layer of sand above a perfectly conducting ground plane at center frequency 9.25 GHz with a bandwidth of 1.5 GHz. A $6' \times 6'$ sand-box on top of a computer controlled turntable was used to contain the sand layer. The antenna footprint covered an area of about $0.27 \sec\theta \; m^2$ on the sand-box and collection of independent backscatter data was facilitated by rotating the sand-box at steps of 5^o. The wide bandwidth of the radar system was used to range-gate the possible unwanted radar backscatter from the sand-box walls and edges. A simplified block diagram of the measurement system is shown in Fig. 17.

An uniform sand with maximum particle dimension of 0.15 mm was chosen to minimize the effect of volume scattering from the sand layer. The effective dielectric constant of the sand medium was measured to be $\epsilon_r = 2.7 + i\,0.05$. The radar was calibrated polarimetrically using STCT [19]. To generate a desired roughness over the sand surface repeatedly, a template was made. The imprint of the template on the surface generated a rough surface with almost an exponential auto-correlation function with $ks = 0.122$ and $kl = 2.69$. The surface roughness statistics were measured using a laser ranging system with a range resolution of 0.1 mm. The backscatter measurements conducted for two layers having thicknesses $d = 2.52$ cm and $d = 3.53$ cm over the angular range $20^o \sim 50^o$.

Figures 18a and 18b show the measured and simulated σ^0 versus incidence angle. All the measured results are shown to be in a very good agreement with the complete second order solution except for the cross-polarized responses at $\theta = 50^o$. For these cases we were limited by the system noise floor. Figures 19a and 19b show the response of the co-polarized coherent phase difference as a function of incidence angle. Both the first-order and second-order solutions are shown and it is obvious that the second-order contribution is insignificant at angles below 40^o.

Figures 20a and 20b compare the measured and theoretical ratio of $\sigma^0_{hhhh}/\sigma^0_{vvvv}$, versus incidence angle. Here it is shown that at high incidence angles first-order results are incapable of accurate prediction of backscattering coefficients whereas the second-order solution provide satisfactory results. Figures 21a and 21b show the the measured and calculated co-polarized degree of correlation versus incidence angle, where a relatively good agreement has been obtained considering the difficulties in the accurate measure-

ment of α [20].

2.2.5 Summary

In this paper, a bistatic polarimetric scattering model for random dielectric surfaces with inhomogeneous permittivity profiles and small surface roughnesses is developed using a perturbation expansion of volumetric polarization current. A complete second-order solution for the backscattering coefficients and the statistics of the phase difference between the elements of scattering matrix is obtained. The validity of the model is verified in a limiting case, where it is shown that the formulation for surface with inhomogeneous permittivity profile reduces to the known formulation for homogeneous rough surfaces. Also, polarimetric backscatter measurements from rough surfaces with known dielectric profiles and roughness statistics were collected and compared with the theoretical calculations. Comparisons with the measured data show excellent agreement. The sensitivity analysis in terms of the surface physical parameters is also performed. It is shown that, in general, the backscatter parameters, such as backscattering coefficients and phase-difference statistics, are more sensitive to ks than kl. The contribution of the second-order solution for calculation of σ^o_{hhhh} is more significant than that for the calculation of σ^o_{vvvv}. The contribution of the second-order solution to overall σ^o_{hhhh} can be as high as 2 dB for $ks \leq 0.3$. It is shown that for continuous inhomogeneous profiles, the backscattering coefficients are insensitive to the variations of moisture content as a function of depth. In the other words, the backscattering coefficients of a surface with a continuous soil moisture profile are equal to those of a homogeneous surface having a moisture content equivalent to that of the inhomogeneous profile at the interface. The only backscatter parameter sensitive to moisture profile is the co-polarized coherent phase difference (ζ_c). However, both the backscattering coefficients and phase-difference statistics are very sensitive to step discontinuities in moisture profile.

A Appendix

In this appendix closed form expressions for the second and third order elements of bistatic scattering matrix of the inhomogeneous rough surface are provided.

$$
\begin{aligned}
S_{hh}^{(2)} = \quad & \tfrac{ik_0^2(\epsilon-1)}{8\pi}\left(1+R_h^i\right)\cos(\phi_s-\phi_i)e^{-i(k_z^s+k_z^i)d}\Big[k_z^s\left(R_h^i-1\right)C_1^h(\mathbf{k}^s,d)C_0^h(\mathbf{k}^i,d) \\
& -k_{1z}^i\left(R_h^i+1\right)C_0^h(\mathbf{k}^s,d)C_1^h(\mathbf{k}^i,d)\Big]\left(\tfrac{1}{2\pi}\right)^2\int_{-\infty}^{\infty}F(\mathbf{k}_\perp^s-\mathbf{k}_\perp)F(\mathbf{k}_\perp-\mathbf{k}_\perp^i)\,d\mathbf{k}_\perp \\
& +\tfrac{ik_0^2(\epsilon-1)^2}{4\pi}\left(1+R_h^s\right)\left(1+R_h^i\right)C_0^h(\mathbf{k}^s,d)C_0^h(\mathbf{k}^i,d)e^{-i(k_z^s+k_z^i)d} \\
& \cdot\left(\tfrac{1}{2\pi}\right)^2\int_{-\infty}^{\infty}F(\mathbf{k}_\perp^s-\mathbf{k}_\perp)F(\mathbf{k}_\perp-\mathbf{k}_\perp^i)\cdot\Big[\tfrac{k_0^2}{k_z+k_{1z}}C_0^h(\mathbf{k},d)\cos(\phi_s-\phi) \\
& \cdot\cos(\phi-\phi_i)-\tfrac{k_zk_{1z}}{\epsilon k_z+k_{1z}}C_0^v(\mathbf{k},d)\sin(\phi_s-\phi)\sin(\phi-\phi_i)\Big]\,d\mathbf{k}_\perp \qquad (81)
\end{aligned}
$$

$$
\begin{aligned}
S_{vv}^{(2)} = \quad & \tfrac{ik_z^i(\epsilon-1)}{8\pi}\left(1-R_v^i\right)e^{-i(k_z^s+k_z^i)d}\Big\{\Big[\left(k_z^s\right)^2\cos(\phi_s-\phi_i)-k_\rho^ik_\rho^s\Big]\left(1+R_v^s\right)C_1^v(\mathbf{k}^s,d) \\
& \cdot C_0^v(\mathbf{k}^i,d)-\Big[k_{1z}^ik_z^s\cos(\phi_s-\phi_i)-k_\rho^ik_\rho^s\tfrac{k_z^s}{k_{1z}^i}\Big]\left(R_v^s-1\right)C_0^v(\mathbf{k}^s,d)C_1^v(\mathbf{k}^i,d)\Big\} \\
& \cdot\left(\tfrac{1}{2\pi}\right)^2\int_{-\infty}^{\infty}F(\mathbf{k}_\perp^s-\mathbf{k}_\perp)F(\mathbf{k}_\perp-\mathbf{k}_\perp^i)\,d\mathbf{k}_\perp \\
& -\tfrac{ik_z^sk_z^i(\epsilon-1)^2}{4\pi}\left(1-R_v^s\right)\left(1-R_v^i\right)C_0^v(\mathbf{k}^s,d)e^{-i(k_z^s+k_z^i)d} \\
& \cdot\left(\tfrac{1}{2\pi}\right)^2\int_{-\infty}^{\infty}F(\mathbf{k}_\perp^s-\mathbf{k}_\perp)F(\mathbf{k}_\perp-\mathbf{k}_\perp^i)\cdot\Big[-\tfrac{k_0^2}{k_z+k_{1z}}C_0^h(\mathbf{k},d)C_0^v(\mathbf{k}^i,d) \\
& \cdot\sin(\phi_s-\phi)\sin(\phi-\phi_i)+\tfrac{k_zk_{1z}}{\epsilon k_z+k_{1z}}C_0^v(\mathbf{k},d)C_0^v(\mathbf{k}^i,d)\cos(\phi_s-\phi) \\
& \cdot\cos(\phi-\phi_i)+\tfrac{k_\rho^ik_\rho k_{1z}}{k_{1z}^i(\epsilon k_z+k_{1z})}C_0^v(\mathbf{k},d)C_1^v(\mathbf{k}^i,d)\cos(\phi_s-\phi)\Big]\,d\mathbf{k}_\perp \\
& +\tfrac{ik_\rho^sk_z^i(\epsilon-1)^2}{4\pi}\left(1+R_v^s\right)\left(1-R_v^i\right)C_1^v(\mathbf{k}^s,d)e^{-i(k_z^s+k_z^i)d} \\
& \cdot\left(\tfrac{1}{2\pi}\right)^2\int_{-\infty}^{\infty}F(\mathbf{k}_\perp^s-\mathbf{k}_\perp)F(\mathbf{k}_\perp-\mathbf{k}_\perp^i)\,\tfrac{k_\rho}{\epsilon k_z+k_{1z}}C_1^v(\mathbf{k},d) \\
& \cdot\Big[k_zC_0^v(\mathbf{k}^i,d)\cos(\phi-\phi_i)+k_\rho\tfrac{k_\rho^i}{k_{1z}^i}C_1^v(\mathbf{k}^i,d)\Big]\,d\mathbf{k}_\perp \qquad (82)
\end{aligned}
$$

$$
\begin{aligned}
S_{vh}^{(2)} = \quad & -\tfrac{ik_0k_z^s(\epsilon-1)}{8\pi}\left(1+R_h^i\right)\sin(\phi_s-\phi_i)e^{-i(k_z^s+k_z^i)d}\Big[k_{1z}^i\left(1-R_v^s\right)C_0^v(\mathbf{k}^s,d)C_1^h(\mathbf{k}^i,d) \\
& +k_z^s\left(1+R_v^s\right)C_1^v(\mathbf{k}^s,d)C_0^h(\mathbf{k}^i,d)+\Big]\left(\tfrac{1}{2\pi}\right)^2\int_{-\infty}^{\infty}F(\mathbf{k}_\perp^s-\mathbf{k}_\perp)F(\mathbf{k}_\perp-\mathbf{k}_\perp^i)\,d\mathbf{k}_\perp \\
& +\tfrac{ik_0k_z^s(\epsilon-1)^2}{4\pi}\left(1-R_v^s\right)\left(1+R_h^i\right)C_0^v(\mathbf{k}^s,d)C_0^h(\mathbf{k}^i,d)e^{-i(k_z^s+k_z^i)d} \\
& \cdot\left(\tfrac{1}{2\pi}\right)^2\int_{-\infty}^{\infty}F(\mathbf{k}_\perp^s-\mathbf{k}_\perp)F(\mathbf{k}_\perp-\mathbf{k}_\perp^i)\cdot\Big[\tfrac{k_0^2}{k_z+k_{1z}}C_0^h(\mathbf{k},d) \\
& \cdot\sin(\phi_s-\phi)\cos(\phi-\phi_i)+\tfrac{k_zk_{1z}}{\epsilon k_z+k_{1z}}C_0^v(\mathbf{k},d)\cos(\phi_s-\phi)\sin(\phi-\phi_i)\Big]\,d\mathbf{k}_\perp \\
& -\tfrac{ik_0k_\rho^s(\epsilon-1)^2}{4\pi}\left(1+R_v^s\right)\left(1+R_h^i\right)C_1^v(\mathbf{k}^s,d)C_0^h(\mathbf{k}^i,d)e^{-i(k_z^s+k_z^i)d}\left(\tfrac{1}{2\pi}\right)^2
\end{aligned}
$$

$$\cdot \int_{-\infty}^{\infty} F(\mathbf{k}_\perp^s - \mathbf{k}_\perp) F(\mathbf{k}_\perp - \mathbf{k}_\perp^i) \cdot \tfrac{k_\rho k_z}{\epsilon k_z + k_{1z}} C_1^v(\mathbf{k}, d) \sin(\phi - \phi_i)\, d\mathbf{k}_\perp \qquad (83)$$

$$\begin{aligned} S_{hv}^{(2)} = \quad & -\tfrac{ik_0 k_z^i (\epsilon-1)}{8\pi} (1 - R_v^i) \sin(\phi_s - \phi_i) e^{-i(k_z^s + k_z^i)d} \Big[k_{1z}^i (1 + R_h^s)\, C_0^h(\mathbf{k}^s, d) C_1^v(\mathbf{k}^i, d) \\ & + k_z^s (1 - R_h^s)\, C_1^h(\mathbf{k}^s, d) C_0^v(\mathbf{k}^i, d) + \Big] \left(\tfrac{1}{2\pi}\right)^2 \int_{-\infty}^{\infty} F(\mathbf{k}_\perp^s - \mathbf{k}_\perp) F(\mathbf{k}_\perp - \mathbf{k}_\perp^i)\, d\mathbf{k}_\perp \\ & + \tfrac{ik_0 k_z^i (\epsilon-1)^2}{4\pi} (1 + R_h^s)(1 - R_v^i)\, C_0^h(\mathbf{k}^s, d) e^{-i(k_z^s + k_z^i)d} \\ & \cdot \left(\tfrac{\triangle}{2\pi}\right)^2 \int_{-\infty}^{\infty} F(\mathbf{k}_\perp^s - \mathbf{k}_\perp) F(\mathbf{k}_\perp - \mathbf{k}_\perp^i) \cdot \Big[\tfrac{k_0^2}{k_z + k_{1z}} C_0^h(\mathbf{k}, d) C_0^v(\mathbf{k}^i, d) \\ & \cdot \cos(\phi_s - \phi) \sin(\phi - \phi_i) + \tfrac{k_z k_{1z}}{\epsilon k_z + k_{1z}} C_0^v(\mathbf{k}, d) C_0^v(\mathbf{k}^i, d) \sin(\phi_s - \phi) \\ & \cdot \cos(\phi - \phi_i) + \tfrac{k_\rho k_{1z}}{\epsilon k_z + k_{1z}} \tfrac{k_\rho^i}{k_{1z}^i} C_0^v(\mathbf{k}, d) C_1^v(\mathbf{k}^i, d) \sin(\phi_s - \phi) \Big]\, d\mathbf{k}_\perp \end{aligned} \qquad (84)$$

$$\begin{aligned} S_{hh}^{(3)} = \quad & -\tfrac{k_0^2 (\epsilon-1)}{24\pi} (1 + R_h^i)\, e^{-i(k_z^s + k_z^i)d} \cos(\phi_s - \phi_i) \cdot \Big\{ \Big[(k_z^s)^2 + (k_{1z}^i)^2 \Big] (1 + R_h^s) \\ & \cdot C_0^h(\mathbf{k}^i, d) C_0^h(\mathbf{k}^s, d) + 2 k_z^s k_{1z}^i (1 - R_h^s)\, C_1^h(\mathbf{k}^i, d) C_1^h(\mathbf{k}^s, d) \Big\} \\ & \cdot \tfrac{1}{(2\pi)^4} \int_{-\infty}^{\infty} F(\mathbf{k}_\perp^s - \mathbf{k}_\perp) F(\mathbf{k}_\perp - \mathbf{k}'_\perp) F(\mathbf{k}'_\perp - \mathbf{k}_\perp^i)\, d\mathbf{k}_\perp d\mathbf{k}'_\perp \\ & + \tfrac{k_0^2 (\epsilon-1)^2}{8\pi} (1 + R_h^i)(1 + R_h^s)\, C_0^h(\mathbf{k}^i, d) C_0^h(\mathbf{k}^s, d) e^{-i(k_z^s + k_z^i)d} \tfrac{1}{(2\pi)^4} \end{aligned}$$

$$\begin{aligned} & \cdot \int_{-\infty}^{\infty} F(\mathbf{k}_\perp^s - \mathbf{k}_\perp) F(\mathbf{k}_\perp - \mathbf{k}'_\perp) F(\mathbf{k}'_\perp - \mathbf{k}_\perp^i) \Big[\tfrac{k_0^2 k'_{1z}}{k'_z + k'_{1z}} C_1^h(\mathbf{k}', d) \cos(\phi' - \phi_i) \\ & \cos(\phi_s - \phi') - \tfrac{k'_z (k'_{1z})^2}{\epsilon k'_z + k'_{1z}} C_1^v(\mathbf{k}', d) \sin(\phi' - \phi_i) \sin(\phi_s - \phi') \Big]\, d\mathbf{k}_\perp d\mathbf{k}'_\perp \\ & + \tfrac{k_0^2 (\epsilon-1)^2}{8\pi} (1 + R_h^i)(1 - R_h^s)\, C_0^h(\mathbf{k}^i, d) C_1^h(\mathbf{k}^s, d) e^{-i(k_z^s + k_z^i)d} \tfrac{1}{(2\pi)^4} \\ & \cdot \int_{-\infty}^{\infty} F(\mathbf{k}_\perp^s - \mathbf{k}_\perp) F(\mathbf{k}_\perp - \mathbf{k}'_\perp) F(\mathbf{k}'_\perp - \mathbf{k}_\perp^i) \Big[\tfrac{k_0^2 k_z^s}{k'_z + k'_{1z}} C_0^h(\mathbf{k}', d) \cos(\phi' - \phi_i) \\ & \cdot \cos(\phi_s - \phi') - \tfrac{k_z^s k'_z k'_{1z}}{\epsilon k'_z + k'_{1z}} C_0^v(\mathbf{k}', d, 0) \sin(\phi' - \phi_i) \sin(\phi_s - \phi') \Big]\, d\mathbf{k}_\perp d\mathbf{k}'_\perp \\ & - \tfrac{k_0^2 (\epsilon-1)^2}{8\pi} (1 + R_h^i)(1 + R_h^s)\, C_0^h(\mathbf{k}^s, d) e^{-i(k_z^s + k_z^i)d} \tfrac{1}{(2\pi)^4} \int_{-\infty}^{\infty} d\mathbf{k}_\perp d\mathbf{k}'_\perp \\ & F(\mathbf{k}_\perp^s - \mathbf{k}_\perp) F(\mathbf{k}_\perp - \mathbf{k}'_\perp) F(\mathbf{k}'_\perp - \mathbf{k}_\perp^i) \Big[k_z C_0^h(\mathbf{k}^i, d) - k_{1z}^i C_1^h(\mathbf{k}^i, d) \Big] \Big[\tfrac{k_0^2}{k_z + k_{1z}} \\ & \cdot C_0^h(\mathbf{k}, d) \cos(\phi - \phi_i) \cos(\phi_s - \phi) - \tfrac{k_z^s k_{1z}}{\epsilon k_z + k_{1z}} C_0^v(\mathbf{k}, d) \sin(\phi - \phi_i) \sin(\phi_s - \phi) \Big] \\ & + \tfrac{k_0^2 (\epsilon-1)^3}{4\pi} (1 + R_h^i)(1 + R_h^s)\, C_0^h(\mathbf{k}^s, d) C_0^h(\mathbf{k}^i, d) e^{-i(k_z^s + k_z^i)d} \\ & \cdot \tfrac{1}{(2\pi)^4} \int_{-\infty}^{\infty} F(\mathbf{k}_\perp^s - \mathbf{k}_\perp) F(\mathbf{k}_\perp - \mathbf{k}'_\perp) F(\mathbf{k}'_\perp - \mathbf{k}_\perp^i) \Big\{ \\ & - \tfrac{k_0^4}{(k_z + k_{1z})\left(k'_z + k'_{1z}\right)} C_0^h(\mathbf{k}', d) C_0^h(\mathbf{k}, d) \cos(\phi_s - \phi) \cos(\phi - \phi') \cos(\phi' - \phi_i) \end{aligned}$$

$$
\begin{aligned}
&+\tfrac{k_0^2 k_z k_{1z}}{(\epsilon k_z+k_{1z})\left(k'_z+k'_{1z}\right)} C_0^h(\mathbf{k}',d) C_0^v(\mathbf{k},d)\sin(\phi_s-\phi)\sin(\phi-\phi')\cos(\phi'-\phi_i)\\
&+\tfrac{k_0^2 k'_z k'_{1z}}{(k_z+k_{1z})\left(\epsilon k'_z+k'_{1z}\right)} C_0^v(\mathbf{k}',d) C_0^h(\mathbf{k},d)\cos(\phi_s-\phi)\sin(\phi-\phi')\sin(\phi'-\phi_i)\\
&+\tfrac{k_z k_{1z} k'_z k'_{1z}}{(\epsilon k_z+k_{1z})\left(\epsilon k'_z+k'_{1z}\right)} C_0^v(\mathbf{k}',d) C_0^v(\mathbf{k},d)\sin(\phi_s-\phi)\cos(\phi-\phi')\sin(\phi'-\phi_i)\\
&+\tfrac{k'_\rho k'_z k_\rho k_{1z}}{(k_z+k_{1z})\left(k'_z+k'_{1z}\right)} C_1^v(\mathbf{k}',d) C_0^v(\mathbf{k},d)\sin(\phi_s-\phi)\sin(\phi'-\phi_i)\Big\}\, d\mathbf{k}_\perp d\mathbf{k}'_\perp \qquad (85)
\end{aligned}
$$

$$
\begin{aligned}
S_{vv}^{(3)} = \quad & -\tfrac{k_z^i(\epsilon-1)}{24\pi}\left(1-R_v^i\right)e^{-i(k_z^s+k_z^i)d}\Big\{k_z^s\Big(\left[\left(k_{1z}^i\right)^2+\left(k_z^s\right)^2\right]\cos(\phi_s-\phi_i)-2k_\rho^i k_\rho^s\Big)\\
&\cdot\left(R_v^s-1\right)C_0^v(\mathbf{k}^s,d)C_0^v(\mathbf{k}^i,d)+\Big(\left[\left(k_{1z}^i\right)^2+\left(k_z^s\right)^2\right]\tfrac{k_\rho^i k_\rho^s}{k_{1z}^i}-2\left(k_z^s\right)^2 k_{1z}^i\\
&\cdot\cos(\phi_s-\phi_i)\Big)\left(R_v^s+1\right)C_1^v(\mathbf{k}^s,d)C_1^v(\mathbf{k}^i,d)\Big\}\\
&\cdot\tfrac{1}{(2\pi)^4}\int_{-\infty}^{\infty}F(\mathbf{k}_\perp^s-\mathbf{k}_\perp)F(\mathbf{k}_\perp-\mathbf{k}'_\perp)F(\mathbf{k}'_\perp-\mathbf{k}_\perp^i)\,d\mathbf{k}_\perp d\mathbf{k}'_\perp\\
&+\tfrac{k_z^i(\epsilon-1)^2}{8\pi}\left(1-R_v^i\right)\left(R_v^s-1\right)C_0^v(\mathbf{k}^s,d)e^{-i(k_z^s+k_z^i)d}\tfrac{1}{(2\pi)^4}\int_{-\infty}^{\infty}\\
&\cdot F(\mathbf{k}_\perp^s-\mathbf{k}_\perp)F(\mathbf{k}_\perp-\mathbf{k}'_\perp)F(\mathbf{k}'_\perp-\mathbf{k}_\perp^i)\Big\{-\tfrac{k_0^2 k_z^s k'_{1z}}{k'_z+k'_{1z}}C_0^v(\mathbf{k}^i,d)C_1^h(\mathbf{k}',d)\\
&\cdot\sin(\phi_s-\phi')\sin(\phi'-\phi_i)+\tfrac{k_z^s}{\epsilon k'_z+k'_{1z}}\Big[k'_z C_0^v(\mathbf{k}^i,d)\cos(\phi'-\phi_i)+\tfrac{k_\rho^i k'_\rho}{k_{1z}^i}\\
&\cdot C_1^v(\mathbf{k}^i,d)\Big]\Big[\left(k'_{1z}\right)^2\cos(\phi^s-\phi')-k_\rho^s k'_\rho\Big]C_1^v(\mathbf{k}',d)\Big\}\,d\mathbf{k}_\perp d\mathbf{k}'_\perp\\
&+\tfrac{k_z^i(\epsilon-1)^2}{8\pi}\left(1-R_v^i\right)\left(R_v^s+1\right)C_1^v(\mathbf{k}^s,d)e^{-i(k_z^s+k_z^i)d}\tfrac{1}{(2\pi)^4}\int_{-\infty}^{\infty}\\
&F(\mathbf{k}_\perp^s-\mathbf{k}_\perp)F(\mathbf{k}_\perp-\mathbf{k}'_\perp)F(\mathbf{k}'_\perp-\mathbf{k}_\perp^i)\Big\{\tfrac{k_0^2\left(k_z^s\right)^2}{k'_z+k'_{1z}}C_0^v(\mathbf{k}^i,d)C_0^h(\mathbf{k}',d)\\
&\cdot\sin\left(\phi_s-\phi'\right)\sin\left(\phi'-\phi_i\right)-\tfrac{k'_{1z}}{\epsilon k'_z+k'_{1z}}\Big[k'_z C_0^v(\mathbf{k}^i,d)\cos(\phi'-\phi_i)+\tfrac{k_\rho^i k'_\rho}{k_{1z}^i}\\
&\cdot C_1^v(\mathbf{k}^i,d)\Big]\Big[\left(k_z^s\right)^2\cos(\phi^s-\phi')-k_\rho^s k'_\rho\Big]C_0^v(\mathbf{k}',d)\Big\}\,d\mathbf{k}_\perp d\mathbf{k}'_\perp\\
&+\tfrac{k_z^i(\epsilon-1)^2}{8\pi}\left(1-R_v^i\right)\left(R_v^s-1\right)e^{-i(k_z^s+k_z^i)d}\tfrac{1}{(2\pi)^4}\int_{-\infty}^{\infty}F(\mathbf{k}_\perp^s-\mathbf{k}_\perp)F(\mathbf{k}_\perp-\mathbf{k}'_\perp)\\
&F(\mathbf{k}'_\perp-\mathbf{k}_\perp^i)\Big\{\tfrac{k_0^2 k_z^s}{k_z+k_{1z}}\left[k_z C_0^v(\mathbf{k}^i,d)-k_{1z}^i C_1^v(\mathbf{k}^i,d)\right]C_1^v(\mathbf{k}^s,d)\\
&\cdot C_0^h(\mathbf{k},d)\sin(\phi^s-\phi)\sin(\phi-\phi^i)+\Big[-\tfrac{k_z^s k_{1z}}{\epsilon k_z+k_{1z}}C_1^v(\mathbf{k}^s,d)C_0^v(\mathbf{k},d)\\
&\cdot\cos(\phi^s-\phi)+\tfrac{k_\rho}{\epsilon k_z+k_{1z}}\tfrac{\epsilon k_z^s k_\rho^s}{k_{1z}^s}C_0^v(\mathbf{k}^s,d)C_1^v(\mathbf{k},d)\Big]\Big(\Big[\left(ks_z\right)^2\cos(\phi-\phi^i)\\
&-k_\rho^i k_\rho\Big]C_0^v(\mathbf{k}^i,d)+\Big[k_\rho^i k_\rho\tfrac{k_z}{k_{1z}^i}-k_{1z}^i k_z\cos(\phi-\phi^i)\Big]C_1^v(\mathbf{k}^i,d)\Big)\Big\}\,d\mathbf{k}_\perp d\mathbf{k}'_\perp\\
&+\tfrac{k_z^i(\epsilon-1)^3}{4\pi}\left(1-R_v^i\right)\left(R_v^s-1\right)C_0^v(\mathbf{k}^s,d)C_0^v(\mathbf{k}^i,d)e^{-i(k_z^s+k_z^i)d}
\end{aligned}
$$

$$\cdot\frac{1}{(2\pi)^4}\int\limits_{-\infty}^{\infty}F(\mathbf{k}_\perp^s-\mathbf{k}_\perp)F(\mathbf{k}_\perp-\mathbf{k}'_\perp)F(\mathbf{k}'_\perp-\mathbf{k}_\perp^i)\Bigg\{$$

$$\begin{aligned}
&\frac{k_0^4k_z^s}{(k_z+k_{1z})\left(k'_z+k'_{1z}\right)}C_0^h(\mathbf{k},d)C_0^h(\mathbf{k}',d)\sin(\phi^s-\phi)\cos(\phi-\phi')\sin(\phi'-\phi^i)\\
+&\frac{k_0^2k_z^sk'_{1z}k'_z}{(k_z+k_{1z})\left(\epsilon k'_z+k'_{1z}\right)}C_0^h(\mathbf{k},d)C_0^v(\mathbf{k}',d)\sin(\phi^s-\phi)\sin(\phi-\phi')\cos(\phi'-\phi^i)\\
+&\frac{k_0^4k_z^sk_{1z}k_z}{(\epsilon k_z+k_{1z})\left(k'_z+k'_{1z}\right)}C_0^v(\mathbf{k},d)C_0^h(\mathbf{k}',d)\cos(\phi^s-\phi)\sin(\phi-\phi')\sin(\phi'-\phi^i)\\
-&\frac{k_z^sk_{1z}k_zk'_{1z}k'_z}{(\epsilon k_z+k_{1z})\left(\epsilon k'_z+k'_{1z}\right)}C_0^v(\mathbf{k},d)C_0^v(\mathbf{k}',d)\cos(\phi^s-\phi)\cos(\phi-\phi')\cos(\phi'-\phi^i)\\
-&\frac{k_z^sk'_zk_{1z}k_\rho k'_\rho}{(\epsilon k_z+k_{1z})\left(\epsilon k'_z+k'_{1z}\right)}C_0^v(\mathbf{k},d)C_1^v(\mathbf{k}',d)\cos(\phi^s-\phi)\cos(\phi'-\phi^i)\Bigg\}\mathbf{k}_\perp d\mathbf{k}'_\perp\\
&+\frac{k_z^i(\epsilon-1)^3}{4\pi}\left(1-R_v^i\right)\left(R_v^s-1\right)C_0^v(\mathbf{k}^s,d)C_1^v(\mathbf{k}^i,d)e^{-i(k_z^s+k_z^i)d}\\
&\cdot\frac{1}{(2\pi)^4}\int\limits_{-\infty}^{\infty}F(\mathbf{k}_\perp^s-\mathbf{k}_\perp)F(\mathbf{k}_\perp-\mathbf{k}'_\perp)F(\mathbf{k}'_\perp-\mathbf{k}_\perp^i)\cdot\Bigg\{\\
&\frac{k_0^2k_z^sk_\rho^ik'_\rho}{(k_z+k_{1z})\left(\epsilon k'_z+k'_{1z}\right)}C_0^h(\mathbf{k},d)C_0^v(\mathbf{k}',d)\sin(\phi^s-\phi)\sin(\phi-\phi')\\
-&\frac{k_z^sk_{1z}k_zk'_{1z}k_\rho^ik'_\rho}{k_{1z}^i(\epsilon k_z+k_{1z})\left(\epsilon k'_z+k'_{1z}\right)}C_0^v(\mathbf{k},d)C_0^v(\mathbf{k}',d)\cos(\phi^s-\phi)\cos(\phi-\phi')\\
-&\frac{k_z^sk_{1z}k_\rho^ik_\rho\left(k'_\rho\right)^2}{k_{1z}^i(\epsilon k_z+k_{1z})\left(\epsilon k'_z+k'_{1z}\right)}C_0^v(\mathbf{k},d)C_1^v(\mathbf{k}',d)\cos(\phi^s-\phi)\Bigg\}d\mathbf{k}_\perp d\mathbf{k}'_\perp\\
&+\frac{k_z^ik_\rho^s(\epsilon-1)^3}{4\pi}\left(1-R_v^i\right)\left(1+R_v^s\right)C_1^v(\mathbf{k}^s,d)C_0^v(\mathbf{k}^i,d)e^{-i(k_z^s+k_z^i)d}\\
&\cdot\frac{1}{(2\pi)^4}\int\limits_{-\infty}^{\infty}F(\mathbf{k}_\perp^s-\mathbf{k}_\perp)F(\mathbf{k}_\perp-\mathbf{k}'_\perp)F(\mathbf{k}'_\perp-\mathbf{k}_\perp^i)\Bigg\{\\
&\frac{k_0^2k_zk_\rho}{(\epsilon k_z+k_{1z})\left(k'_z+k'_{1z}\right)}C_1^h(\mathbf{k},d)C_0^h(\mathbf{k}',d)\sin(\phi-\phi')\sin(\phi'-\phi^i)\\
-&\frac{k_\rho k_zk'_zk'_{1z}}{(\epsilon k_z+k_{1z})\left(\epsilon k'_z+k'_{1z}\right)}C_1^v(\mathbf{k},d)C_0^v(\mathbf{k}',d)\cos(\phi-\phi')\cos(\phi'-\phi^i)\\
-&\frac{k'_zk'_\rho(k_\rho)^2}{(\epsilon k_z+k_{1z})\left(\epsilon k'_z+k'_{1z}\right)}C_1^v(\mathbf{k},d)C_1^v(\mathbf{k}',d)\cos(\phi'-\phi_i)\Bigg\}d\mathbf{k}_\perp d\mathbf{k}'_\perp\\
-&\frac{k_z^ik_\rho^s(\epsilon-1)^3}{4\pi}\left(1-R_v^i\right)\left(1+R_v^s\right)C_1^v(\mathbf{k}^s,d)C_1^v(\mathbf{k}^i,d)e^{-i(k_z^s+k_z^i)d}\\
&\cdot\frac{\triangle^3}{(2\pi)^4}\int\limits_{-\infty}^{\infty}F(\mathbf{k}_\perp^s-\mathbf{k}_\perp)F(\mathbf{k}_\perp-\mathbf{k}'_\perp)F(\mathbf{k}'_\perp-\mathbf{k}_\perp^i)\Bigg\{
\end{aligned}$$

$$\begin{aligned}
&\frac{k_zk'_{1z}k_\rho k_\rho^ik'_\rho}{k_{1z}^i(\epsilon k_z+k_{1z})\left(\epsilon k'_z+k'_{1z}\right)}C_1^v(\mathbf{k},d)C_0^v(\mathbf{k}',d)\cos(\phi-\phi')\\
&+\frac{k_\rho^i(k_\rho)^2\left(k'_\rho\right)^2}{k_{1z}^i(\epsilon k_z+k_{1z})\left(\epsilon k'_z+k'_{1z}\right)}C_1^v(\mathbf{k},d)C_1^v(\mathbf{k}',d)\Bigg\}d\mathbf{k}_\perp d\mathbf{k}'_\perp
\end{aligned}\tag{86}$$

References

[1] Y. Oh, K. Sarabandi, and F.T. Ulaby, "An empirical model and an inversion technique for radar scattering from bare soil surfaces," *IEEE Trans. Geosci. Remote Sensing,* vol. 30, pp. 370-382, Mar. 1992.

[2] O.M. Philips, "The Dynamics of the Upper Ocean,", 2nd Ed., NewYork: Cambridge University Press, 1978.

[3] S.O. Rice, "Reflection of electromagnetic wave by slightly rough surfaces," *Communication in Pure and Applied Mathematics,* vol. 4, pp. 351-378, 1951.

[4] M. Nieto-Vesperinas, "Depolarization of electromagnetic waves scattered from slightly rough random surfaces: A study by means of the extinction theorem," *J. Opt. Soc.,* 72(5), pp. 539-547, 1982.

[5] G.S. Agarwal, "Interaction of electromagnetic waves at rough dielectric surfaces," *Phys. Rev. B,* no. 15, pp. 2371-2383, 1977.

[6] L. Tsang, J. Kong, and R.T. Shin, *Theory of Microwave Remote Sensing,* John Wiley and Sons, New York, 1985.

[7] P. Beckmann and A. Spizzichino, *The Scattering of Electromagnetic Waves from Rough Surfaces*, Pergamon, New York, 1963.

[8] D. Winebrenner and A. Ishimaru, "Investigation of a surface field phase perturbation technique for scattering from rough surfaces," *Radio Science,* vol. 20, no. 2, pp. 161-170, Mar-Apr, 1985.

[9] E. Rodriguez and Y. Kim, "A unified perturbation expansion for surface scattering," *Radio Science,* vol. 27, no. 1, pp. 79-93, Jan-Feb, 1992.

[10] A.K. Fung and G.W. Pan, "A scattering models for perfectly conducting random surfaces: I. model development, II. range of validity," *IEEE Trans. Geosci. Remote Sensing,* vol. 8, no. 11, pp. 1579-1605, 1987.

[11] A.K. Fung, Z. Li, and K.S. Chen, "Backscattering from a randomly rough dielectric surface," *IEEE Trans. Geosci. Remote Sensing,* vol. 30, pp. 356-369, Mar. 1992.

[12] T. Chiu and K. Sarabandi, "Scattering solutions for slightly rough surfaces with inhomogeneous dielectric profiles," Radiation Laboratory Report no. RL-946, the University of Michigan, 1997.

[13] K. Sarabandi, "Derivation of phase statistics from the Mueller matrix," *Radio Science,* vol. 27, no. 5, pp. 553-560, September-October 1992.

[14] M.T. Hallikainen, F.T. Ulaby, M.C. Dobson, M.A. El-Rayes, and L. Wu, "Microwave dielectric behavior of wet soil — part I: empirical models and experimental observations," *IEEE Trans. Geosci. Remote Sensing,* vol. GE-23, no. 1, pp. 25-34, January 1985.

[15] Sarabandi,K., and T.C. Chiu "Electromagnetic scattering from slightly rough surfaces with inhomogeneous dielectric profile," *IEEE Trans. Antennas Propagat.,* vol. 45, no. 9, Sept. 1997.

[16] E.G. Njoku, and J. Kong, "Theory for passive microwave remote sensing of near-surface soil moisture," *J. Geophys. Res.,* vol. 28, pp. 1022-1033, 1990.

[17] F.G. Tricomi, *Integral Equations*, New York: Interscience Publishers, 1957.

[18] R. DeRoo, R. Hartikka, N. Peplinski, and A. Zambetti, , Bistatic Measurement Facility User's Manual, Radiation Laboratory, the University of Michigan, August, 1994.

[19] K. Sarabandi and F.T. Ulaby, "A convenient technique for polarimetric calibration of radar systems," *IEEE Trans. Geosci. Remote Sensing,* vol. GE-23, no. 1, pp. 25-34, January 1985.

[20] K. Sarabandi, Y. Oh, and F.T. Ulaby, "Measurement and calibration of differential Mueller matrix of distributed targets," *IEEE Trans. Antennas Propagat.,* vol. 40, pp. 1524-1532, Dec. 1992.

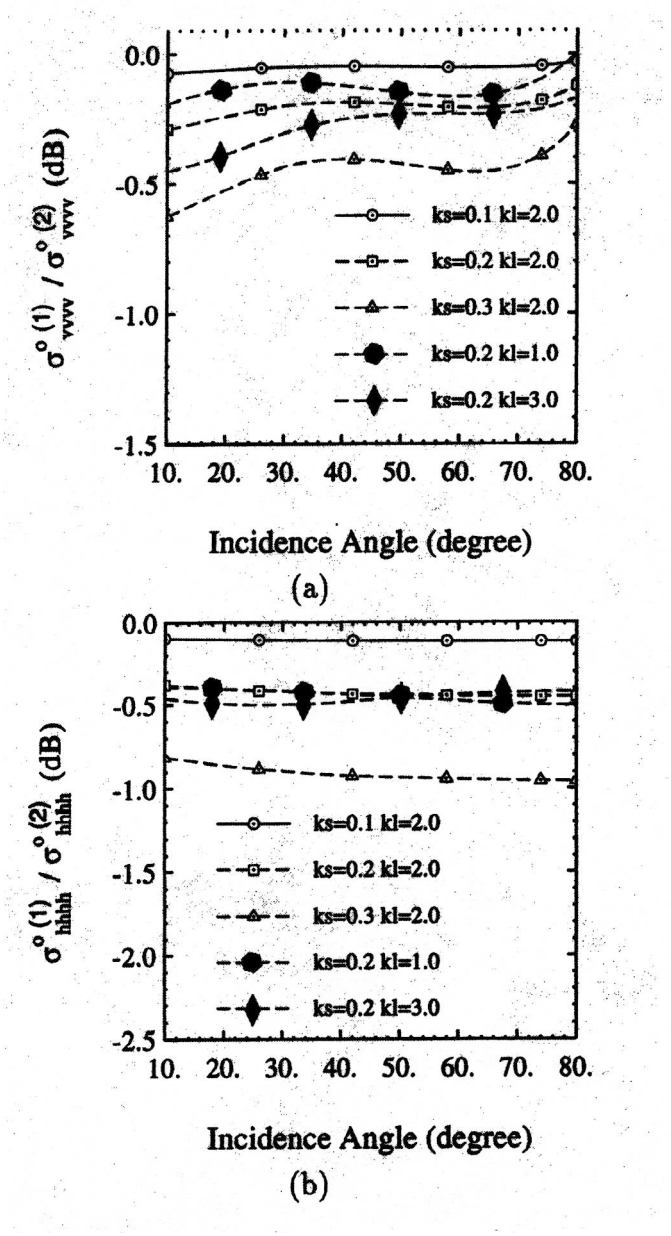

Figure 5: Ratio of the first-order to the complete second-order solution of a homogeneous rough surface with $m_v = 0.2\,(\epsilon = 8.0 + i2.51$ at 1.25 GHz) as a function of incidence angle for different values of ks and kl .

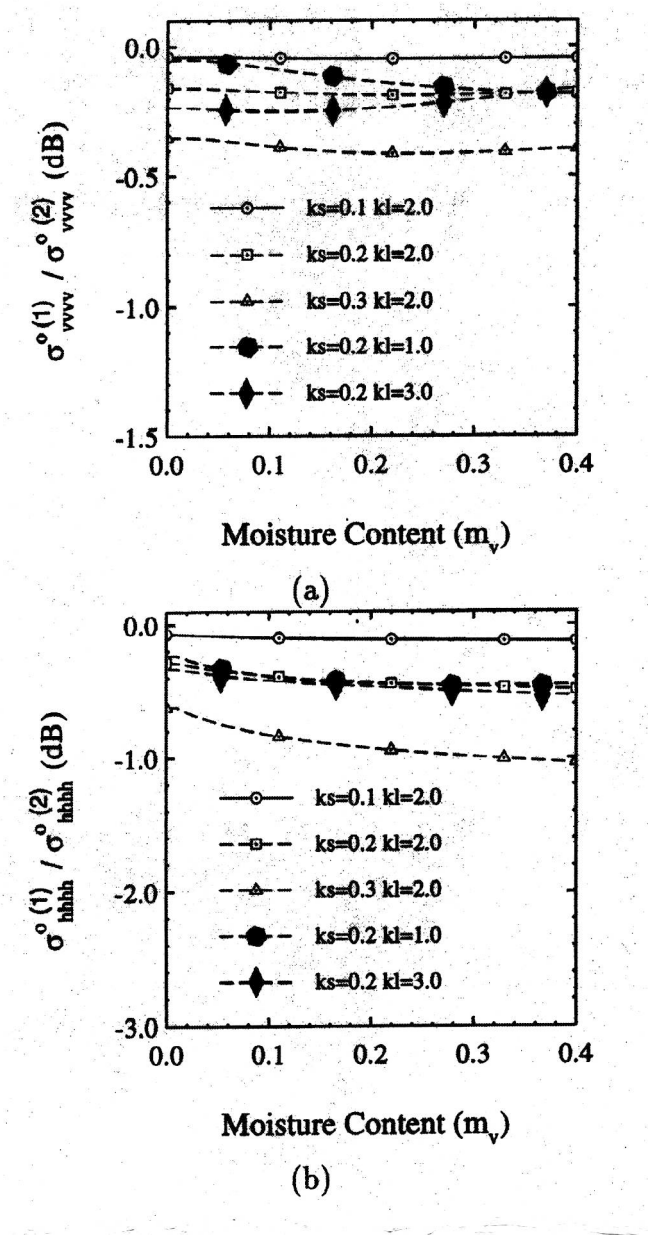

Figure 6: Ratio of the first-order to the complete second-order solution of a homogeneous rough surface as a function of moisture content for different values of ks and kl at $\theta = 45°$.

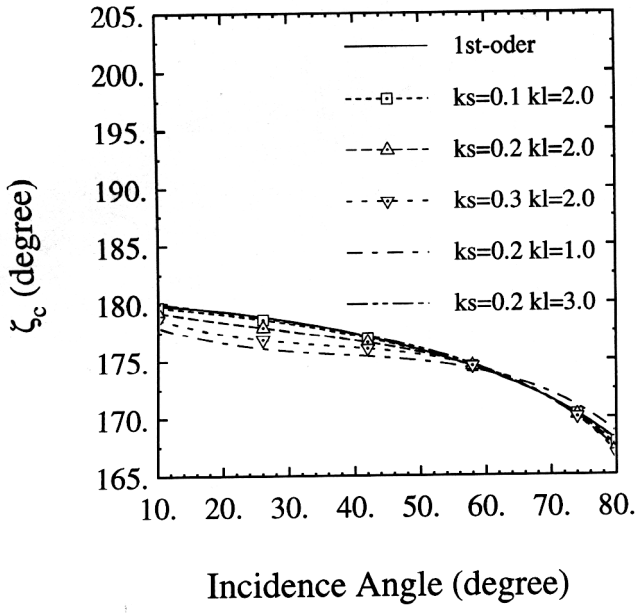

Figure 7: Co-polarized coherent phase difference of homogeneous rough surface with $m_v = 0.2(\epsilon = 8.0 + i2.51$at 1.25 GHz) as a function of incidence angle for different values of ks and kl.

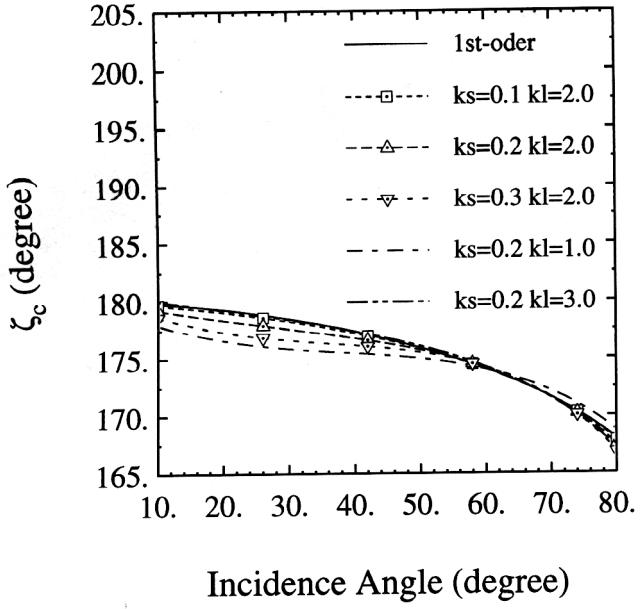

Figure 8: Co-polarized coherent phase difference of homogeneous rough surface as a function of moisture content for different values of ks and kl at $\theta = 45°$.

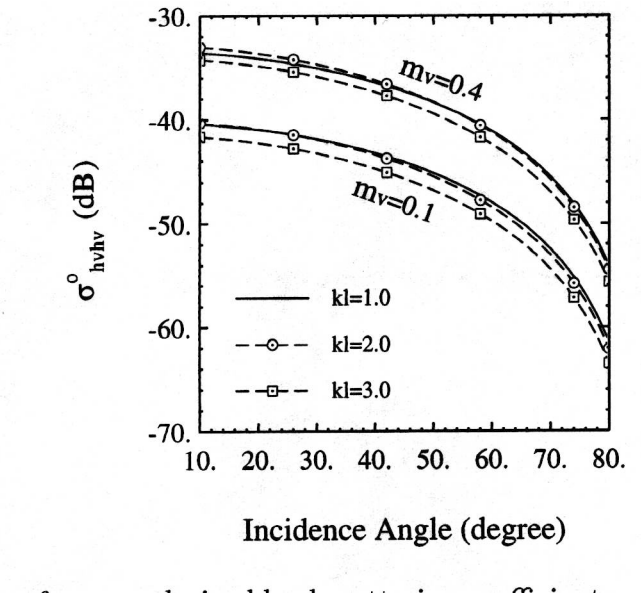

Figure 9: Variations of cross-polarized backscattering coefficient as a function of incidence angle, moisture content ($\epsilon = 4.89 + i0.92$ for $m_v = 0.1$ and $\epsilon = 1.46 + i7.5$ for $m_v = 0.4$ at 1.25 GHz) and correlation length for a surface with $ks = 0.2$.

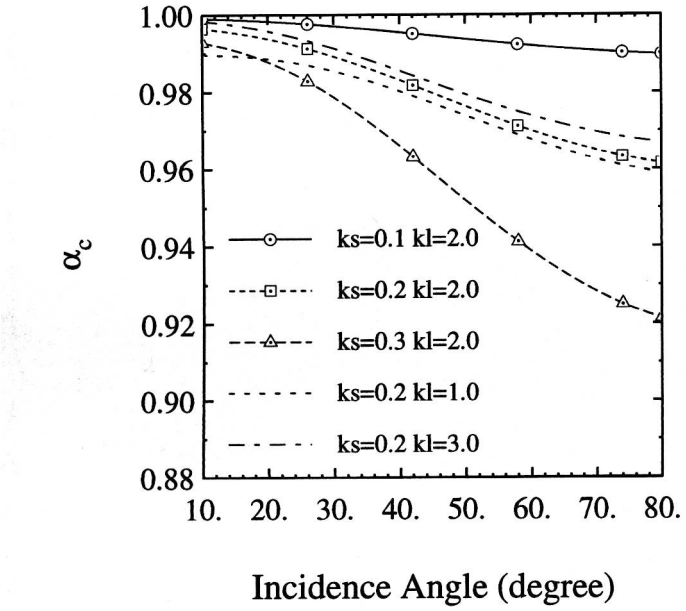

Figure 10: Sensitivity of co-polarized degree of correlation to incidence angle for different values of ks and kl and moisture $m_v = 0.2$ ($\epsilon = 8.0 + i2.51$ at 1.25 GHz).

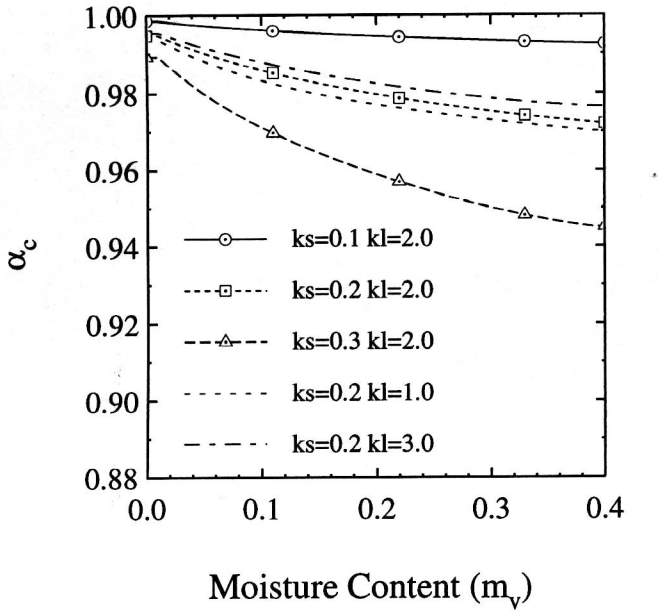

Figure 11: Sensitivity of co-polarized degree of correlation to soil moisture content for different values of ks and kl $\theta = 45°$. α_c does not show much sensitivity to kl.

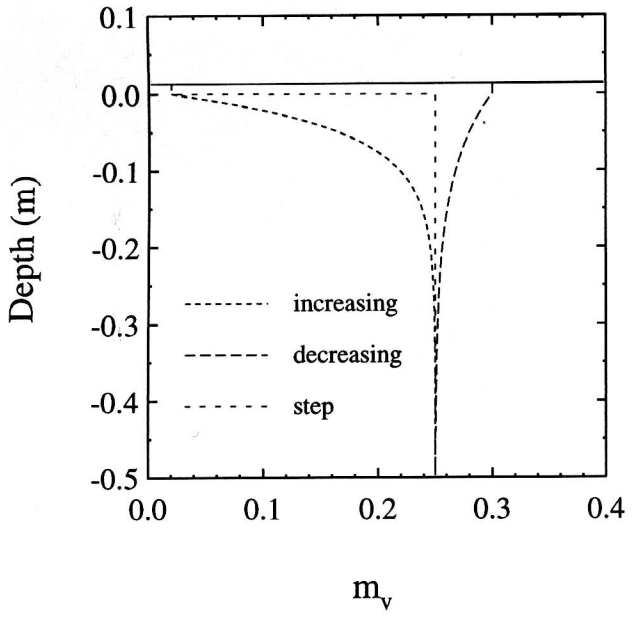

Figure 12: Three different moisture profiles used in the backscattering simulations: increasing exponential with $\beta = 20$, decreasing exponential with $\beta = 10$, and step.

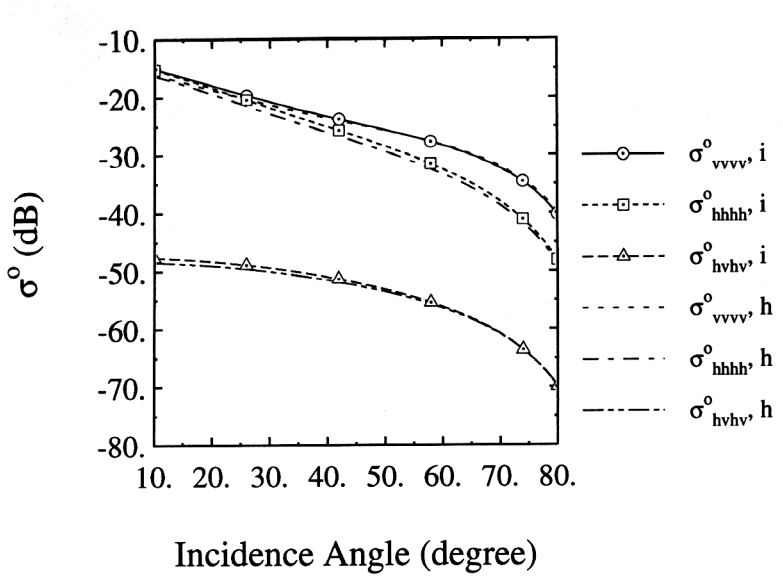

Figure 13: Comparison of backscattering coefficients calculated for the homogeneous and increasing exponential moisture profiles for a rough surface with $ks = 0.2$ and $kl = 2$.

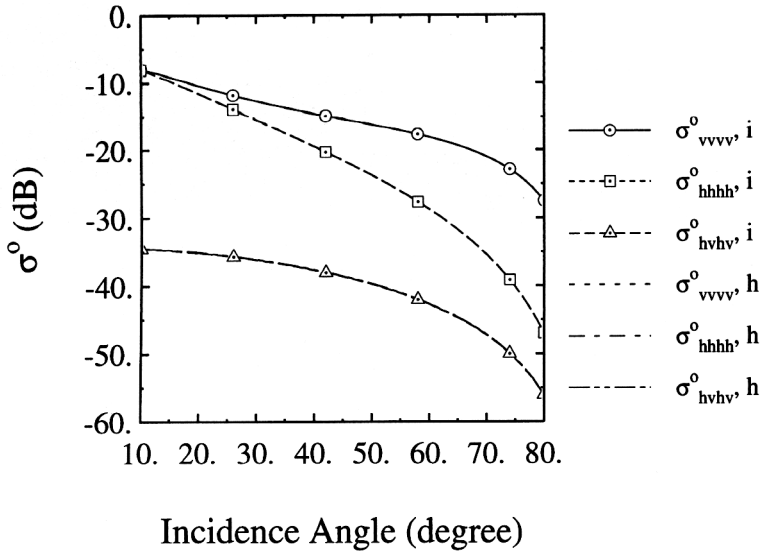

Figure 14: Comparison of backscattering coefficients calculated for the homogeneous and decreasing exponential moisture profiles for a rough surface with $ks = 0.2$ and $kl = 2$.

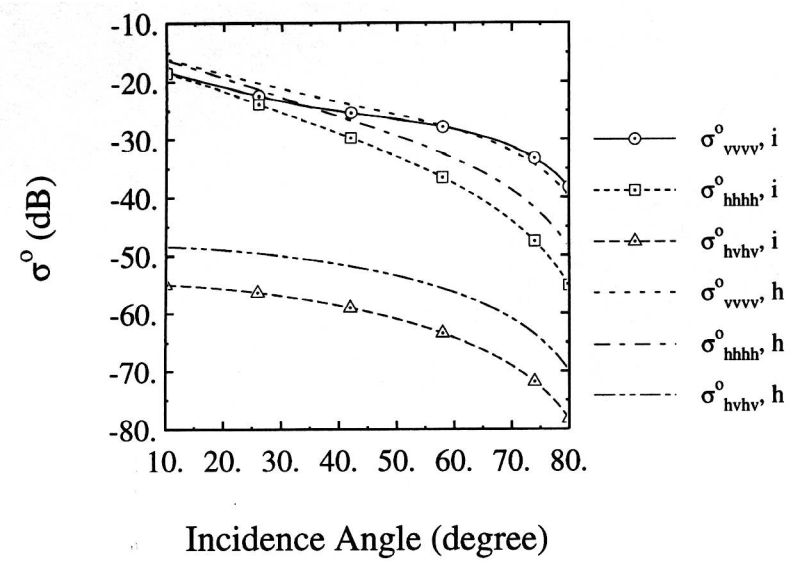

Figure 15: Comparison of backscattering coefficients calculated for the homogeneous and step moisture profiles for a rough surface with $ks = 0.2$ and $kl = 2$.

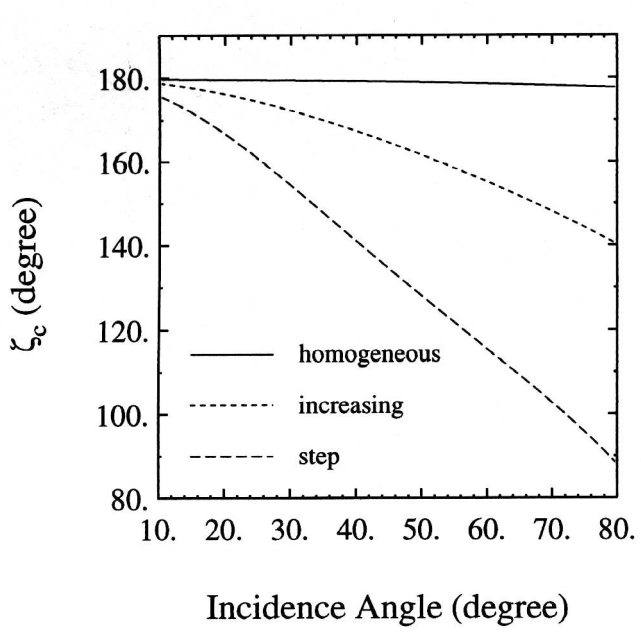

Figure 16: Co-polarized coherent phase difference calculated for the homogeneous, increasing exponential, and step moisture profiles for a rough surface with $ks = 0.2$ and $kl = 2$.

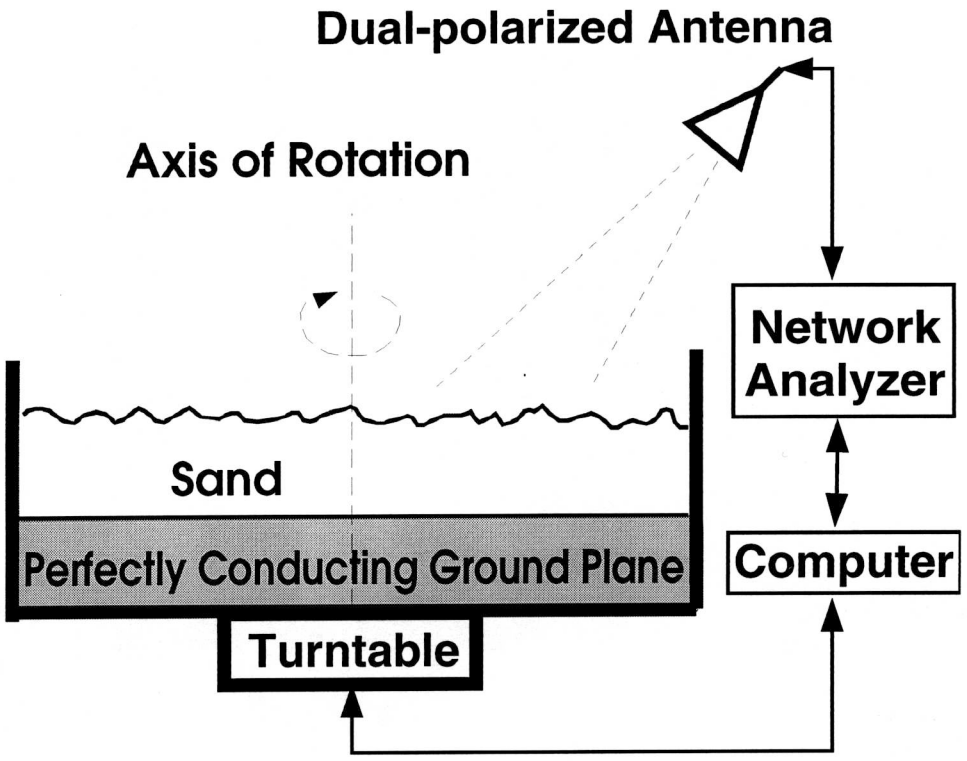

Figure 17: Simplified block diagram of the experimental setup.

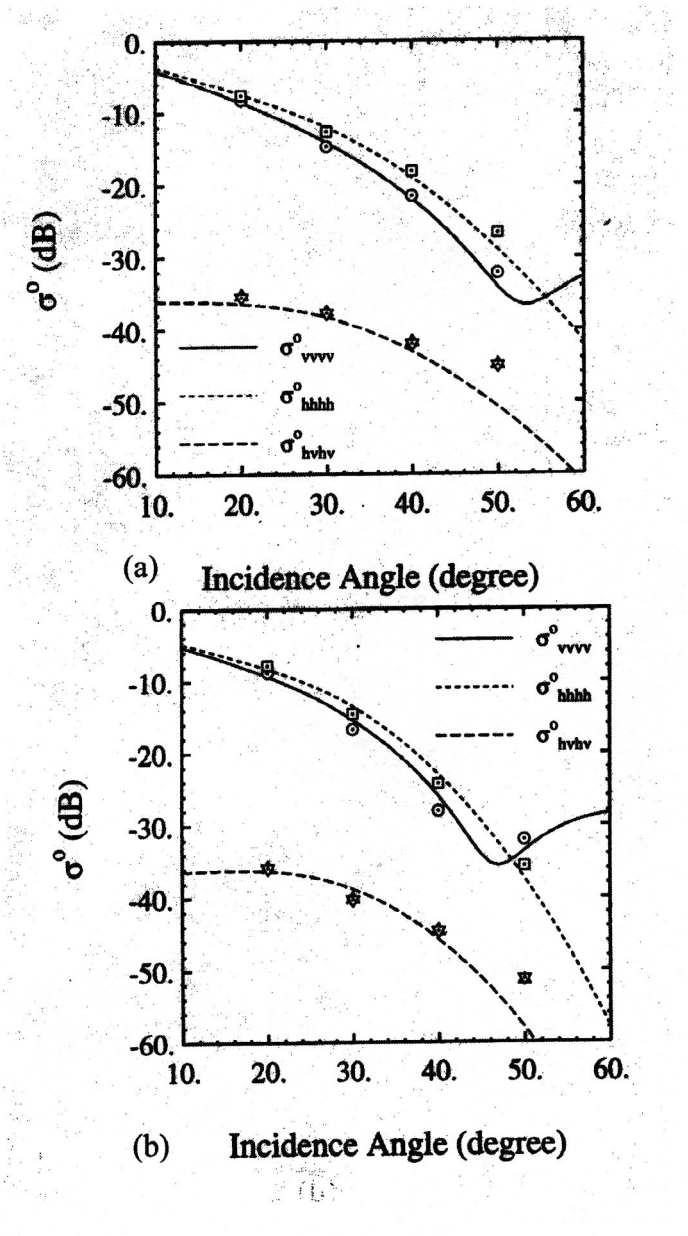

Figure 18: Comparison of the measured and the calculated $\sigma^0_{hhhh}/\sigma^0_{vvvv}$ for a sand layer of thickness 2,52 cm (a) and 3.53 cm (b) above a perfectly conducting ground plane at 9.25 GHz.

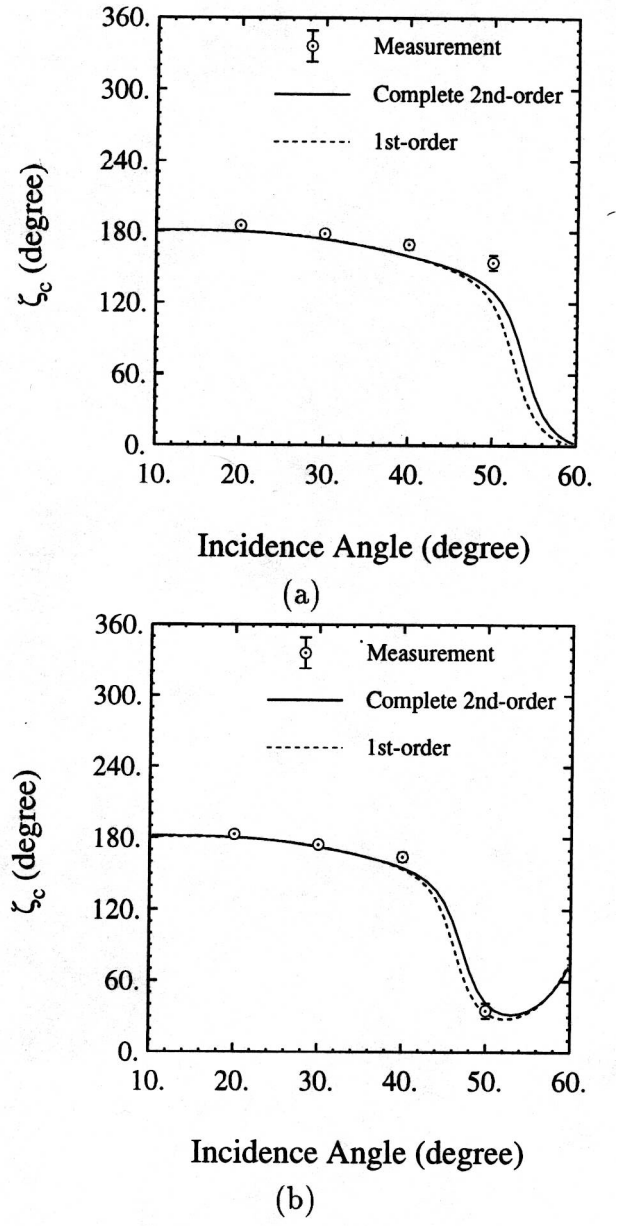

Figure 19: Comparison of the measured and the calculated co-polarized degree of correlation for a sand layer of thickness 2.52 cm (a) and 3.53 cm (b) above a perfectly conducting ground plane at 9.25 GHz.

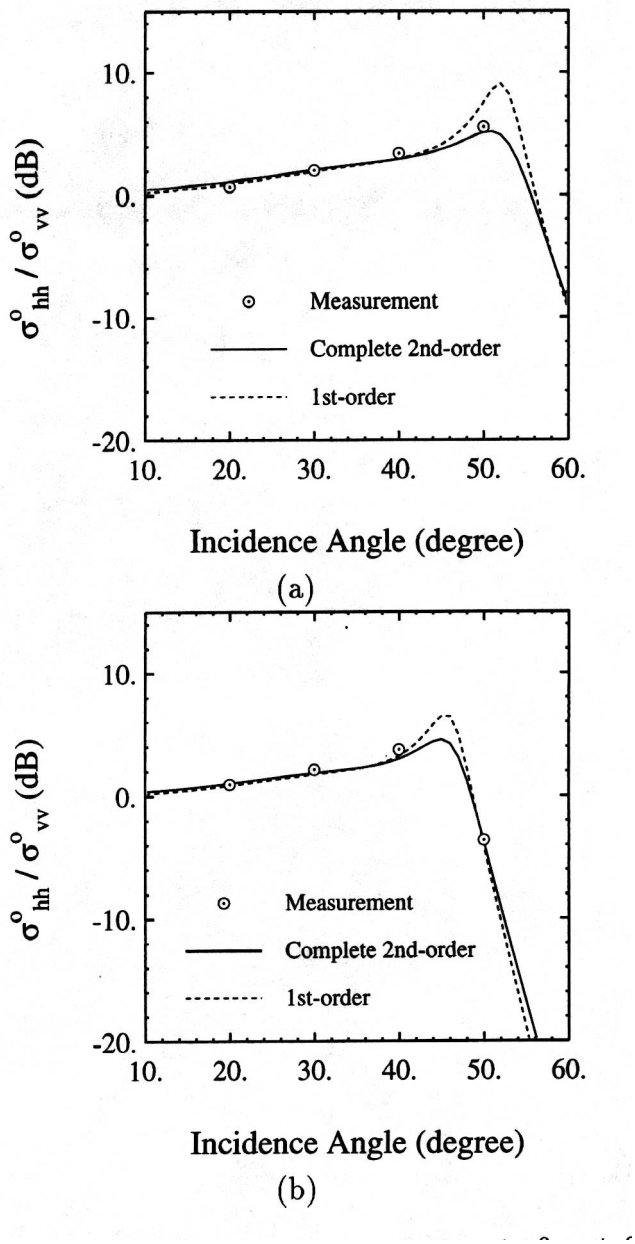

Figure 20: Comparison of the measured and the calculated $\sigma^0_{hhhh}/\sigma^0_{vvvv}$ for a sand layer of thickness 2.52 cm (a) and 3.53 cm (b) abov e a perfectly conducting ground plane at 9.25 GHz.

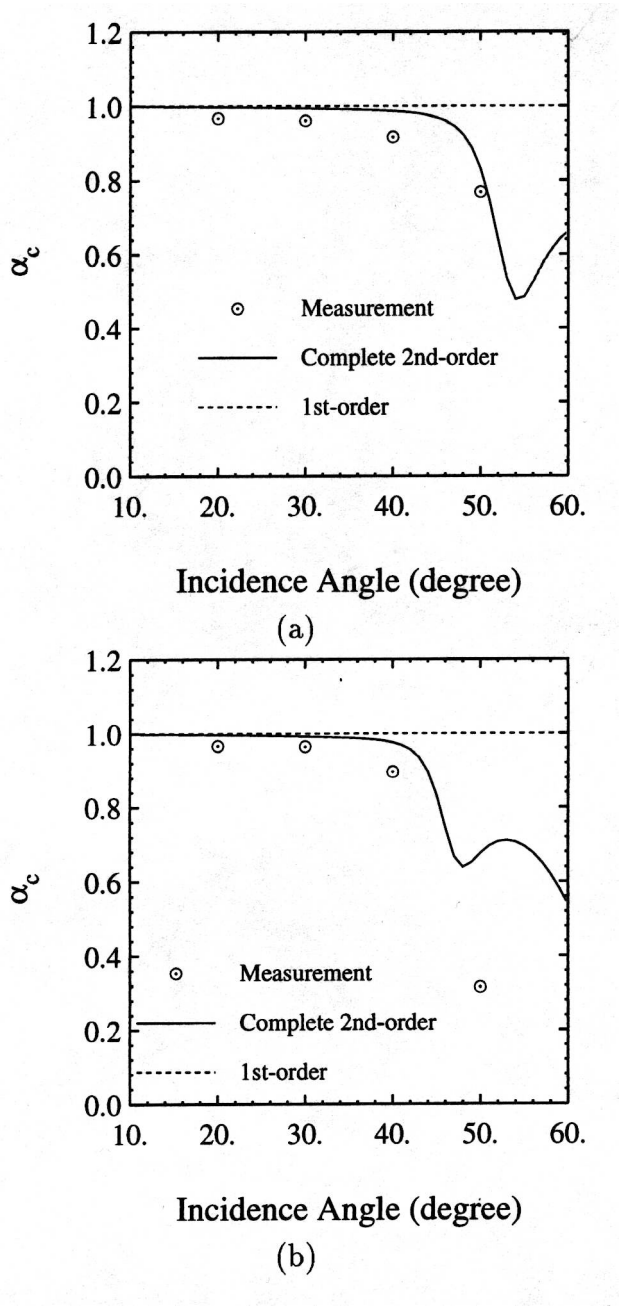

Figure 21: Comparison of the measured and the calculated co-polarized degree of correlation for a sand layer of thickness 2.52 cm (a) and 3.53 cm (b) above a perfectly conducting ground plane at 9.25 GHz.